

## **Chapter 1**

### **Introduction**

#### **1.1 Purpose**

The sea breeze phenomenon is a coupled atmospheric and oceanic response to the differential heating rates of land and water. The onshore directed sea breeze (using the meteorological convention) is a mesoscale phenomenon that occurs along many of the world's tropical and temperate coastlines when the land is warmer than the sea due to solar insolation and properties associated with the land-water energy balance. Additionally, the sea breeze circulation is a result of small-scale air pressure differences in the coastal zone, so it occurs only when the prevailing synoptic flows are not prohibitively strong (Simpson, 1994). Due to the mesoscale nature of the phenomenon, determining the onset of the sea breeze development is quite often difficult and consequently is a significant challenge for meteorologists. This is compounded by the lack of monitoring information over the ocean and along the shoreline, and the fact that most operational models are run at course resolutions unable to resolve dynamics within the sea breeze circulation. Accurate forecast of the sea breeze is important to New Jersey for a number of reasons. The sea breeze has the potential to propagate tens of kilometers inland, it also effects nearby large urban centers such as Philadelphia and New York. The potential developments of small-scale, slow-moving thunderstorms are possible at the sea breeze front due to surface wind convergence, when outflow boundaries from thunderstorms intersect the sea breeze. Wind convergence at the sea

breeze front along with the recirculation characteristics of the sea breeze cell can also play a role in the transport of pollutants and pollen to areas well away from their source resulting in adverse air quality and increases in potential health problems. Similarly, sea breeze transport and dispersion can be of vital importance in the event of the accidental or intentional releases of hazardous chemicals. The sea breeze circulation will impact efficient energy management (i.e., temperature forecasts will impact load forecasts and subsequent energy allocations; wind field perturbations will affect wind energy system citing, design, and operations). However, the most common and beneficial impact of the sea breeze, for the state's inhabitants and many seasonal tourists, is the advection of the cool marine air onshore, which provides welcome relief from the hot summertime temperatures.

The sea breeze's rapid onshore rush of marine air and the subsequent decrease in lower tropospheric air temperatures can have important ramifications for both public and marine meteorological forecasting as well as for the tourism industry. Coastal inhabitants frequently travel en masse to the New Jersey coastline to seek relief from hot summertime temperatures in the adjacent Philadelphia and New York metropolitan areas. Tourism comprises the second largest revenue base in the state of New Jersey, most of which occurs during the warmer months along the state's one hundred and twenty-seven mile shoreline. Energy availability along the state's barrier islands is a constant summertime concern due to the one to two magnitude increases in summertime population which can increase energy demand beyond available supply. Concurrent with the dramatic increase in summertime tourism is an added increase in pollution

from automobile emissions and from power plants struggling to cope with the extreme demand for electricity.

Since the sea breeze is such an important facet of the weather along the coast, it is incumbent upon the research community to gain a better understanding of the relationships responsible for the phenomenon, especially the vital land-sea temperature gradient. Although variations in the air temperature are well observed, the same cannot be said for variations in sea surface temperature (SST) and the air immediately above it. However, advances in remote sensing technologies have recently allowed for high-resolution observations of the SST. These observations have located small-scale variations in both space and time of SST in the coastal zone known as coastal upwelling (Glenn et al., 2004). Since coastal upwelling is especially present during the summer months, study of the relationship between coastal upwelling and the sea breeze is essential. In order to attain accurate forecasts of the sea breeze, we must look to the sea to measure the potential impact of small-scale ocean temperature variations that are crucial in the development of certain sea breeze cases.

Coastal upwelling refers to the offshore transport of warmer surface water offshore caused by a wind stress acting parallel to the coast. Along the New Jersey coast, upwelling occurs in response to the semi-persistent southwesterly winds that occur during the summer months. The surface water is replaced by colder bottom water, which results in colder sea surface temperature (SST) along the coast (Glenn et al., 1996).

Coastal upwelling can lead to precipitous decreases in the temperature of the ocean adjacent to the immediate shoreline. While the sea breeze and coastal upwelling

are distinctly separate phenomena, they at times occur concurrently. The relationship between coastal upwelling and the sea breeze circulation has not yet been fully investigated; however numerical weather prediction modeling can provide significant insight into this relationship.

The purpose of this thesis will be to provide evidence showing the effect of coastal upwelling on the development and characteristics of the New Jersey sea breeze. My hypothesis is: Coastal upwelling can enhance the New Jersey sea breeze by leading to farther inland penetration of the sea breeze front, bringing cooler marine air farther inland during the summer months when upwelling is occurring. By altering SSTs in mesoscale modeling simulations of sea breeze cases, this thesis will investigate the sensitivity of the sea breeze to nearshore variations in SST, as well as attempting to show that given a certain SST the sea breeze circulation can be “turned on and off”. Additionally, variations in the structure and behavior of the sea breeze circulation cell between upwelling and non-upwelling coastal ocean regimes will be examined. A third issue to be addressed by this thesis, is whether or not the presence of localized coastal upwelling present irregularities in the shape of the sea breeze front distinctly different from the shape of the sea breeze front on non-upwelling days or days with cold water along the entire coastline.

These issues will be investigated by the utilization of The National Center for Atmospheric Research’s (NCAR’s) high-resolution Weather Research Forecast (WRF) Model, as well as observational evidence obtained via remote sensing; namely, using the Doppler Radar operated by the National Weather Service (NWS), and sea surface temperature analyses from the Advanced Very High Resolution Radiometer (AVHRR)

on board the National Oceanographic and Atmospheric Administration's (NOAA) Polar Orbiting Environmental Satellites (POES). The study area comprises the central and southern portion of New Jersey, including Raritan Bay, southeastern Pennsylvania, and the northern portion of Delaware, including Delaware Bay (Figure 1 a-c).

These issues are all quite important in regards to operational high-resolution meteorological forecasts in and near the coastal zone. A complete understanding of the sea breeze–coastal upwelling relationship in both behavior and structure will certainly benefit the tourist industry and the public utilities while providing more accurate meteorological forecasts to the public, marine, aviation, and private communities. Additionally, improved forecasting for coastal areas will enhance utility reliability and security during periods of peak energy demand.

Chapter 1 of this thesis will provide a basic background regarding the development and behavior of the sea breeze with an emphasis on the importance of the synoptic wind flow aloft and background on coastal upwelling along the New Jersey shore. Chapter 2 will focus on the primary means used to study the sea breeze and upwelling phenomena, including the use of remote sensing in the form of visible satellite imagery and SST from orbiting satellites and tracking the thin line of radar reflectivity from Doppler radar caused by the congregation of insects and birds along the convergence at the sea breeze front. Chapter 3 will discuss the methods used to perform the mesoscale modeling case studies discussed in this study. Chapter 4 will provide more in depth discussion of the typical evolution of a sea breeze event and the evolution of a sea breeze event influenced by a coastal upwelling regime in the coastal ocean. Chapter 5 will dissect the case study and sensitivity experiments performed,

along with detailed comparisons between the individual cases. Chapter 6 will discuss conclusions and possible future work.

This thesis will show the rather distinct differences between an upwelling enhanced sea breeze and a typical sea breeze. This will include differences in the inland penetration of the sea breeze front, the vertical depth of the sea breeze front and return current, and distinct differences in the sensible weather that would be expected in the coastal zone during sea breeze events.

### **1.2 Characteristics of the Sea Breeze**

Study of the sea breeze has gone on for centuries, mainly due to the influence of the phenomenon on marine weather, however most of these studies have been almost entirely observation based. The lack of modern remote sensing based meteorological instrumentation had limited all study to the inland movement of the sea breeze front onshore (Simpson, 1994). Technology has advanced to the point where in depth monitoring and modeling of the sea breeze circulation can now take place, allowing meteorologists for the first time an opportunity to study the 3-dimensional sea breeze circulation, as well as continuing studies of the inland propagation of the sea breeze front. While it has been understood for quite some time that the difference in land-sea temperatures was the impetus behind the formation of sea breezes, study of the full depth of the sea breeze from surface to the return current at the top of the sea breeze is now possible.

While the study of the sea breeze has been ongoing since the time of the Greeks for use in marine military battles (Simpson, 1994), much is still to be learned as to not

only how the sea breeze circulation behaves, but how it initially forms. Traditional theory explains that on a clear day with calm conditions and no surface pressure gradient, the air over the land will be heated disproportionately more than the air over the ocean due to the differing heat capacities of soil and seawater. In a hydrostatic world, this would cause the vertical pressure gradients to be much larger in the column of air over the land. This will lead toward greater air pressure aloft over land, creating a horizontal pressure gradient. The evacuation of air aloft of the land surface (the return current) coupled with air convergence aloft from the sea will lower surface pressures at the land surface and raise surface pressures at the ocean surface due to conservation of mass. This surface pressure gradient will result in a flow from the sea to the land at the surface, while also completing the circuit of the sea breeze circulation (Pielke, 1984). Figure 2 illustrates the vertical dimension of the sea breeze circulation. Tjim et al. (1999) using a mesoscale model found that as the sea breeze initially develops, the height of the sea breeze circulation can reach as high as 1000 m, with a poorly developed return current above it. As the event continues, the sea breeze circulation decreases in depth but increases in strength.

The return current, which is the flow from land to sea aloft is the subject of some controversy in the literature. Frizzola and Fisher, (1963) in their study of the New York City area sea breeze found that the return current was difficult to identify on days with a strong opposing synoptic flow. Banta (1993) confirms this, as he found very little evidence of a return current associated with the Monterey Bay sea breeze system.

The most important factors in the development of the sea breeze circulation cell are horizontal temperature gradient across the land-sea interface, the synoptic flow at

the surface, and the gradient flow aloft (Simpson, 1994). Considering the very fine scales at which these variables occur in the sea breeze circulation cell, the study method of choice in recent years has been the use of high-resolution mesoscale numerical models.

As computing speeds have increased over the last few decades, the most widely utilized means to study the sea breeze has been through the use of numerical modeling. Modeling studies have progressed from simple linear models in the early days, to synoptic and now mesoscale spatial resolution models that are now able to fully resolve the sea breeze with reasonable accuracy.

The advent of numerical modeling has also allowed for some of the first investigations of the sea breeze circulation cell in the vertical direction. Previous studies using tethered balloons at Atlantic City International Airport and Ocean City found that the sea breeze may arrive at some height above the surface prior to the passage of the sea breeze front at the surface (Angell and Pack, 1965). The entire vertical height of the sea breeze circulation has been found to vary several hundred meters depending on the synoptic flow aloft (Simpson, 1994). The return current, which is located in the upper part of the sea breeze circulation cell, is an offshore wind through which rising air from the land surface is able to move back over the ocean. Air divergence aloft of the ocean surface allows for the air, which was returned to the ocean by the return current, to move back towards the ocean surface, shown by downward vertical velocities over the ocean. Thus, the return current is the above surface completion of the sea breeze circulation cell.

### **1.3: Outside Factors Affecting Sea-Breeze Behavior**

The overall synoptic flow is an important factor in the development, characteristics, and behavior of the sea breeze. It has been found that a weak offshore-directed wind is best for the development of the sea breeze as it intensifies the sea breeze perturbation by increasing the horizontal land-sea temperature gradient (Estoque 1962; Zhong and Takle, 1993). Arritt (1993) conducted a series of sensitivity studies to investigate the effect of the strength and direction of the synoptic flow on the sea breeze circulation. An onshore synoptic flow acts to reduce the overall temperature gradient at the coastline, thus allowing for an onshore wind of only a few meters per second (m/s) to disrupt the sea breeze circulation. The most intense sea breezes occur with a weak to moderate synoptic offshore flow as it increases the temperature gradient in the coastal zone while also allowing for large upward motion at the convergence zone due to strong convergence frontogenesis. Geostrophic flows of greater than 11 m/s allow for convergence frontogenesis, although in these cases the sea breeze front remains offshore or at the immediate coastline only. Due to the proximity of the statically stable environment over the ocean, upward motion is suppressed, resulting in lesser horizontal velocities and a weaker sea breeze circulation.

The intensity of the sea breeze circulation is strongly correlated to the offshore wind component aloft (Simpson, 1994). Changes in the offshore synoptic wind can lead to large changes in the strength of wind and upward motion at the sea breeze front due to stronger low-level convergence. The most intense sea breezes occur when the offshore synoptic wind is strong enough to reduce the penetration speed of the sea breeze front (Bechtold et al., 1991).

An observational study (Kwiatkowski, 1999) of the New Jersey sea breeze was conducted to investigate the impact of offshore winds at 850 mb on the inland penetration of the sea breeze. While the study used only five case studies, indications were that an offshore directed wind of 10 m/s was enough to allow a sea breeze to penetrate inland approximately 15-20 km, but then retreat back towards the shoreline. Two of these cases, June 7 and May 19, 1996 had land-sea temperature gradients of 11°C and 18°C respectively.

An observational study of the New York City area sea breeze (Frizzola and Fisher, 1963) found that with a wind flow directed onshore aloft, the circulation cell begins earlier in the day, thus allowing for inland penetration of up to 25 to 30 km. With an opposing gradient wind flow, the sea breeze develops during the afternoon hours and is generally relegated to within a few kilometers of the immediate coastal zone. Observational evidence further suggests that frontal penetration onshore is negated by offshore directed gradient winds greater than 15 knots and land-sea temperature gradients of less than 10°C.

The speed of penetration of the sea breeze front is a function of the onshore wind (Pearson et al., 1983). Laboratory experiments in a salt tank conducted by Simpson and Britter (1980) indicated that an offshore wind would act to both slow the inland penetration of the sea breeze by approximately three-fifths of the magnitude of the offshore component of the wind, while also reducing the depth of the sea breeze. Additionally, it has been found that when the opposing flow is adequate for a penetrating sea breeze the speed at which propagation occurs increases throughout the day. In the presence of opposing synoptic wind flow, the inland penetration rate of the

sea breeze corresponds to that of a gravity current (Atkins and Wakimoto, 1997). By definition (Simpson, 1997), a gravity current describes the motion of a dense fluid moving into a less dense fluid.

It has been established that the synoptic wind flow aloft is an important factor in the development and behavior of the sea breeze circulation. Strong offshore flow aloft can be prohibitive to the development of the sea breeze, and when strong enough can negate its development completely. The effectiveness of the offshore synoptic wind flow to alter the representation of the sea breeze in simulations must be considered in any study of both the inland penetration as well as the vertical depth of the sea breeze.

#### **1.4: Small-scale Variations in the Sea Breeze Front**

Previous studies of the sea breeze found in the literature indicate that small-scale variations in the sea breeze front occur at small-scale spatial resolutions and are primarily the result of small geographic features such as barrier islands, bays, and estuaries. These variations in the sea breeze circulation can lead to significant implications for sensible weather.

Variations in the sea breeze frontal structure have been found when barrier islands exist offshore. Mahrer and Segal (1985) simulated the effects of the shape and size of islands on the effect of the sea breeze using a simple numerical model. Stronger winds and upward vertical velocities were found on circular islands than for elongated ones. This is attributed to the fact that the sea breeze will develop on all sides of the island and converge in the center.

As the sea breeze propagates onshore, additional variations in the structure of the sea breeze front occur due to various irregularities in the shape of the coastline configuration. A modeling study by McPherson (1970), intended to investigate small-scale variations in the sea breeze front caused by an irregularly shaped coastline, utilized a straight west to east coastline with a large square bay in the center of the grid and the ocean located to the south (Figure 3). It was found that immediately inland from the center of the bay, surface wind divergence was found. This wind divergence negated the development of the sea breeze in this region by producing downward vertical velocities. It was also found that convergence was increased immediately inland of the east and west sides of the mouth of the bay forming two separate bay breezes, where the coastline curvature is convex. As the simulation day progressed, a sea breeze developed inland of the center of the bay and joined with the two breezes on either side of the bay. As the simulation continued, the combined sea breeze took on an orientation parallel to the coast, regardless of the curvature of the bay.

These studies hold important significant along the coast of New Jersey due to presence of numerous barrier islands, bays, and estuaries in the coastal zone. A simulation using the WRF model showing these irregularities along the coast of New Jersey will be presented in Section 4.3.

### **1.5: Offshore Characteristics of the Sea Breeze**

The sea breeze does not only exist along the coast, but also well offshore. As warm air rises over the land, the resultant pressure gradient results in a flow of air from over the ocean to the land. As the sea breeze circulation moves farther onshore, the area

over the ocean from which air moves onshore expands. This sea breeze feeder area expands offshore resulting in a larger region of onshore directed winds. At the farthest offshore extent of this sea breeze feeder exists a region of light, divergent winds. The wind further offshore from this divergence zone returns to the direction and magnitude of the overall surface synoptic flow. Observational studies of this phenomenon have been limited due to a lack of offshore observation sites. Remote sensing and numerical modeling has provided new opportunities to study this poorly understood aspect of the sea breeze circulation.

Prior to the advent of high-resolution numerical modeling or advanced remote sensing technologies, Angell and Pack (1965) found evidence by tracking tetroons released along the coast that the sea breeze front existed for some time offshore prior to breaching the shoreline. As technology has advanced, several methods have been developed to study the offshore portion of the sea breeze circulation.

Banta et al. (1993) used a Doppler lidar to investigate the offshore extension of the sea breeze cell along the coast of Monterey Bay. They defined the offshore extent of the sea breeze to be the point where an onshore component of the wind ceased. It was found that the “offshore sea breeze” began rather close to shore, between 1 and 10 km, and then propagated farther offshore as the event progressed. Interestingly, the speed at which the offshore sea breeze front moved offshore increased throughout the afternoon, to as much as 2 m/s between 1800 and 1900 GMT.

Modern day study of the sea breeze has included investigations of the completed circuit of the sea breeze circulation. Originally, theory suggested that the offshore

extent of the sea breeze circulation would be approximately equal to that of the inland penetration.

Zhong and Takle (1993) and Stephan et al. (1999) found that the sea breeze circulation cell extends offshore about twice the inland penetration distance. Additionally, Finkle et al. (1995) and Chiba et al. (1999) found that the seaward extent of the sea breeze circulation cell contained a feeder flow and subsidence over the ocean. However, the results of the Chiba et al. (1999) study contradicted those of Zhong and Takle (1993) in that the inland extent of the sea breeze was measured to be 25 km while the offshore extent of the circulation extends to about 10 km offshore. They found that offshore subsidence was localized near the coastline.

Simpson (1994) examined a Gemini XI photograph of India taken in 1966 (Figure 5). The photograph distinctly shows the sea breeze front along both the eastern and western coasts, as well as a large area offshore, which is cloud free. This cloud free zone indicates that the entire width of the sea breeze circulation cell is roughly 100 to 120 km on this day, most of which is centered offshore. Fett and Tag (1984) found a similar coastal cloud-free zone offshore of Florida corresponding to the offshore sea breeze (Figure 4). Sun glint effect shown in satellite imagery implies calm seas where large-scale wind and sea breeze wind meet. Somewhere in between the onshore and offshore sea breeze front must exist a divergence zone.

These studies hold important significant along the coast of New Jersey due to heavy marine traffic in the offshore waters. A simulation using the WRF model showing the offshore extent of the sea breeze circulation offshore in relation to the onshore penetration of the sea breeze will be presented in Section 4.5.

### **1.6: Coastal Upwelling along the New Jersey Coast**

It has been established that the primary driving factor in the development of the sea breeze circulation is the land-sea temperature differential. Along the New Jersey Coast, as with many other coastlines, there can be large variations in the sea temperature over just a few kilometers (Glenn et al., 2004). Along the New Jersey Coast, coastal upwelling is driven by a persistent south to southwesterly wind regime which through Ekman pumping pushes solar heated surface water offshore which is subsequently replaced by colder bottom water (Glenn et al, 1996). The nearshore temperature variations can be seen each summer at Rutgers University's Long-term Ecological Observatory at 15 meters depth (LEO-15) (Glenn et al., 2000) in conductivity-temperature-depth (CTD) measurements, as well as the through the use of Advanced Very-High Resolution (AVHRR) polar orbiting satellite imagery (Schofield et al., 2002). Evidence suggests that coastal upwelling along the coast occurs in several distinct upwelling centers along the coast. Though the use of a theoretical wind driven coastal ocean model, Song et. al. (2001) discovered that these variations along the coast are driven to a significant degree by varying bathymetric features which are present on the continental shelf within a few kilometers of the shoreline (Figure 6), particularly in the regions of Barnegat Inlet, the Mullica River Estuary, and Townsend-Hereford Inlet (Glenn et al., 1996).

Additionally, strong stratification is possible during the summer months. The surface to bottom temperature gradient is as much as 10°C, separated by a strong thermocline (Chant, 2001). An upwelling favorable wind can easily bring the

thermocline to the surface in a matter of days, especially in the typical upwelling centers already mentioned (Glenn et al., 1996).

Within these coastal upwelling centers, SST readings can vary by more than 10°C over several kilometers in both the cross-shelf and along-shelf directions. The impact of these large ranging mesoscale variations in coastal ocean temperature have not been fully examined in regards to sea breeze development and behavior. However, localized enhancements in sea breeze frontal strength and cooler temperatures along coastal communities have been shown through observations of Doppler radar reflectivity (Section 4.4).

Classic Ekman theory indicates that the optimal wind direction for the development of upwelling along a coastline would be one that was parallel to the shoreline, with no cross-shore component. The coastline of New Jersey is oriented from southwest to northeast from Cape May to the southern portion of Long Beach Island, then south to north up to Sandy Hook. A study by Inghram and Eberwine (1984) found that along the New Jersey coast south of Tuckerton, a wind coming from 250 degrees was optimal for the appearance of colder bottom water reaching the surface at the National Ocean Service Tide Station at the Atlantic City Pier. Best fit linear analyses from their study indicate that changes in upwelling/downwelling wind strengths produce slightly more temperature variability in July and August, than during the month of June. This is attributed to less temperature difference between the surface and the bottom water during the month of June than during the remainder of the summer months. A similar study by Hicks and Miller (1980) found that surf temperature decreases of greater than 9.3° C occurred along the New Jersey coast north

of Long Beach Island after two days of persistent south to southwest winds during the months of July, August, and September. While these temperature variations may only exist for just a few tens of kilometers in the cross-shore direction, observational evidence in Section 4.4 will show that these upwelling centers can play an important role in the onshore propagation of the sea breeze front.

One of the few studies to examine the sea breeze-coastal upwelling relationship was performed by Clancy et al. (1979) using a coupled four-layer atmospheric, two layer oceanic numerical model with homogeneous terrain and coastline. While the coupled model was simplistic, the results are quite important to this discussion. Resulting from Coriolis deflection, surface winds generally become more along-shore as the sea breeze event progresses (Simpson, 1996). This may enhance the effect from this wind stress on Ekman pumping along the coast. It was found that as the sea breeze event progresses, along-shore winds from the sea breeze added slightly to coastal upwelling by forcing more surface water offshore. The colder upwelled surface water in the nearshore ocean resulted in a stronger and shallower sea breeze. This stronger sea breeze resulted in a better-defined sea breeze front that penetrated inland twice that of a non-upwelling enhanced sea breeze front, as well as propagating inland more rapidly.

Furthermore, Clancy et al. (1979) discovered that the sea breeze is affected by coastal upwelling, and upwelling is enhanced by the sea breeze. The colder nature of the marine air in the coastal zone over several days will act to produce more stable conditions, thus resulting in a net reduction in the magnitude of the along-shore sea breeze wind by reducing the nearshore temperature gradient, resulting in very little

additional Ekman transport of surface water offshore, and therefore very little variation in SST would be expected during a single sea breeze event.

## **CHAPTER 2**

### **Sea-Breeze Observations: Identification and Characteristics**

The Glossary of Meteorology (Huschke, 1959) defines the sea breeze as:

“A coastal local wind that blows from sea to land, caused by the temperature difference when the sea surface is cooler than the adjacent land. Therefore, it usually blows on relatively calm, sunny, summer days; and alternates with the oppositely directed, usually weaker, nighttime land breeze. As the sea breeze regime progresses, the wind develops a component parallel to the coast, owing to the Coriolis deflection.”

#### **2.1: Surface Observational Evidence**

There are several methods by which to detect the presence of a sea breeze. Prior to modern times, the primary method in which to study the sea breeze was through in-situ surface observations. The sea breeze front is similar to a synoptic-scale cold front in that it is usually characterized by a wind shift. In a sea breeze, this wind shift is greater than 30 degrees in one hour (Bourne et al., 1998), generally from an offshore component to an onshore component, accompanied by an increase in horizontal wind speed. This results in a decrease in surface temperature as cooler marine air is advected onshore. Dry, sinking air is generally found immediately inland of the sea breeze front, then moist marine air is advected onshore by the onshore wind. As a result, relative humidity decreases and then rapidly increases as the sea breeze front passes (Simpson,

1994). Figures 7-a, 7-b, and 7-c show the effects of a passing sea breeze at Tuckerton for wind direction, wind speed, and relative humidity.

Onshore surface convergence leads to increased upward vertical motion as the sea breeze front breaches the shoreline. As this air is forced upward to the convective condensation level (CCL), a thin line of cumulus clouds forms, denoting the head of the sea breeze front. The head of the sea breeze occurs at the highest point along the sea breeze front and is the location at which the cool, dense air from the sea breeze meets the opposing synoptic wind flow. The opposing wind flow moves over the head of the sea breeze forming Kelvin-Helmholtz billows through which the marine and continental air are mixed (Simpson, 1994; Simpson, 1997). This mixing frequently results in the formation of cumulus clouds along the entire length of the sea breeze front. With the advent of remote sensing technologies, the head of the sea breeze front can be seen on the visible satellite imagery and detected by Doppler radar. As a result, determination of the maximum inland penetration of the sea breeze has become possible.

## **2.2: Remote Sensing of the Sea Breeze and Coastal Upwelling**

### **2.2.1: Weather Surveillance Radar - 88D Doppler Radar**

The most accurate method to identify the sea breeze front is through imagery of radar reflectivity from the National Weather Service (NWS) Weather Surveillance Radar (WSR-88D) network. WSR-88D has the capability of being utilized in two different modes determined by atmospheric conditions. Radar reflectivity is measured in decibels (dBZ) using a logarithmic scale to measure the amount of transmitted power

returned to the radar. As precipitation moves into the range of the radar beam, the radar is automatically set to precipitation mode, which detects reflectivity in the range of 5 dBZ to 75 dBZ or greater. When precipitation is absent or extremely light, the radar is operated in clear-air mode. Clear-air mode can detect reflectivity in the range of -28 dBZ to 28 dBZ. The more sensitive clear-air mode is best to detect aggregations of birds and insects, as well as sharp thermal and density discontinuities in the lowest levels of the troposphere.

When the WSR-88D is operated in clear-air mode, the volume scan is performed through a smaller range of elevation angles. The antenna can thus be rotated more slowly and still complete a volume scan in a comparable length of time. Clear-air mode volume scans complete in 10 minutes, while precipitation mode volume scans complete in 6 minutes, allowing for more frequent, yet less sensitive, updates during active weather. This slower, clear-air mode, results in more power per unit volume being transmitted over a similar amount of time, which enables a finer resolution (Crum and Alberty, 1993). The higher resolution obtained from clear-air mode volume scans allows for a visual representation of the sea breeze front in near real-time (Figure 8a). Figure 8b shows a hand-drawn analysis of the sea breeze front along the coast and the Delaware Bay breeze extending southeast to northwest across Cape May County.

The sea breeze front frequently takes on the appearance of a narrow band of higher reflectivity, often less than 3 kilometers wide. This thin line of reflectivity generally becomes more noticeable after the sea breeze front has moved several kilometers onshore. As the front continues inland the reflectivity signature begins to decrease and becomes narrower, likely due to weakened convection during the evening

hours as solar insolation decreases (Atkins and Wakimoto, 1997). This line frequently takes on a scalloped shape, which is the result of mesoscale variations in the head of the sea breeze front.

It has been well established in literature that one effective means of observing the sea breeze front is from the utilization of radar echoes, however the exact cause of this fine line of higher reflectivity associated with the sea breeze front is still under debate. Atlas (1960) found that stable elevated layers commonly contained transition zones where strong gradients of wind, humidity, and temperature, which are often found in the transition from sea breeze circulation to the base of the return current were found. These transition zones had a strong correlation to higher reflectivity clear-air echoes. It was concluded that gradients in the refractive index are highly correlated to the appearance of clear-air echoes at the sea breeze front. At the onset of the formation of a sea breeze, an air mass boundary forms when there is an increase in vapor pressure and a decrease in temperature, both resulting in an increase in the refractive index. In addition, turbulence and wind shear at the interface between the sea breeze circulation and the synoptic flow can act to enhance the refractive index. This occurs both at the surface and at the interface of the sea breeze circulation cell and the return current.

Eastwood and Rider (1961) conducted a study along the coast of the English Channel in southeastern England to explain the appearance of the sea breeze front on radar. The authors were able to correlate the motion of a line of higher reflectivity in the radar echoes to variations in the wind direction and speed, as well as relative humidity.

The authors found that birds are often present in the vicinity of the sea breeze front as they can easily soar in the updrafts associated with the rising motion along the head of the sea breeze front. Additionally, the lower tropospheric wind convergence focused at the sea breeze front has been shown to lead to a convergence of insects, which in turn may explain the higher density of birds in the area of the sea breeze front (Simpson, 1964; Pedgeley, 1990; Achtemeier, 1991, Russell and Wilson, 2001).

Additional evidence has been shown from a small study conducted in Israel. Meteorological observations have often identified the presence of a sea breeze frontal passage from the Mediterranean Sea. However, they were very rarely associated with a line of higher reflectivity on Doppler radar due to dry subsidence aloft which often negates the density of birds and insects at an elevation where the radar can see them. However, during times of high honey buzzard migration, distinct lines of high reflectivity have been shown to exist, which mimic the passage of the sea breeze front in surface meteorological observations (Alpert et al., 2000).

### **2.2.2: AVHRR SST Imagery**

The Advanced Very High Resolution Radiometer (AVHRR) has been an operational component on NOAA polar orbiting satellites for more than two decades. While more sophisticated and higher-resolution sensor datasets are presently available, the data acquired are of sufficient resolution to determine the sea surface temperature in coastal regions and to identify regions of coastal upwelling. Presently, there are four operational AVHRR satellites, each orbiting at an altitude of 850 kilometers. Polar orbiting satellites are designed to complete 14 orbits daily, thereby creating global

coverage twice daily, on ascending and descending passes, with a resolution of 1.1 kilometers at nadir (Sabins, 1987). The satellites have five bands, each focusing on different wavelengths ranging from visible to thermal. Sea surface temperature can be derived from the AVHRR dataset from channels 4 and 5. This data can then be plotted to obtain 2-dimensional images of sea surface temperature. Rutgers University's Institute of Marine and Coastal Sciences maintains a SeaSpace satellite tracking system where AVHRR data is collected, converted to SST, earth located, and plotted (Figure 9). The data obtained from the satellite is level 1 B geo-corrected data, with a latitude and longitude assigned for each pixel location in the AVHRR metadata. The data is plotted in 2-dimensions using Terascan's auto-navigation software supplied by SeaSpace Corporation, Inc.

### **2.2.3: Visible Satellite Imagery from AVHRR and MODIS**

Visible cloud products can be derived from the AVHRR dataset by the utilization of channel 1. The raw visible satellite imagery is useful in identifying the formation of the thin cloud band that commonly occurs along the head of the sea breeze front (Figure 10).

To obtain a detailed view of the sea breeze front, up to and including the scalloped nature of the clouds within the front satellite imagery, considerable resolution is required. The Moderate Resolution Imaging Spectroradiometer (MODIS) satellite can provide imagery at a spatial resolution of up to 250 meters at nadir. Figure 11 is an example of the thin line of cumulus clouds along the sea breeze front taken by the MODIS instrument on the Terra satellite. The sea breeze front is established several

kilometers inland, extending from Sandy Hook to northern Cape May County. Clouds extending west through northern Cape May County are the result of the Delaware Bay Breeze. Significant convergence can be noted to the build up of cumulus cloud activity and brighter cloud tops at the intersection of the sea breeze and the bay breeze.

Additional sea breezes can be seen in this image along the coast of the Delmarva Peninsula, Long Island, Connecticut, and eastern facing shores of Massachusetts, New Hampshire, and Maine.

## **CHAPTER 3**

### **Sea Breeze Modeling**

#### **3.1: Modeling Studies of Sea-Breeze – Upwelling Behavior**

The vast majority of studies involving numerical modeling of the sea breeze have focused on the effect of the overall synoptic flow on the development and inland penetration of the sea breeze (Section 1.3). However, very few have investigated the impact of the coastal ocean on the sea breeze. This is quite interesting due to the fact that the sea breeze is to the first order a result of the land-sea temperature gradient, and in particular the response to the gradient of temperature in the first ten to twenty kilometers of the coastline in the along-shore direction. It is in this critical region of the coastal ocean where the variability of sea surface temperature is the greatest during the warmer months of the year.

Both sea breezes and coastal upwelling occur on the mesoscale level; thus it is necessary to use a mesoscale model to examine the relationship between the two. Clancy et al. (1979) used a simple coupled oceanic – atmospheric model to investigate the interaction between the two phenomena. The results of the study indicated that upwelling did increase the strength of the sea breeze, and in turn the sea breeze increased the magnitude of coastal upwelling. The coupled relationship was found to be strongest in enhancing the sea breeze and to a lesser extent enhancing the magnitude of coastal upwelling. This is due to the much longer time scales necessary in order to effect change in the magnitude of coastal upwelling. Very little variation in SST should be expected over the course of a single sea breeze event. Therefore, it is expected that

the modeling results of the study here will be biased only slightly using prescribed SST as a bottom boundary condition for an entire day of simulation.

### **3.2: Weather Research Forecast Model**

The Weather Research and Forecast (WRF) Model was chosen for these studies due to the flexibility of the model for both research and operational forecasting applications, particularly in the mesoscale range of 1-10 kilometers for the horizontal spatial resolution. The model was introduced as a community model in 2000 by the National Center for Atmospheric Research (NCAR), the National Center for Environmental Prediction (NCEP), the Forecast Systems Laboratory (FSL), the U.S. Air Force Weather Agency (AFWA), and the University of Oklahoma Center for the Analysis and Prediction of Storms (CAPS). Version 2.0 of the WRF code was released in the Spring of 2004 and included the ability to perform multiple domains nests, and an emphasis on an Eulerian mass coordinate. The model code utilizes an Arakawa-C grid in the horizontal, as well as a third-order Runge-Kutta technique for time-steps (<http://www.wrf-model.org>).

These sets of experiments were run with WRF at a horizontal resolution of 2 kilometers, with a time-step of 12 seconds. Thirty-one staggered vertical levels were used in the model runs, of which eighteen vertical levels exist in the lower 1 km of the atmosphere to provide a high resolution view of the vertical nature of the sea breeze circulation. A high spatial resolution of 2 kilometers was chosen to best view the dynamics of the sea breeze phenomenon. The model was run for 48 hours of simulated

time using the 1200 GMT ETA model from NCEP at a 22 km spatial resolution for boundary forcing and initial conditions.

The WRF model output at 2 km spatial resolution was converted from WRF-binary format to Grid Analysis and Display System (GrADS) control file format using the wrf2ctl program from NCAR (<http://www.wrf-model.org>). Model output images were then processed at 1 hour time increments using GrADS. Two-dimensional maps of 2 m temperature, wind speed, wind direction, relative humidity, and vertical velocity at 500 meters were produced for each hour of simulation time. Two-dimensional vertical cross sections of temperature, wind direction, wind speed, and relative humidity were also produced for each hour of simulation time. Wind direction vectors in the output images show each third vector for ease of viewing; therefore vector spacing shown is every 6 km.

A spatial resolution of 2 km was chosen in order to achieve a solution of the mesoscale nature of the sea breeze circulation cell. A study by Colby (2004) on the use of high resolution mesoscale modeling found that running a mesoscale model at a resolution of 4 kilometers or greater can lead to a valuable understanding of the nature and structure of the sea breeze. Less detailed models with resolutions of less than 12 km may be more useful for real-time operational forecasting of such phenomenon since they can generate a sea breeze with less computational time and overall error, with better resolution of the larger synoptic-scale features. However, they are not able to fully resolve the sea breeze as in the higher resolution experiments. It should be noted that in this study of the New England sea breeze, the sea breeze in the lower resolution

simulations did not penetrate more than 20 km inland, whereas significant penetration was seen in higher resolution simulations.

Nevertheless, as a result of this study, a significantly fine resolution is necessary to resolve both the sea breeze circulation in the horizontal and the vertical, but also to investigate the impact of varying nearshore SST on the inland penetration and development of the sea breeze circulation. For example, when initial simulations of the cases presented in this thesis were run at a spatial resolution of 4 km, inland penetration of the sea breeze was diminished and the structure of the sea breeze front was poorly defined. Therefore a spatial resolution of 2 km was chosen to provide optimal detail of the sea breeze circulation while still maintaining a realistic representation of the sea breeze as compared to radar.

### **3.3: AVHRR Satellite SST**

For the most accurate initial conditions, it was necessary to use SST data that was of a higher-resolution than was available in the ETA model boundary conditions (30 km). The ETA model utilizes the Real-Time Global Sea Surface Temperature Analysis (RTG\_SST) developed by NCEP's Ocean Modeling Branch (OMB). This dataset utilizes GOES satellite derived SST analyses and averages them into data bins with horizontal spatial resolution of 0.5 degrees. Summertime coastal upwelling often occurs on spatial scales of tens of kilometers, thus the RTG\_SST dataset would unlikely provide any useful definition of either the magnitude or the extent of offshore coastal upwelling.

A far superior SST analysis in terms of horizontal resolution is supplied by NOAA/NASA AVHRR Ocean Pathfinder Sea Surface Temperature datasets, which are made available by the Physical Oceanography Distributed Active Archive Center (PO.DAAC) at NASA's Jet Propulsion Laboratory (JPL) (<http://podaac.jpl.nasa.gov>). Version 5.0 of the dataset contains daily SST data for the Mid-Atlantic Bight Region at a spatial resolution of 4 kilometers.

The dataset is in HDF format, requiring a conversion to WRF-readable format prior to ingestion into the model. The conversion was completed by the utilization of HDF-tools developed by The National Center for Supercomputing Applications (NCSA) at the University of Illinois at Urbana-Champaign (UIUC) and then encoding the output into a GRIB file, which is the model output data format of choice at NCEP and the preferred file format for ingestion into the WRF model. The GRIB file was encoded using NCEP's GRIB encoder software written in FORTRAN. Alterations of the SST in a number of the simulations described later were performed between extracting the data from HDF format and encoding the GRIB file.

## **CHAPTER 4**

### **The New Jersey Sea-Breeze**

#### **4.1: Prior Studies of the New Jersey Sea Breeze**

The New Jersey sea breeze phenomenon is poorly understood since only a handful of studies have been undertaken to attempt to explain the very nuances that makes it unique. These studies (Kwiatkowski, 1999; Frizzola and Fisher, 1963), discussed in Section 1.3 of this thesis, focused on the generation and inland penetration of the sea breeze in the presence of offshore directed synoptic flow. Prior studies of the sea breeze have focused on simple numerical modeling experiments, or on observationally based data from other parts of the world. Very little research has been done on the small scale features which make the New Jersey sea breeze unique.

This chapter will discuss the more intricate details of the New Jersey sea breeze phenomenon. Section 4.2 will discuss the frequency at which sea breezes occur along the coast, highlighting the importance of why small-scale variations in the sea breeze are important and must be more thoroughly studied. Section 4.3 will discuss the small-scale variations which occur with a typical sea breeze, which are mainly due to variations in the coastline configuration (McPherson, 1970) and the presence of barrier islands (Mahrer and Segal, 1985). Section 4.4 will discuss the properties and behavior of upwelling enhanced sea breezes. Section 4.5 will highlight the behavior of the sea breeze offshore, including evidence from the literature and WRF model runs conducted

for this study showing an area of divergence offshore indicating the offshore extent of the sea breeze.

#### **4.2: New Jersey Sea Breeze Climatology**

The sea breeze is an important mesoscale feature along the New Jersey shore mainly due to the fact that occurs so frequently. A climatology compiled for this thesis of sea breeze fronts passing Tuckerton was performed using historical data from 1996 to 2002. The method used was that of Bourne et al. (1998) who developed a method for identifying sea breeze frontal passages along the Swedish coast using observational data. Upper level winds for this climatology are taken from NCAR reanalysis data. During this time, 211 sea breeze fronts were seen to have reached and passed the site according to continuous observational data (Figure 12). The data indicate that sea breeze formation and penetration onshore occurred in every month except February during this six year period. This highlights the importance of the sea breeze to the climatology of the coastal zone even during the cooler months of the year.

Sea surface temperature off the New Jersey coastline is quite variable during the summer due to upwelling, but the extent of coastal upwelling can vary from year to year (Figure 13) due to the overall position of the subtropical Bermuda High offshore as well as the frequency of storm systems moving through the coastal waters and the severity of the previous winter. The Bermuda High often becomes semi-permanent during the summer months with a persistent southwest wind which pushes the surface water offshore. A severe winter produces strong mixing events which mixes the nearshore waters enough to degrade the two layer ocean system offshore, resulting in less upwelling events. A study of coastal upwelling performed offshore Tuckerton (Glenn

et al., 2004) found that seasonal air temperature variation is the primary signal in the sea surface temperature off of the coast of New Jersey (Figure 14) during the summer. Coastal upwelling was found to be the secondary signal. Additionally, the authors found that the most variance in offshore SST occurred during the months of July and August, further supporting the findings of Inghram and Eberwine (1984).

As this indicates, the sea breeze – coastal upwelling relationship can vary on time scales from as little as days to weeks to as long as months to years. An example of this on a small temporal scale is that the sea breeze can have day to day variations in the extent of inland penetration due to several factors. Figures 15, 16, and 17 show adaptations taken from NWS WSR-88D reflectivity imagery of consecutive sea breeze events on June 29, June 30, and July 1, 2002. These images show the maximum extent of inland penetration for the day according to reflectivity measurements. On the synoptic level, June 29 had northwesterly winds between 5 and 6 m/s at the 850 mb level, while June 30 and July 1 had offshore northerly winds at 850 mb less than 5 m/s. These three days represent the end of a period of coastal upwelling along the New Jersey coast. The most significant upwelling signature occurred on June 29, with SST between 17.5° and 19°C in a large area nearshore and 22°C or greater offshore and along the coast north of Asbury Park. On June 30 the SST was between 19.5° and 21° in a smaller area nearshore and 22°C or greater elsewhere. By July 1, the area of upwelling was confined to the immediate shoreline, with temperatures of 19.5° to 21°C and elsewhere greater than 22°C.

### **4.3: Typical New Jersey Sea Breeze**

The New Jersey sea breeze is unique for no other reason than the irregularities along the majority of the coastline. Numerous small inlets and estuaries, barrier islands, and the influence of the Delaware and Raritan Bay breezes can create irregularities not only in the shape of the sea breeze front, but also on the overall sea breeze dynamics. Idealized numerical modeling studies are noted in the literature describing the effect of coastline curvature and barrier islands on the ocean-side sea breeze.

The results of the McPherson (1970) study indicated that irregularities in the coastline configuration could result in variations in the shape of the sea breeze front. A WRF case study simulation was performed for a sea breeze event on April 16, 2004 to show this effect of the coastline configuration on the variability of the shape of the sea breeze front. Figures 18 and 19 show the results of a WRF model run for a sea breeze occurring on April 16, 2004. Figure 18 shows the output from the WRF model at 1800 GMT. At this time, the sea breeze has formed along the coastline south of Sandy Hook. The sea breeze front develops distinct lobes around Great Egg Harbor Bay and Great Bay which distorts the shape of the sea breeze front from a straight parallel line along the coast. Figure 19 shows the progression of the sea breeze front by 2000 GMT when the perturbations in the shape of the sea breeze front had diminished, and the sea breeze front was more generally parallel to the entire coast.

Mahrer and Segal (1985) simulated the effects of the shape and size of islands on the effect of the sea breeze and found that circular islands contributed more towards a stronger sea breeze circulation than elongated islands. This has important ramifications for the New Jersey sea breeze. The barrier islands north of Long Beach

Island are elongated, generally less than 1 km wide. South of Long Beach Island there are a number of smaller islands, while still somewhat elongated in nature, have a more circular geometry. This would indicate that the islands from Atlantic City south would experience increased upward vertical velocities and subsequently stronger horizontal wind speeds, especially at the onset of the sea breeze event.

Additionally, New Jersey's barrier islands are tourist magnets during the summer months. These areas over the past few decades have transformed the once quiet shoreline into a narrow stretch of urban environs the entire length of the coast. A study by Yoshikado (1990) found that the sea breeze frequently increased in intensity immediately following passage through the coastal urban complex of Tokyo. While small coastal cities such as Atlantic City would not have the same convective characteristics of Tokyo, Atlantic City can create a "mini urban heat island" that would be enough to intensify the sea breeze front just west of major tourist locations along the coast. The low-level temperature gradient may be enough to favor the development of a "minor sea breeze" in the morning hours prior to the development of the "major sea breeze". Banta et al. (1993) described the existence of a transient precursor to the primary sea breeze during a study of the Monterey Bay sea breeze.

Recall the results of the McPherson (1970) study that indicated a convex coastline is sea breeze favorable. This is important when considering the variations occurring in the shape of the sea breeze front, because the overall shape of the New Jersey shoreline is generally convex (Figure 20). The northern portion of the New Jersey shoreline combines with Long Island to form a large concave coastline in the vicinity of New York Harbor. At the southern edge of the harbor is Sandy Hook, which

according to the curvature argument would be a favorable location for sea breeze development. This is confirmed by the frequency of the sea breeze front in the area shown by radar reflectivities. The coastline is generally convex from Sandy Hook south to Atlantic City. The sea breeze is strongest and penetrates the furthest inland in this area on light to moderate offshore synoptic flow days. South of Atlantic City, the coastline takes on a more concave shape. Very rarely does the sea breeze front extend much farther south than Ocean City and Great Egg Harbor Bay. While the concave nature of this bay and the general coastline would likely retard the formation of the sea breeze area, an additional factor of considerable interest to this area is the Delaware Bay Breeze.

The Delaware Bay Breeze is a phenomenon that has almost been completely neglected in scientific studies, and the paucity of observational data in the region precludes verification of its behavior and development. However, mesoscale model simulations show that the bay breeze propagates through most of Cape May, Cumberland, and Salem Counties producing a general southwest wind flow initially, which shifts to a west-southwest wind later due to the Coriolis deflection.

The bay breeze intersects with the ocean-side sea breeze over northeastern Cape May County in the vicinity of Great Egg Harbor Bay, resulting in large reflectivity values and strong upward vertical velocities. It is in this area of strong low-level convergence that cloud tops are highest (Figure 20) and that thunderstorms occasionally form.

Radar reflectivity indicates that the north to south oriented sea breeze front commonly rides along the boundary of the west to east oriented bay breeze front. As

the bay breeze penetrates farther north into southern New Jersey, the southern most point of radar reflectivity of the primary sea breeze appears to move north as well.

Figure 21 (a-c) shows this situation quite well as the bay breeze can be seen pushing the southern most part of the sea breeze front farther north, and perhaps accelerating this part of the sea breeze front inland more rapidly than the northern portion of the front.

This case shows particularly well that the sea breeze need not take on the shape of the coastline, especially when driven by external forces such as the bay breeze.

Additionally, this case shows the effects of divergence in and around Raritan Bay.

There is a distinct thin line of reflectivity which develops near Sandy Hook and moves along the Raritan Bay shoreline in a clock-wise manner. However, at no time does a bay breeze circulation appear to develop separate from the primary sea breeze.

While the Raritan Bay breeze has been shown to occur in reflectivity data, it only seems to occur on very weak synoptic flow days when the primary sea breeze penetrates greater than 30 km. This analysis seems to confirm the findings of Kwiatkowski (1999) in regards to a rare and nearly imperceptible Raritan Bay breeze. Kwiatkowski (1999)

however is somewhat incorrect that the primary sea breeze takes on a straight-line shape. While the sea breeze may take on a straight-line shape at times, it is shown here that it might take on a rather irregular shape (Figures 18 and 19), usually coinciding when additional forcing from the Delaware Bay breeze and when the effects from larger bays are considered. Another important outside forcing to consider is the effect of coastal upwelling.

#### **4.4: Upwelling Enhanced Sea Breeze**

While local coastline curvature and geometry may play an important role in the dynamics and structure of the sea breeze circulation at the immediate coast, the synoptic flow and coastal upwelling seem to play the biggest role farther inland. Assuming a suitable wind flow aloft, variation in the structure and the extent of inland penetration of the sea breeze is hypothesized to be due to the temperature distribution in the coastal zone.

Figures 22 and 23 show a strong far-penetrating sea breeze on June 4, 1994 and the sea surface temperature from the AVHRR satellite. The sea breeze penetrates well past Philadelphia just prior to dissipation. The SST from June 5, 1994 indicates coastal upwelling occurring along the entire coastline. Nearshore SSTs are approximately 14° to 15°C while offshore SST are 17°C or greater. Synoptic winds at 850 mb were from the northwest at 8 m/s.

While any degree of coastal upwelling may enhance the strength of the sea breeze, it is those localized upwelling events that are the focus of this study. A number of sea breezes have been recorded where the sea breeze front moved significantly farther inland in an area adjacent to a coastal upwelling center.

Figures 24 and 25 show the image adapted from radar reflectivity and Sea Surface Temperature for June 26, 2001. These figures show a significant penetration in Southern New Jersey directly northwest of the small coastal upwelling center located near Tuckerton. While SST is quite warm, there is an approximately 3°C temperature differential between the upwelling center and areas a few kilometers offshore and along the remainder of the coastline.

June 23, 2000 is a case of upwelling localized along the coast of Long Beach Island (Figure 26) and an associated sea breeze (Figure 27). SSTs for this event were 15° to 17°C nearshore from Long Beach Island to Asbury Park, while elsewhere SSTs ranged from 18° to 21°C. The radar reflectivity indicates a sea breeze that was moving towards the southwest. The sea breeze attains maximum penetration west of Barnegat Light to Brant Beach, just west of the primary upwelling center (Figure 26). The sea breeze did not develop south of Atlantic City or north of Asbury Park where upwelling was not occurring.

#### **4.5: The Offshore New Jersey Sea Breeze**

Little is currently known about the offshore characteristics of the sea breeze circulation. As referenced in Section 1.5, numerical modeling and some observational data has suggested that the sea breeze circulation extends offshore roughly two to three times farther than the distance of the sea breeze front onshore to the coastline. It is in this region where the sea breeze feeder flow exists resulting in a surface flow directed onshore. Additionally, surface wind divergence and associated subsidence just seaward of this feeder flow is suggested by Simpson (1994) and Fett and Tag (1984).

This phenomenon appears to occur offshore the New Jersey coast as well. NWS Doppler radar reflectivity has indicated the presence of an “offshore sea breeze front” on a number of occasions. SST imagery from July 25, 2003 indicates coastal upwelling occurring from Asbury Park down to Cape May (Figure 28). Radar reflectivity (Figure 29) indicates a parallel sea breeze along the coast on July 26, however also shown is the apparent offshore extent of the sea breeze. This offshore sea breeze appears to

correspond quite well to the offshore SST front where SST ranges from 16° to 17°C nearshore to 23°C or greater just east of the oceanic temperature front. A similar appearance of this offshore sea breeze occurred on August 2, 2001 (Figure 30), however the SST analysis (Figure 31) shows little variation in ocean temperature. While no observational data exists to prove that the thin lines of reflectivity indicated on these days is the offshore extent of the sea breeze circulation, the lines of reflectivity do appear to mirror the shape of the inland sea breeze front, and are situated in a position roughly two to three times farther offshore than the distance the sea breeze has penetrated onshore in both cases. To investigate this radar evidence of the apparent offshore extent of the sea breeze circulation cell, a modeling case study of a sea breeze which occurred on April 16, 2004 was conducted.

The simulation of the sea breeze event which occurred on April 16, 2004 shows a long band of calm to near calm winds several kilometers offshore (Figure 32 a-f). This zone of light winds represents the divergence of winds returning to the surface from the sea breeze circulation aloft. Seaward of this zone, the winds are offshore in the general direction of the surface synoptic wind. Landward of this zone, winds are onshore as this portion of the sea breeze circulation represents the sea breeze feeder flow as described by Finkle et al. (1995). A vertical cross-section from 2000 GMT along the 39.0°N line of latitude directly through this calm zone band indicates sinking air in the center of this band where wind vectors begin to diverge (Figure 32 g).

As the simulation continues, the band of light, divergent winds moves farther offshore proportional to the inland penetration of the sea breeze front, concurrent with the findings of Zhong and Takle (1993), Stephan et al. (1999), and Chiba et al. (1999).

It appears that the band of light, divergent winds occurs roughly two to three times farther offshore than the inland penetration of the sea breeze. This concurs with the findings of Stephan et al. (1999) and Chiba et al. (1999).

## **CHAPTER 5**

### **Case Studies**

#### **5.1: Introduction**

In order to test the hypothesis that varying degrees of coastal upwelling can impact the development and behavior of the New Jersey sea breeze, a suite of numerical modeling case studies have been compiled to examine the sensitivity of coastal ocean temperatures to the development and behavior of the sea breeze circulation cell. The suite of case studies focus on three base cases in which a sea breeze was known to have developed by use of NWS Mount Holly Doppler Radar located at Fort Dix located in Central Ocean County, New Jersey (Figures 33 and 34). The three base case days chosen were June 28, July 5, and July 6, 2004. The July 5 and July 6 sea breeze events were chosen due to a synoptic offshore directed wind and the presence of coastal upwelling. However, upwelling on July 5 was localized to a small area off Long Beach Island north to Asbury Park, while upwelling on July 6 was a larger scale phenomenon along the coast from Atlantic City to Point Pleasant. Winds at the 850 mb level are offshore directed generally less than 5 m/s on July 5 (Figure 35), while on July 6, 850 mb winds increase to between 7.5 and 12.5 m/s (Figure 36), thus exceeding the critical 11 m/s threshold determined by Kwiatkowski (1996) as a hindrance to sea breeze circulation development and inland penetration in the northern portion of the study area. The June 28 case is unique in this set of cases as it has a synoptic onshore directed wind throughout the day, and the embedded sea breeze lends to enhance the strength of the

onshore wind. Coastal upwelling is present along the entire coastline of New Jersey on June 28, however offshore temperatures are several degrees warmer than the offshore temperatures in the July 5 and July 6 cases. Very little difference was found between the upwelling and non-upwelling SST regimes for the onshore wind case on June 28. A decision was made to discard these results and to focus on the results from the offshore flow cases.

The sea breezes that formed on these days varied in their shape, speed of inland penetration, and final inland distance of penetration. Visual comparisons of radar imagery to WRF model predictions at 2000 GMT show that the model simulations of the actual sea breeze front are realistic in both temporal and spatial scales in all three cases. Unlike classical theory, the sea breeze front in all three cases does not move inland exactly parallel to the shoreline. The sea breeze fronts in the July 5 and July 6 cases appear to have a maximum inland penetration at the latitude of Long Beach Island, the most convex portion of the New Jersey coastline, in agreement with the findings of McPherson (1970) and the WRF model case study described in Section 4.3. Meanwhile, sea breeze penetration reaches a minimum along the shoreline of Cape May County, the southern part of a concave portion of New Jersey's Atlantic shoreline.

Section 5.2 will discuss the July 5, 2004 case study simulations, including a simulation using the actual forcing and SST for July 5, 2004, a simulation using forcing from July 5, 2004 and the SST from July 16, 2004 (a non-upwelling day), and a simulation using the forcing from July 5, 2004 and the SST from July 16, 2004 with 4 degrees Celsius added to the SST uniformly to bring the values into the climatological

maximum range of 26 to 28° C. These simulations will then be compared and contrasted and the conclusions discussed at the end of the section.

Section 5.3 will discuss the July 6, 2004 case study simulations, including a simulation using the actual forcing and SST for July 6, 2004 and a simulation using forcing from July 5, 2004 and the SST from July 16, 2004. These simulations will then be compared and contrasted and the conclusions discussed at the end of the section.

Section 5.4 will discuss a sensitivity test performed to show the impact of uniform SST of 15° and 17°C. These simulations use the forcing from July 6, 2004. These simulations will then be compared and contrasted and the conclusions discussed at the end of the section.

## **5.2: July 5, Northern Upwelling, Offshore Wind, Weak 850mb Flow**

The first in the series of case studies focuses on July 5, 2004, a day that had weak 850 mb winds from the northwest at less than 5 m/s at 1200 GMT throughout the state.

### **5.2.1: Synoptic Conditions**

The New Jersey region was under the influence of a weak Bermuda type high pressure area to the southeast. A slow moving cold front to the west was located in the Great Lakes southwestward, and the associated warm front was located in central New York state to southeastern New England. No rainfall had occurred during the past day. Overnight surface low temperatures had reached minimums of 23°C at both Philadelphia International Airport and at Atlantic City International Airport. Daytime

high temperatures at these locations reached maximums of 34°C. These observations correspond quite well to the model simulation high temperatures throughout the region. However, the surface low temperatures at Philadelphia were slightly too warm in the model simulation.

## **5.2.2: Simulations**

### **5.2.2.1: July 5, 2004 SST**

The base case model simulation has several interesting features. Throughout the simulation, the model produces a sea breeze and a Delaware Bay breeze of moderate strength and duration. The sea breeze begins around 1600 GMT and penetrates up to 30 km inland, especially in the areas to the west of the upwelling center. Farther south, where the SST (Figure 37) is still rather cool compared to the land surface, the sea breeze attains a maximum penetration of 18-20 km and begins to slowly retreat shoreward by 2200 GMT. No sea breeze is detected in southern Cape May County. Here the sea breeze has been negated by the effects of a rather strong Delaware Bay breeze which was producing west to northwest winds to the Cape May oceanfront. The bay breeze penetrates up to 24 km inland, especially in Cumberland County. The presence of the Bay Breeze is also quite evident along the Delaware coast. A Raritan Bay breeze also develops along the south facing shoreline of the bay. This bay breeze helps to increase convergence in east central Monmouth County at the intersection with the sea breeze.

Surface air temperatures on land at 1200 GMT are generally 24° to 26°C throughout interior New Jersey, except 26° to 27°C in the greater Philadelphia area. Near the coast, temperatures ranged from 21° to 24°C, except near the area of upwelling where air temperatures were 19° to 21°C. This represents an approximate 2° to 4° C land-sea temperature gradient within 10 km of the ocean.

By 1600 GMT, the approximate start time of the sea breeze in most locations, temperatures ranged from 32° to 34°C throughout interior New Jersey, and closer to the coast ranged from 31° to 33°C on the mainland, and 20° to 24°C along the barrier islands. The land-sea temperature gradient in the 10 km zone from the coast is approximately 10° to 14°C.

As the sea breeze begins to move onshore, the temperature gradient is increased, especially near Point Pleasant and again near Great Egg Harbor Bay as the surface air temperature exceeds 35°C in isolated pockets by 1800 GMT. At this point the sea breeze begins to accelerate inland, as much as 6 km in one hour. The temperature gradient across the sea breeze front exceeds 10°C across an area of 3 to 6 km.

By 2000 GMT the sea breeze has penetrated up to 18 to 24 km inland, except just southwest of Great Egg Harbor Bay. Air temperatures in the small region still exceed 35°C, while adjacent areas were under the influence of cooler marine air. The temperature gradient across the sea breeze front decreases to between 3° and 5°C in the areas west of Long Beach Island southward, although the temperature gradient remains as high as 10°C in northern areas adjacent to the upwelling center.

At 2200 GMT, the sea breeze has reached its maximum penetration distance onshore, between 24 and 30 km north of Long Beach Island, while the front has begun

to slowly retreat in Southern New Jersey, between 12 and 18 km. The temperature gradient across the front has been reduced to less than 5°C in most areas as the marine airmass, advected onshore, had been modified by the warm land surface. By 0000 GMT, the sea breeze has slowly begun to retreat shoreward as the land temperature had fallen to between 26° and 28°C and the surface temperatures on the barrier islands were a few degrees warmer than the nearby SST. Figure 38 a-d show the 2 m air temperature and wind vector plot for 2000 and 2200 GMT.

Vertical velocity is an excellent proxy for the location of the sea breeze front. Upward vertical velocities at 500 m indicate the head of the sea breeze front, as this region is indicative of strong surface convergence. Negative vertical velocities are often found just seaward of the line of positive vertical velocities associated with the sea breeze front. The sea breeze front moves inland along the coastline, matching exactly the convergence seen in the wind vector field. Figure 39 a-b show vertical velocity at 500 m for 1700 and 2200 GMT.

Variations in the vertical velocity along the front are also shown in the model results. Areas of no or little upward vertical velocity can be seen at 1600, 1700, and 1800 GMT in the areas around Great Bay and Great Egg Harbor Bay. This corresponds to the surface divergence findings along concave coastlines by McPherson (1970). Additionally, areas just to the southwest of these divergence zones have increased upward vertical velocities indicating increased surface convergence. The intersection of the sea breeze and the Delaware Bay breeze also occurs just to the southwest of Great Egg Harbor Bay. This is the location of the largest upward vertical motion at 500 m. A small area of upward vertical velocity develops south of Raritan Bay after 1700

GMT. This area remains stationary until 2200 GMT when it moves slowly south while dissipating.

Cross-sectional plots of air temperature indicate slight inversions develop as the cool, dense marine air moves onshore, however the air near the surface moderates as the day progresses, disrupting the inversion offshore. Very little difference in the vertical temperature structure is noted within the sea breeze circulation either offshore or onshore seaward of the sea breeze front. Figure 40 a-c show the vertical cross-sections of air temperature and wind vectors along 39.4°, 39.8°, and 40.2°N lines of latitude at 2000 GMT.

#### **5.2.2.2: July 16, 2004 SST**

Little difference in surface wind field and in the inland penetration of the sea breeze front is noted from the actual case. Although the difference in the 10 m wind speed indicates that slightly reduced surface convergence occurred at the front with the warmer sea surface temperatures (Figure 41). However, the 2 m surface temperatures are quite different in the marine airmass as would be expected from the change in SST.

Similar to the actual case, the sea breeze front appears in the model output at approximately 1600 GMT. At this time, the land-sea temperature gradient within 10 km of the coastline is approximately 7° to 10°C. By 1800 GMT, the temperature gradient is 7° to 10°C. Figure 42 a-d show the 2m air temperature and wind vectors for 1600 GMT and 1800 GMT.

Temperature differences inland from the sea breeze front are less than 1°C as would be expected since the only variable that was changed between the simulations is

the SST. Air temperatures near the coast are quite different. The barrier islands and the areas immediately inland from the coast have temperatures which are 3° to 6°C warmer with the warmer SST, especially along the central part of the coastline where the SST has increased the most. This occurs while the SST is warmer by 5° to 7.5°C along the central portion of the coast, and 2.5° to 5°C warmer along the southern and northern parts of the coastline.

The warmer temperatures in the marine airmass leads to decreased temperature gradients across the sea breeze front. At 1800 GMT this gradient is between 6° and 8°C across an area of 2-3 km in width. By 2000 GMT, the marine airmass has been modified by the warm land surface, shown by the temperature gradient across the front of only about 4°C.

While the wind direction vectors show very little difference in the maximum extent of sea breeze penetration, it should be remembered that the vectors were shown at 6 km increments while the simulation occurred at a 2 km resolution (Figure 43). The vertical velocity at 500 m indicates slightly more inland intrusion for the actual case than for the warmer sea surface temperature run. Cross-sectional vertical profiles indicate that the vertical extent of the sea breeze circulation ascends to near 550 m, while the return current is noted to approximately 1400 m. Very little temperature variation in the vertical is detected in the cross-sectional plots.

### **5.2.2.3: Climatological Maximum SST**

Surprisingly, the July 16, 2004 SST was unable to impart significant changes on the sea breeze circulation or on inland penetration of the sea breeze front. Can a

realistic increase in the nearshore SST affect changes in the sea breeze circulation?

This question is tested here using the climatologically maximum possible SST for the region. The maximum value of SST observed offshore at LEO-15 (Figure 14) is between 27° to 28°C. A value of 4°C was added to the July 16 sea surface temperature to bring values to within this 27° to 28°C range (Figure 44).

The result of simulating the case study with climatological extreme values led to a no sea breeze solution. The wind vector field throughout the period was devoid of perturbations from the synoptic wind flow at the surface. Inland 2 m maximum air temperatures were relatively unchanged, while temperatures along the barrier island and near coastal areas increased to between 29° and 31°C. The maximum land-sea temperature gradient within 10 km of the coastline at 1200 GMT was -2° to -3°C as the ocean surface temperature was warmer than the land surface. By 1800 GMT, the land-sea temperature gradient increased to between 5° to 6°C. By 2200 GMT, the land-sea temperature gradient had remained nearly constant. Figure 45 a-d shows air temperature and wind for 1800 and 2200 GMT.

In the vertical, very little can be evaluated in regards to the lack of a sea breeze circulation. The atmosphere remains fairly isothermal in the marine layer with regard to height along the 39.4°N, 39.8°N, and 40.2°N cross-sections offshore. The air temperature in the lower levels of the boundary layer warmed throughout the simulation due to solar heating.

### **5.2.3: Results and comparison**

The three simulations presented in the case study attest to the effectiveness of coastal upwelling along the coast to influence the sea breeze circulation in a number of ways. For a case with moderate offshore synoptic wind flow aloft there appears to be a critical land-sea temperature gradient, which is required to initiate or cancel sea breeze development. While this exact figure was not pinpointed in these simulations, it was found that a land-sea temperature gradient of 7° to 10°C within 10 kilometers of the entire coastline produced a qualitatively similar sea breeze circulation as one with a land-sea temperature gradient of nearly 14°C focused along a portion of the coastline and as much as 10°C along the remainder of the coastline. Meanwhile, a simulation with exactly similar synoptic conditions with a land-sea temperature gradient of 5° to 6°C was unable to produce a sea breeze circulation.

### **5.3: July 6, Central Upwelling, Offshore Wind, Strong 850mb Flow**

The second in the series of case study days focuses on July 6, 2004, a day that had strong 850 mb winds from the west-northwest between 7.5 and 12.5 m/s at 1200 GMT throughout the state. Minimum temperature at Philadelphia International Airport was 22°C in the observations and is fairly well documented in the model results. At Atlantic City International Airport the observation was 18°C and in the model the low temperature was approximately 3°C warmer. Maximum temperatures of 30°C at Philadelphia was 1-2°C cooler than expected from the model simulations, this appears to be due to additional observed cloud cover than was shown in the model. At Atlantic

City International Airport maximum temperatures reached 31°C in both the model and in observations.

### **5.3.1: Synoptic Conditions**

The cold front located to the west the day prior had moved through the region overnight and was located greater than 200 kilometers offshore by 1200 GMT. A broad area of high pressure (1021 mb) was located near southern Hudson Bay in Canada and was moving southeastward toward the region.

### **5.3.2: Simulations**

#### **5.3.2.1: July 6, 2004 SST**

The base case for the strong offshore wind set of experiments features the development of an Atlantic sea breeze throughout much of the coastline, except once again along Cape May county where a Delaware Bay Breeze develops creating an offshore wind throughout the length of the simulation. In this case, it appears that the Delaware Bay Breeze develops around 1600 GMT, and the sea breeze begins to develop along the Atlantic shoreline around 1800 GMT.

Interestingly, the sea breeze in this simulation appears to develop in two distinct areas of increased inland penetration, one north of the upwelling center, and the other to the south of the upwelling center. The sea breeze does not move onshore near the upwelling center until after 2100 GMT. By this time, the sea breeze throughout the areas to the south of the upwelling center had the sea breeze front retreat towards the

coast, apparently due to the additional surface winds from the Delaware Bay breeze. The retreat of the sea breeze front from northern areas was complete after 0200 GMT on July 7.

Surface air temperatures at 1200 GMT throughout inland New Jersey were between 20° and 23°C. SSTs are shown in Figure 46. Along the coast, land temperatures were coldest along the northern barrier islands near the upwelling center, between 19° and 21°C, leading to a land-sea temperature gradient of 5° to 6°C, while the remainder of the coast ranged from 20° to 22°C, with a land-sea temperature gradient of between 2° and 4°C.

Between 1600 and 1800 GMT (Figure 47 a-d), air temperatures along the barrier islands had remained nearly constant, although temperatures inland around Sandy Hook and Atlantic City had risen to as high as 29°C. The land-sea temperature gradient at this time was as high as 6° to 9°C away from the upwelling center, and as much as 10° to 15°C near the upwelling center. At about this time, the beginnings of an onshore wind had begun near Sandy Hook, along Long Beach Island, and near Atlantic City.

Between 2000 and 2300 GMT (Figure 47 e-h), land temperatures near the coast had begun to decrease due to the influence of cooler marine air. Isolated locations of 2m temperatures above 29°C were located within 10 kilometers of the coast, particularly just west of the upwelling center where the sea breeze was confined to the immediate shoreline.

The sea breeze achieves its maximum inland penetration south of Long Beach Island around 2000 GMT when it begins to be slowly pushed back offshore. At this point, the land-sea temperature gradient had been reduced to 5° to 6°C. The maximum

penetration distance was approximately 3 to 6 km. Farther north, the maximum inland penetration of the sea breeze occurs near 2300 GMT along coastal areas north of Long Beach Island. In these areas the sea breeze has pushed inland between 6 and 12 km. The land-sea temperature gradient at 2300 GMT north of LBI was between  $7^{\circ}$  and  $9^{\circ}\text{C}$ .

Vertical cross-sections through latitudes  $39.4^{\circ}$ ,  $39.8^{\circ}$ , and  $40.2^{\circ}\text{N}$  (Figure 48 a-c) indicate that the sea breeze circulation cell develops somewhat irregularly, with the surface front of the sea breeze pushing inland. However, the circulation of the sea breeze is displaced increasingly offshore with increasing height and increasing time. This is due to the strong synoptic flow aloft, and is well documented in the literature. As the sea breeze front moves onshore, the vertical extension of the sea breeze circulation is almost completely vertical, with the head of the sea breeze directly above the surface front. However, as time increases, the top of the sea breeze is pushed farther offshore, while the surface front continues to move inland several kilometers before being pushed back offshore.

The vertical extent of the sea breeze varies dramatically in this simulation along the coast from south to north. Along the  $39.4^{\circ}\text{N}$  cross-section, the sea breeze extends up to 450 m, with a rather weak return current extending up to 1250 m. Along the  $39.8^{\circ}\text{N}$  cross-section, the sea breeze extends to 350 m, with a weak return current noted up to 1250 m. Along the  $40.2^{\circ}\text{N}$  cross-section, the sea breeze extends to 350 m, with no noticeable return current.

The cold, dense air advected onshore by the sea breeze remains very close to the surface, with very little temperature change above 50 m. This creates a strong temperature inversion of greater than  $7^{\circ}\text{C}$  between the surface and 100 m. This

temperature inversion extends well offshore towards the later hours of the simulation as the warm air over land is advected offshore by the overall synoptic flow, which is within several hundred meters of the surface.

Vertical velocity along the cross-sectional lines appears to be at a maximum as the sea breeze circulation initially forms. As the synoptic flow aloft pushes the circulation farther offshore, vertical velocities become very weak or near zero. This is likely due to weakened surface convergence as the sea breeze front retreats farther offshore.

#### **5.3.2.2: July 16, 2004 SST**

At 1200 GMT land temperatures throughout most of interior New Jersey were between 22° and 24°C. Sea surface temperatures are from July 16, 2004 (Figure 41). Along the coast, temperatures at 1200 GMT were between 23° and 26°C, leading to a land-sea temperature gradient of 1° to 2°C. By 1800 GMT, inland temperatures had risen to between 28° and 31°C, while temperatures along coastal sections had risen to 27° to 30°C. This represents a nearly 4°C land-sea temperature gradient for areas south of Point Pleasant, and a 6° to 7° temperature gradient north towards Sandy Hook.

In response to these temperature gradients, the sea breeze does make some inland penetration north of Asbury Park, while to the south the sea breeze impacts along the beach before being pushed offshore by 1900 GMT. While the sea breeze does form along the north coast, it only penetrates roughly 6 km inland in only a small portion of coastal Monmouth County. Here too the sea breeze retreats offshore due to the strong

synoptic flow aloft and the diminished land-sea temperature gradient. Figure 49 a-h show air temperature and wind vector plots for 1600, 1800, 2000, and 2300 GMT.

Vertical cross-sections through latitudes  $39.4^{\circ}$ ,  $39.8^{\circ}$ , and  $40.2^{\circ}$  show the sea breeze remaining primary offshore. An additional feature shown by the cross-sectional profiles is the lack of a return current. The sea breeze circulation is not a straight up vertical entity, instead there is a west to east tilt with increasing height. This appears to be due to the strong winds aloft, and the effect increases with time as the sea breeze front retreats offshore. Vertical velocity cross-sections along the same latitudinal lines indicate that upward motion is strong as the sea breeze front initially moves onshore, but quickly diminishes as the front regresses offshore.

The vertical height of the sea breeze is also impacted by the strong offshore synoptic flow. Along the  $39.4^{\circ}\text{N}$  cross-sectional line, the sea breeze circulation reaches a maximum depth of 450 m, with very little return current indicated (Figure 50 a). Along the  $39.8^{\circ}\text{N}$  cross-section, the height of the sea breeze extends up to 400 m, with little if any return current shown (Figure 50 b). Along the  $40.2^{\circ}\text{N}$  cross-section, the sea breeze extends up to 350 m with no return current shown (Figure 50 c). Along all three cross-sectional lines, the maximum depth of the sea breeze occurs just offshore of the coastline, while the sea breeze front is onshore.

The coolest marine air remains very close to the surface, and makes very little movement onshore. As the sea breeze circulation begins to collapse due to the strong winds aloft, warmer air moves in over the marine layer, creating a weak temperature inversion throughout the lower 100 to 300 m of the boundary layer.

### **5.3.3: Results and comparison**

Although neither sea breeze in these simulations penetrates very far inland, and both retreat back towards the coast due to the strong synoptic flow, there are several noticeable differences between the two. The sea surface temperature is from 7.5° to 10°C warmer along portions of the coast from Tuckerton to Point Pleasant, and greater than 5°C warmer from Central Cape May County to Asbury Park (Figure 51 a). This makes the difference between the actual case in which the sea breeze front penetrated between 3 and 12 km inland and the warmer SST case in which the sea breeze only reached the immediate shoreline. Figure 51 c shows the difference in wind vector at 2200 GMT. The sea breeze penetrates about 6 km farther inland north of the upwelling center in the actual case, and up to 18 km farther inland south of the upwelling center. The retreat of the sea breeze front offshore is noted 1 to 2 hours earlier in the warm SST case.

Air temperatures at 2 meters are dramatically different along the coastal zone. However, very little difference is noted inland since the sea breeze affected only the immediate coastal zone. Figure 51 b shows a plot of the 2 m air temperature difference at 2000 GMT. Air temperatures are greater than 3°C colder in the actual case along the majority of the coastline, excluding Sandy Hook and southern Cape May County. Temperature differences greater than 5°C are noted along the coast from Atlantic City to Asbury Park due to the significantly warmer SSTs in the warm SST simulation.

The most important differences between these simulations occur in the vertical depth of the sea breeze. The depth of the sea breeze circulation is decreased in the actual case with colder SST. In the actual case, the depth of the sea breeze extends up

to 450 m, 325 m, and 275 m along the 39.4°, 39.8°, and 40.2°N vertical cross-sections respectively. In the warmer SST case, the sea breeze circulation extends up to 450 m, 400 m, and 350 m along the same three respective cross-sectional lines. While the depth of the sea breeze is reduced to the strong offshore synoptic wind flow, it is likely that the colder SSTs have increased the density of the marine air in the actual SST case, allowing the sea breeze circulation to push farther inland at the surface, but also reduced the vertical depth of the sea breeze due to the higher density of the marine airmass.

Additionally, analysis of the vertical cross-sections reveal that almost no return current can be identified in the warmer SST case, while a rather weak but present return current can be found in the actual case. This is similar to the findings of Frizzola and Fisher (1963) who found that a return current was difficult to detect in cases with a strong offshore synoptic wind.

#### **5.4 Sensitivity Study**

In order to more fully investigate the impact of varying SSTs on the sea breeze circulation, a sensitivity study was conducted using the synoptic conditions from the July 6 case, utilizing two uniform SSTs of 15°C and 17°C respectively. The actual sea surface temperatures on July 6 were such that the minimum within the upwelling center was approximately between 15° and 16° C. Outside of this upwelling center, SSTs ranged from approximately 17° C to 20° C along the entire stretch of the Atlantic shoreline. By choosing these two uniform temperature regimes in this experiment, it was hoped that the sensitivity of the sea breeze circulation cell could be determined by the  $\Delta T_{SST}=2^{\circ}\text{C}$  between the two cases. The sea breeze circulation shown on NWS

Doppler Radar, and in the WRF model simulation of the actual case, is quite localized to the immediate shoreline, with the maximum extent of inland penetration occurring in the vicinity of Great Bay and Tuckerton, as well as along the northern part of the coast around Sandy Hook.

#### **5.4.1: Uniform 15°C SST**

It would be anticipated that given a uniform SST that the sea breeze circulation would likely expand from what was seen in the actual simulation in both spatial scale, the length of the sea breeze front impacting the coast, as well as inland penetration. The 15°C case does appear to have a significant increase in sea breeze frontal penetration over the actual case. Additionally, the sea breeze front is increased in length, now almost the entire length of the New Jersey coastline, except areas in the far south where the effects of the Delaware Bay Breeze creates a strong enough offshore wind to hold the sea breeze front at the immediate Cape May county shoreline. In comparison to the actual base case, the sea breeze front penetrates approximately 10-18 km farther inland along the northern portion of the coast, and as much as 24 km farther inland in the vicinity of Long Beach Island. The onset of the sea breeze breaching the barrier islands appears to occur around 1700 GMT. Figure 52 a-h show the 2 m air temperature and wind direction plots for 1500, 1800, 2000, and 2200 GMT.

The model indicates that the sea breeze in the 15°C case began to form offshore, indicated by an area of winds with magnitude of less than 1 m/s at around 1400 GMT. As the sea breeze front crossed the coastline at about 1500 GMT, the wind magnitude behind the weak winds shoreward of the sea breeze front quickly increased to 4 to 6

m/s. In this case, maximum inland penetration appears to occur along most of the sea breeze front at approximately 2200 GMT. However, along the southern periphery of the sea breeze front, offshore winds from the developing Delaware Bay Breeze begin to retard and then push back the sea breeze front at approximately 2000 GMT. The entire sea breeze front weakens after 0000 GMT, and soon afterwards the synoptic wind flow returns to the coastal areas.

Surface air temperatures increase during the morning from between 20° and 24°C at 1200 GMT to 29° to 32°C at 2000 GMT for most of the interior of New Jersey. More urbanized areas in the vicinity of Philadelphia reach between 33° and 34°C by 2000 GMT. Temperatures along the immediate coastline warm from between 21° and 24°C at 1200 GMT to between 26° and 30°C just prior to sea breeze genesis along the coast at 1700 GMT. This represents a  $\Delta T_{\text{Land-Sea}} = 11^\circ$  to  $15^\circ\text{C}$  at the time of sea breeze initiation. This temperature difference occurred over a spatial range of approximately 10 km, leading to a  $\Delta T/\Delta x$  of  $1.1^\circ\text{C}/\text{km}$  to  $1.5^\circ\text{C}/\text{km}$ .

In the vertical, the depth of the sea breeze extends up to between 550 and 600 m along the 39.4°, 39.8°, and 40.2° N cross-sectional lines. A weak return current exists up to 1250 m along all three cross-sectional lines. A shallow layer of cold, dense marine air exists in the lower 100 m of the atmosphere. As the sea breeze pushes onshore, this layer becomes shoal as it pushes onshore under the strong synoptic flow aloft.

#### **5.4.2: Uniform 17°C SST**

The 17°C case also develops a sea breeze, however it is much reduced in inland penetration and spatial extent than the 15°C SST case. Comparisons to the actual SST base case show that the 17°C sea breeze front penetrates the coastline between 3 and 6 km more than in the actual base case. This difference is most apparent around Sandy Hook and in the vicinity of Long Beach Island. The onset of the sea breeze front breaching the barrier islands appears to occur around 1800 GMT.

The shape of the sea breeze front is quite similar to that of the actual case, with the greatest amounts of land penetration occurring in the same places. This is likely due along the southern extent of the sea breeze circulation to the slight reduction in 850 mb winds from north to south, and the increased SST difference between the actual SST and the 17°C SST around Raritan Bay in the north.

Wind speeds behind the sea breeze front are less than 1 m/s stronger in the uniform 17°C SST case than in the actual. However, onshore wind speeds were generally 1 m/s weaker in the 17°C SST case. Both the actual and the simulation runs were rather similar in showing the magnitude of the wind speed and direction across the southern part of the state due to the interaction of the Delaware Bay Breeze with the Atlantic sea breeze.

Surface air temperatures at 1200 GMT are generally between 24° and 27°C on land. At 2000 GMT surface air temperatures had risen to between 28° and 33°C. Temperatures along the immediate coastline were between 19° and 24°C at 1200 GMT and between 20° along the barrier islands to as warm as 30° to 32° within a few kilometers of the shoreline at 1800 GMT. This represents a  $\Delta T_{\text{Land-Sea}} = 13^\circ$  to  $15^\circ\text{C}$

over a spatial range of approximately 10 km, and thus a  $\Delta T/\Delta x$  of between  $1.3^{\circ}\text{C}/\text{km}$  and  $1.5^{\circ}\text{C}/\text{km}$  at the time of the sea breeze onset.

In the vertical, the sea breeze circulation extends up to 450 m, 350 m, and 300 m along the  $39.4^{\circ}$ ,  $39.8^{\circ}$ , and  $40.2^{\circ}$  N cross-sectional lines. The synoptic flow forces the sea breeze circulation to remain rather shallow, and ultimately forces it to retreat offshore by 2000 GMT. Cold, dense marine air is present in the lower 30 to 40 m of the troposphere, with depth decreasing slightly as it breaches the shoreline.

#### **5.4.3: Comparison**

There is a significant difference in the inland penetration of the sea breeze between these two cases. In most areas north of Cape May County, the sea breeze has penetrated between 12 and 18 km farther inland in the uniform  $15^{\circ}\text{C}$  SST simulation. Figure 53 a-d shows the difference in wind vector for 1600, 1800, 2000, and 2200 GMT. The temperature gradient within 10 km of the coastline is greater in the uniform  $17^{\circ}\text{C}$  SST case due to the land remaining cooler overnight due to the proximity of the cooler ocean. However, the overall temperature gradient between the ocean and inland areas is slightly higher in the  $15^{\circ}\text{C}$  SST case. The difference in 2 m air temperature between the two cases is shown for 1600, 1800, 2000, and 2200 GMT (Figure 54 a-d).

It is possible that while the temperature gradient in the coastal zone was weaker in the  $15^{\circ}\text{C}$  SST simulation, that the sea breeze penetrated far enough inland that the cold, dense wedge of marine air at the surface could interact more with the warmer temperatures farther inland. Indications of this are visible in the vertical cross-sectional plots. Initially, the sea breeze depth was much greater in the  $15^{\circ}\text{C}$  SST case, indicating

that a colder ocean surface was capable of producing a deeper sea breeze against strong offshore synoptic winds. As the simulation progresses, the depth of the sea breeze shoals significantly as it moves farther onshore (Figures 55 a-b, 56 a-b, and 57 a-b) along all three vertical cross-section lines. The marine air would then contrast with the much warmer inland continental air and would thus be more able to push farther inland underneath the less dense airmass inland from the coastal zone.

An air temperature difference between a continental airmass and a marine airmass of  $3^{\circ}\text{C}$  corresponds roughly to a 1% difference in density. In the cases we are discussing here, the temperature gradient is generally between  $5^{\circ}$  and  $15^{\circ}\text{C}$ , leading to a much greater density gradient. This explains the shallow nature of the sea breeze penetration throughout the lower hundred meters of the troposphere, even in the presence of strong offshore synoptic winds.

Due to the more dense airmass within the sea breeze in the  $15^{\circ}\text{C}$  uniform SST case it was rather unexpected that the vertical depth of the circulation cell would be larger than that of the uniform  $17^{\circ}\text{C}$  SST case. It is suspected that the stronger nature of the sea breeze circulation in the  $15^{\circ}\text{C}$  SST case allowed for the development of a better defined circulation cell than in the  $17^{\circ}\text{C}$  SST case, despite the presence of strong offshore winds aloft.

## **CHAPTER 6**

### **Summary and Conclusions**

A complete understanding of the sea breeze phenomenon is essential to accurate mesoscale atmospheric forecasts of sensible weather in the coastal zone. While New Jersey sea breezes are possible throughout the year, they become most important to meteorological forecasts during the summer months because of the increased tourist population and concerns over energy availability and allocation along with associated environmental issues.

Several factors determine the characteristics of a sea breeze event, including:

- the overall synoptic flow aloft
- the configuration of the coastline
- the temperature gradient between the land and the ocean

New Jersey coastal upwelling influenced changes in SST are most pronounced during the summer months of July and August, which allows for the strongest land-sea temperature gradients in which the sea breeze can develop. The determining factors for the extent of inland penetration are a combination of the synoptic wind flow and the gradient between air temperature in the coastal zone and the temperature of the nearshore ocean surface.

This thesis has focused on the effect of sea surface temperature variation due to coastal upwelling on the sea breeze phenomenon along the coast of New Jersey. The

WRF model was used to examine the effect of varying SSTs on the development and behavior of the New Jersey sea breeze. It has been found that the presence of cooler water in the coastal waters due to upwelling can have a profound effect on the inland penetration of the New Jersey sea breeze. While a critical land – sea temperature gradient required for the development of the sea breeze was not established due to a limited number of sea breeze simulations, it is clear that the temperature gradient in the coastal zone is a highly important indicator of sea breeze development and start time.

The July 6 case study indicated that an increase in nearshore SST of 3° to 7.5°C can have negating influence of several kilometers in inland penetration in the presence of a strong offshore directed flow at 850 mb. The July 5 case study indicates that a similar change in SST can only have an impact on inland penetration to a certain degree, as the inland penetration of the sea breeze between the actual case and the warmer SST case is nearly identical. However, when the temperature of the nearshore ocean is increased to near the climatological maximum value the sea breeze circulation fails to develop. The sensitivity study using uniform 15° and 17°C SST shows the significant difference a two degree differential in the land-sea temperature gradient can hold for the inland penetration of the sea breeze front. This proves that the existence of coastal upwelling along the coast has a significant role in the development and behavior of the sea breeze, and more complete understanding of this relationship is vital to the accurate forecasting of this phenomenon along the coast of New Jersey.

The offshore extent of the sea breeze circulation cell has been investigated through the use of the WRF model and Doppler radar detection. Surface wind divergence along the seaward extent of the circulation was shown in the model results

from the April 16, 2004 simulation. The area of calm divergent winds propagates farther offshore corresponding to the increasing inland penetration of the sea breeze front. The modeling results indicate that the offshore extent of the sea breeze cell is roughly two to three times that of the inland penetration of the sea breeze front, similar to the findings of prior studies and two examples of Doppler radar indicated sea breeze fronts shown previously. Little or no calm region was noted in either the July 5 or July 6 case study simulations. The exact reason for this is unclear, although it is suspected that the strong offshore synoptic flow on both days may have an impact in the disruption of the calm zone offshore.

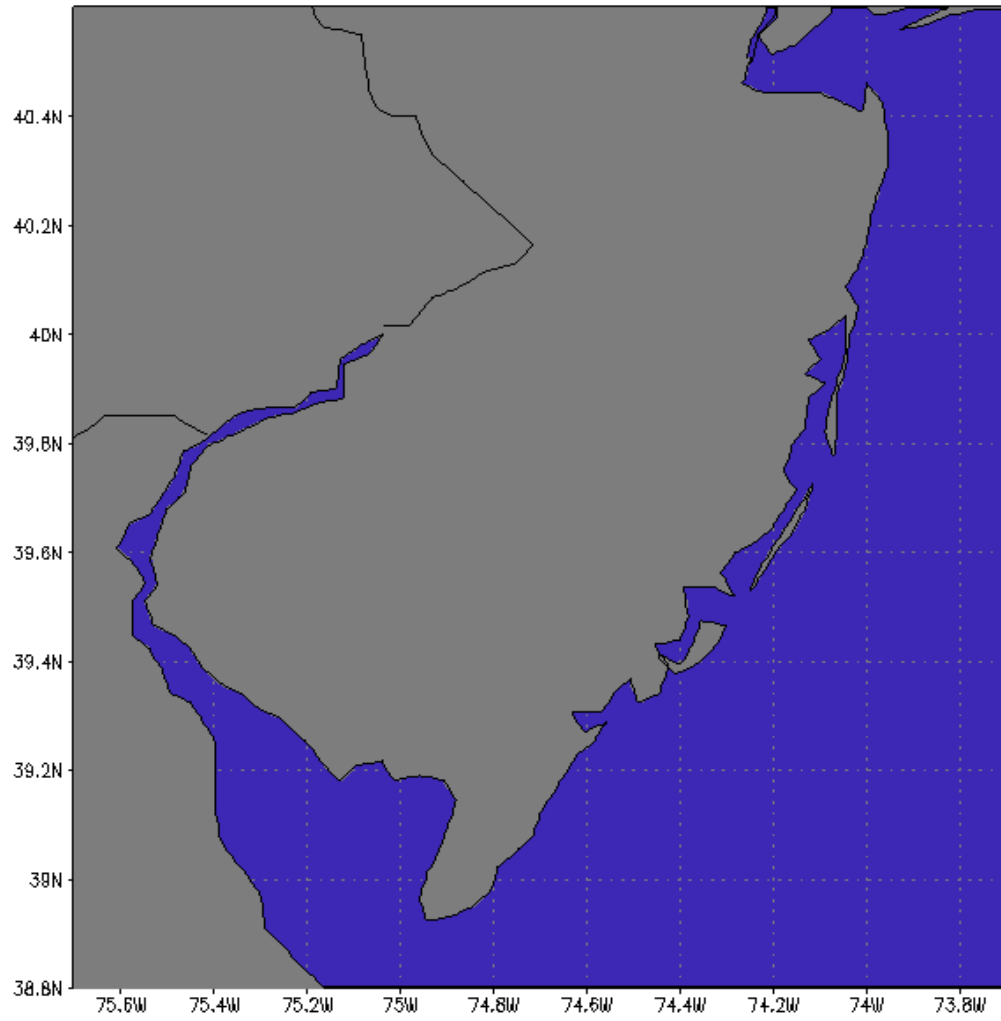
The structure of the sea breeze is influenced by the presence of coastal upwelling. While the depth of the sea breeze appears to be most influenced by the strength of the synoptic flow, sea breeze circulations enhanced by coastal upwelling have cooler, more dense air near the surface which can lead to a more deeply penetrating sea breeze in the lowest levels of the troposphere. It is also a sea breeze which is shallower than a sea breeze during non-upwelling conditions. The July 6 case indicates that the vertical depth of the sea breeze decreased by as much as 100 meters in the presence of coastal upwelling along the coast. However, the sensitivity test indicated that the vertical dimension of the sea breeze was increased with colder SST. A possible cause of these conflicting results is that in the presence of a uniformly cold ocean the sea breeze can become increasingly well defined dynamically. In the case of coastal upwelling enhanced sea breezes, the increased dynamics of the sea breeze circulation occurs over a small region, perhaps only enough to develop a shallow sea breeze in a similar opposing synoptic wind. The difference in SST also appears to have

had an impact on the return current, which was very difficult to detect during the warmer SST simulation.

No significant change in the shape or orientation of the sea breeze front was noticed during these simulations due to the presence of coastal upwelling. Radar reflectivity of the sea breeze front has indicated the presence of irregularly shaped sea breeze fronts during coastal upwelling regimes. Aside from small differences along the extreme southern portion of the state, where the Delaware Bay breeze can interact with the inland penetration of the sea breeze front, alterations in the shape of the sea breeze front were not found to be due to the SST. Instead, the numerical modeling experiments show that variations in the shape and orientation of the sea breeze front are due to the strength of the opposing synoptic flow and variations in the configuration of the coastline. The coastline configuration appears to play a greater role during the initial stages of the sea breeze front penetrating farther inland than expected. This further enhances the argument that the New Jersey sea breeze does not penetrate inland exactly parallel to the coastline as prescribed by idealized conceptual models. Inland penetration distance is generally at a maximum west of Long Beach Island due to the convex nature of the coastline. Towards the southern portion of the state, the Delaware Bay breeze is often responsible for a decreased number of sea breeze fronts moving inland in Cape May County. Instead, the sea breeze front often moves inland along the northern periphery of the Delaware Bay breeze front, with the southern portion of the sea breeze front being pushed progressively farther northwest as the bay breeze penetrates farther inland. Similarly, the northern portion of the sea breeze front

propagates inland clock-wise along the Raritan Bay breeze that is often kept to a minimum due to the concave configuration of the bay.

While this study has shown the considerable effect that coastal upwelling can have on the sea breeze phenomenon in New Jersey, considerable future work is required to attain a complete understanding of the sea breeze – coastal upwelling system. This study has focused on two case study events, with a limited number of SST variations. Simulations should be conducted using a wider range of SST variation with a larger number of varying synoptic upper level wind speeds. Higher spatial resolution simulations with higher resolution SST should be conducted in order to study this relationship in the immediate coastal zone as well as the entire state. The ultimate goal of these studies would be to use a high resolution coupled atmospheric – oceanic model to investigate the coupled response of the sea breeze on coastal upwelling and conversely coastal upwelling on the sea breeze circulation. Accomplishing this task would translate to more accurate forecasts for the tourism industry, the private sector, marine interests, energy consumption, and someday may assist those responsible for homeland security.

**Figures**

**Figure 1a:** Study Region and WRF model domain

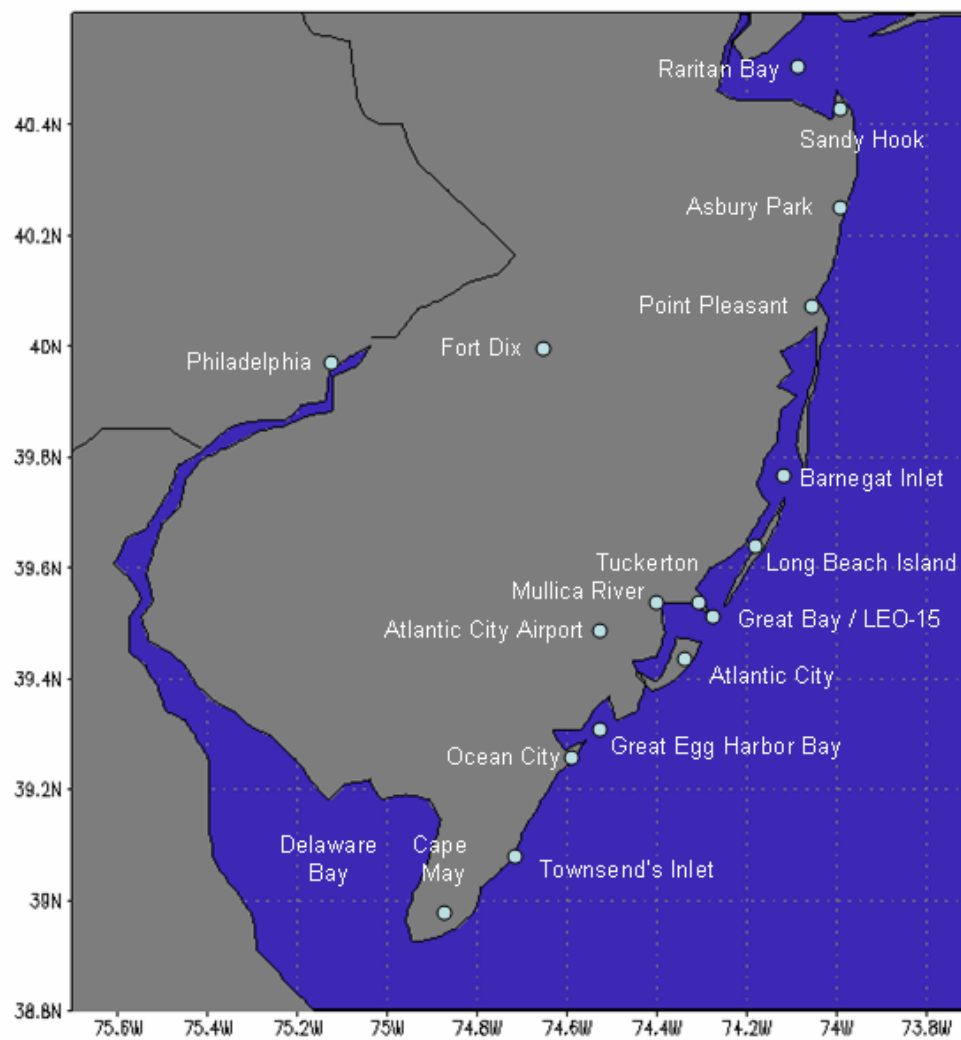


**Figure 1b:** Study Region with site locations

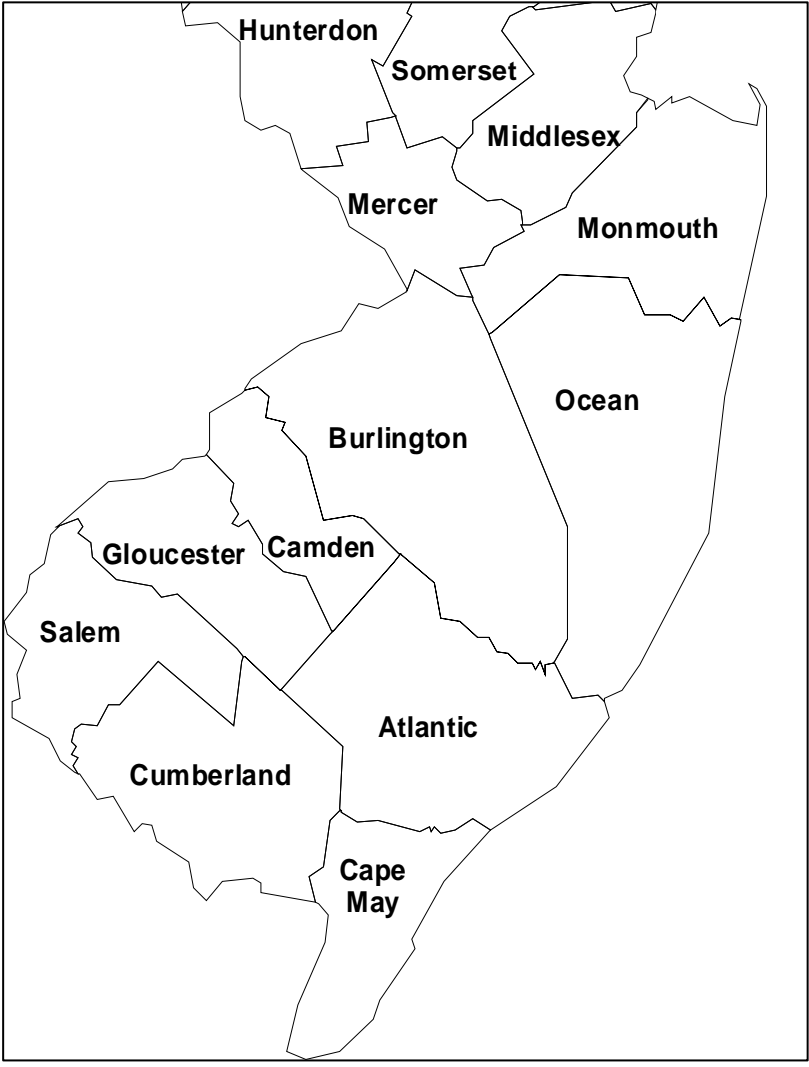


**Figure 1c:** Study Region with county names

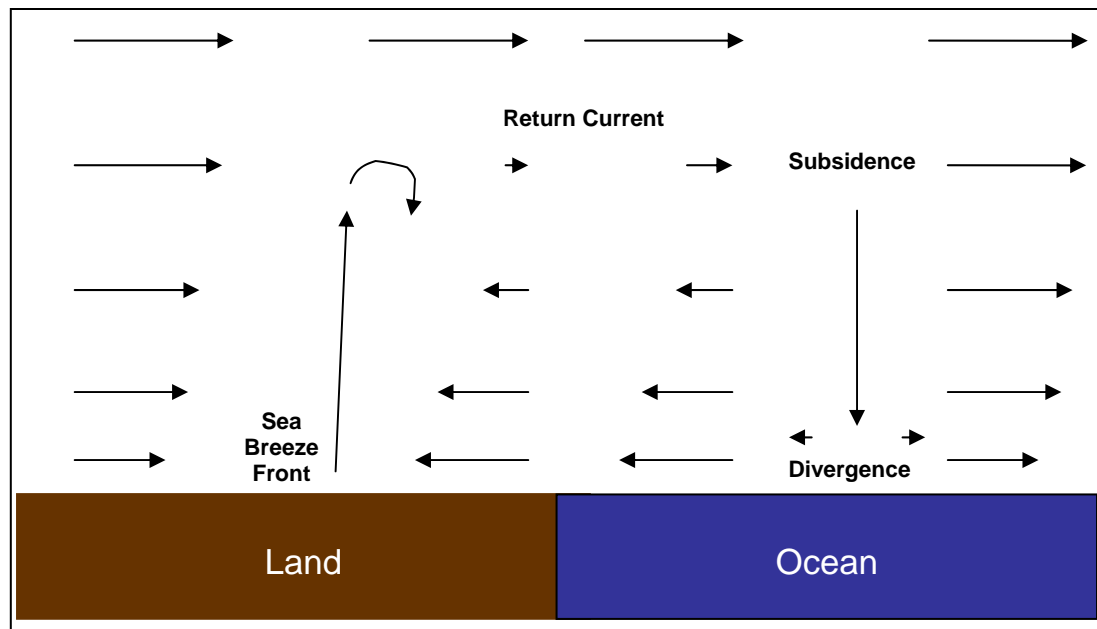


**Figure 2:** Box model of the sea breeze circulation indicating updrafts at the sea breeze front, the return current, and subsidence over the ocean.

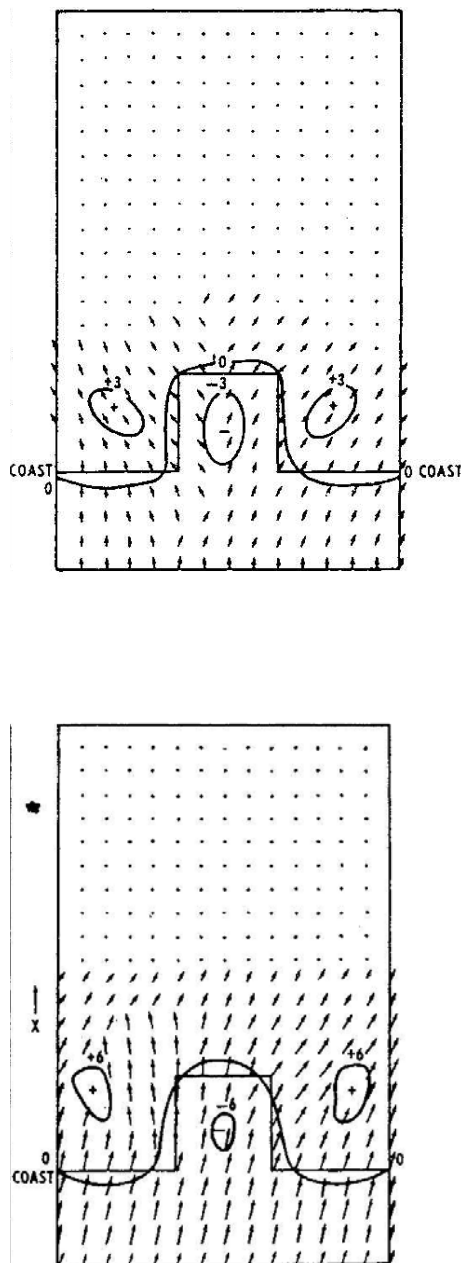


**Figure 3 a-b:** Plot of modeled wind direction and speed vectors at 250 m (m/s) and vertical velocity contours (cm/s) at 850 m for an inland moving sea breeze along a straight coast with a square bay after 2 hr (a, top) and 4 hr (b, bottom) of integration (McPherson, 1970). These figures show increased divergence in the center of the bay, with increased surface wind convergence along either side of the bay.



**Figure 4:** Picture from Gemini XII taken in 1966 showing an area of sun glint offshore from the west coast of Florida. This area is the sight of calm winds due to divergence from the sea breeze circulation (Fett and Tag, 1984).

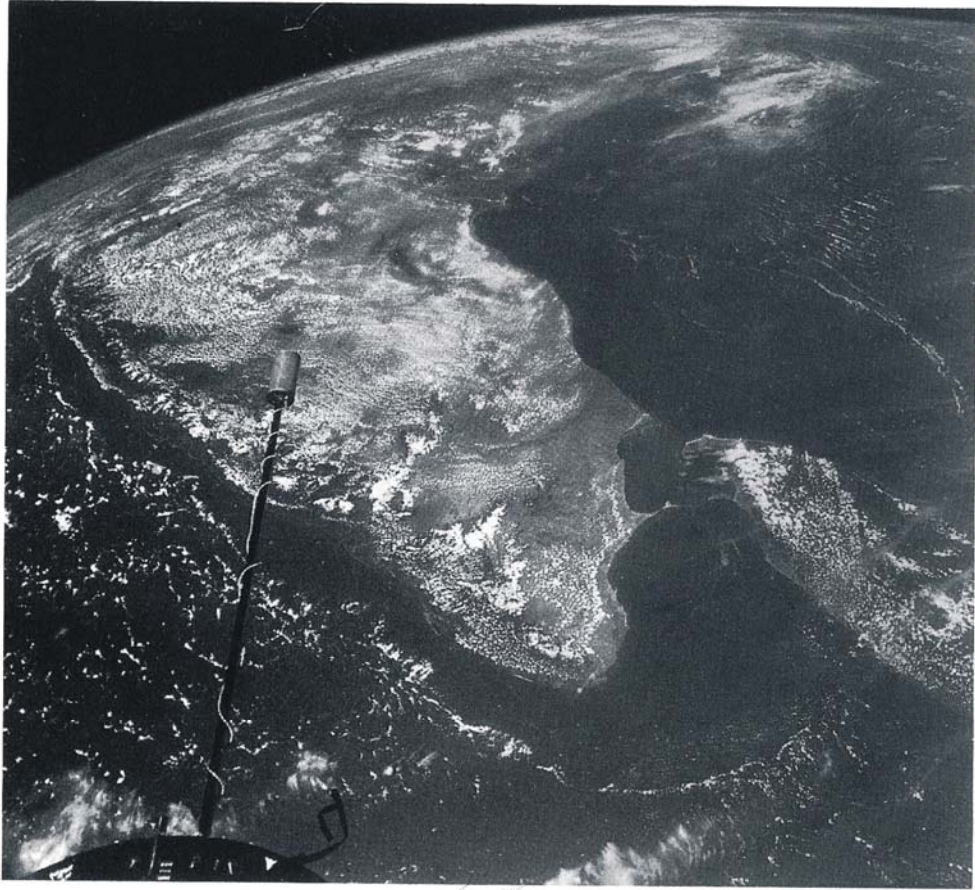


**Figure 5:** Picture from Gemini XI of India taken in 1966. The picture shows a cloud-free area offshore both the east and west coast where sea breezes are occurring. This cloud free zone is due to sinking motion due to the sea breeze circulation (Simpson, 1994).

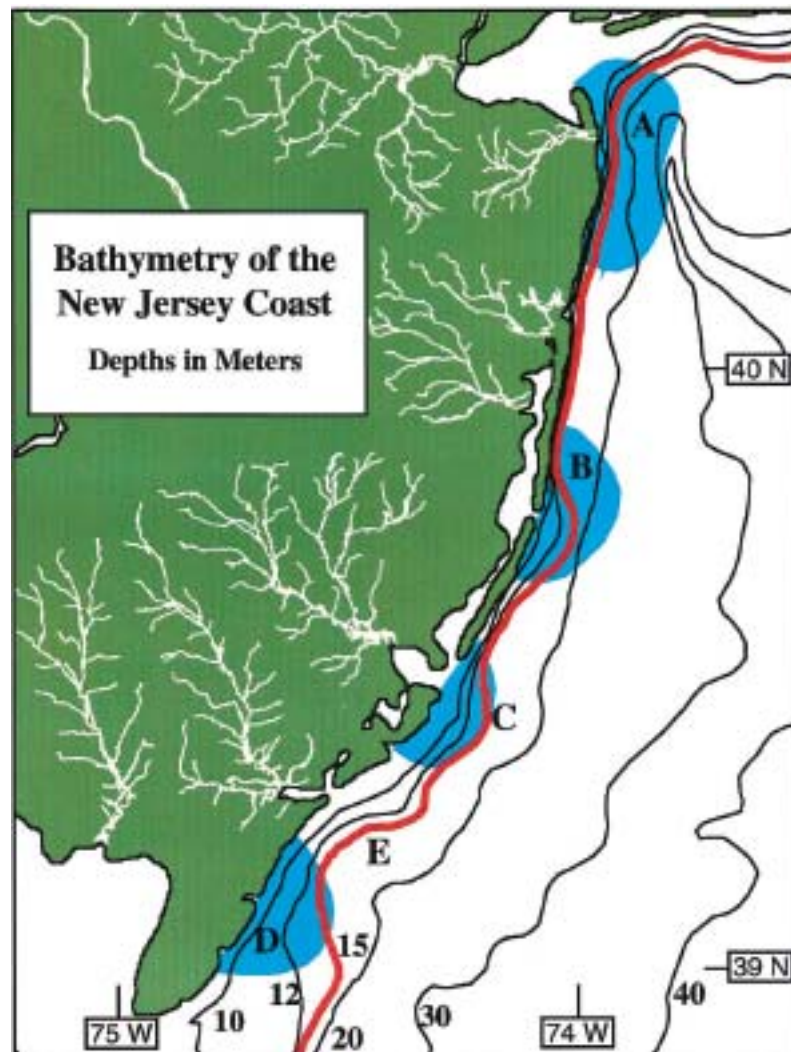


**Figure 6:** Bathymetry along the coast of New Jersey. Areas in blue are typical coastal upwelling centers during the summer months (Song et al., 2001).

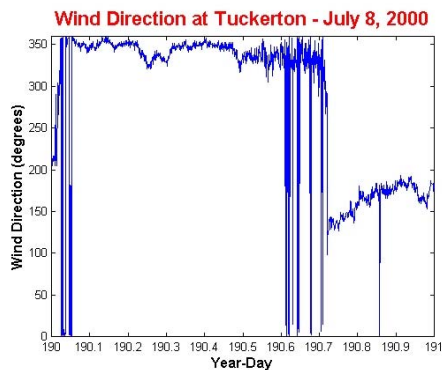


**Figure 7a:** Wind direction at Tuckerton, July 8, 2000 showing passage of sea breeze at Year-Day 190.7. Note the change from a northerly wind to a southerly wind.

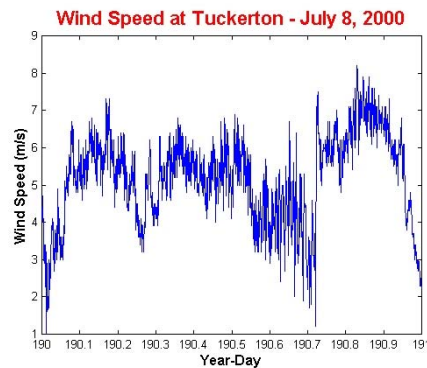


**Figure 7b:** Same as Figure 7a showing increase in wind speed.

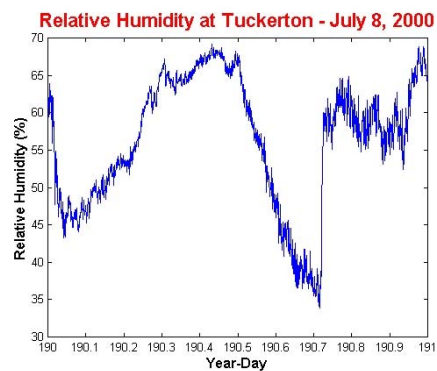


**Figure 7c:** Same as Figure 7a for Relative Humidity. Relative humidity frequently decreases significantly prior to the passage of the sea breeze front, and then increases due to the marine airmass in the sea breeze.

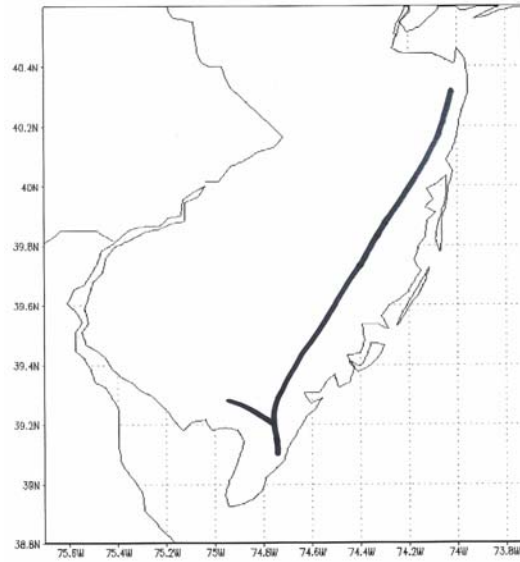
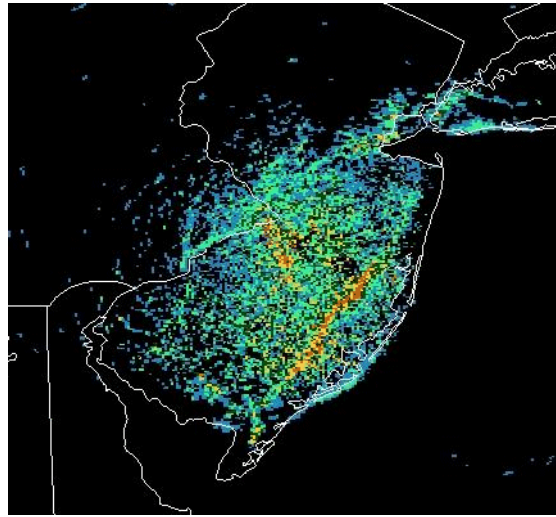


**Figure 8 a-b:** Example WSR-88D reflectivity image (a, top) showing a sea breeze front (red thin line just west of the coast). Hand-drawn representation of the sea breeze and Delaware Bay breeze fronts (b, bottom).

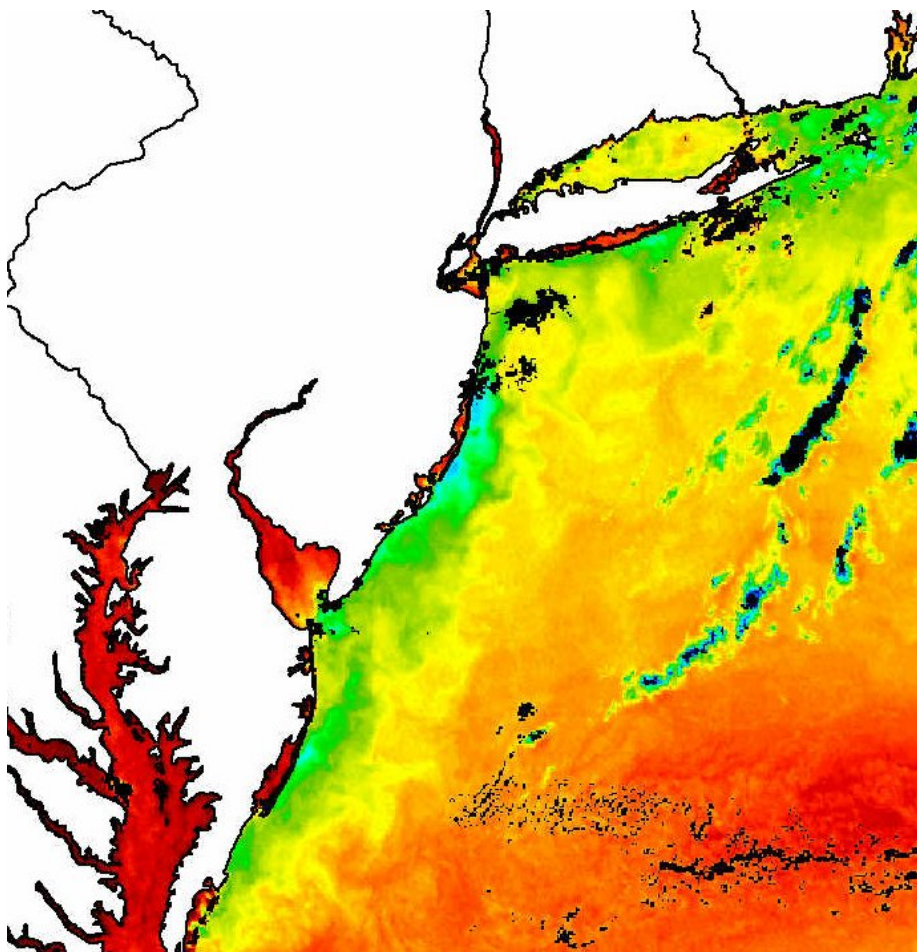


**Figure 9:** AVHRR SST imagery showing coastal upwelling (blue) along the New Jersey coast.

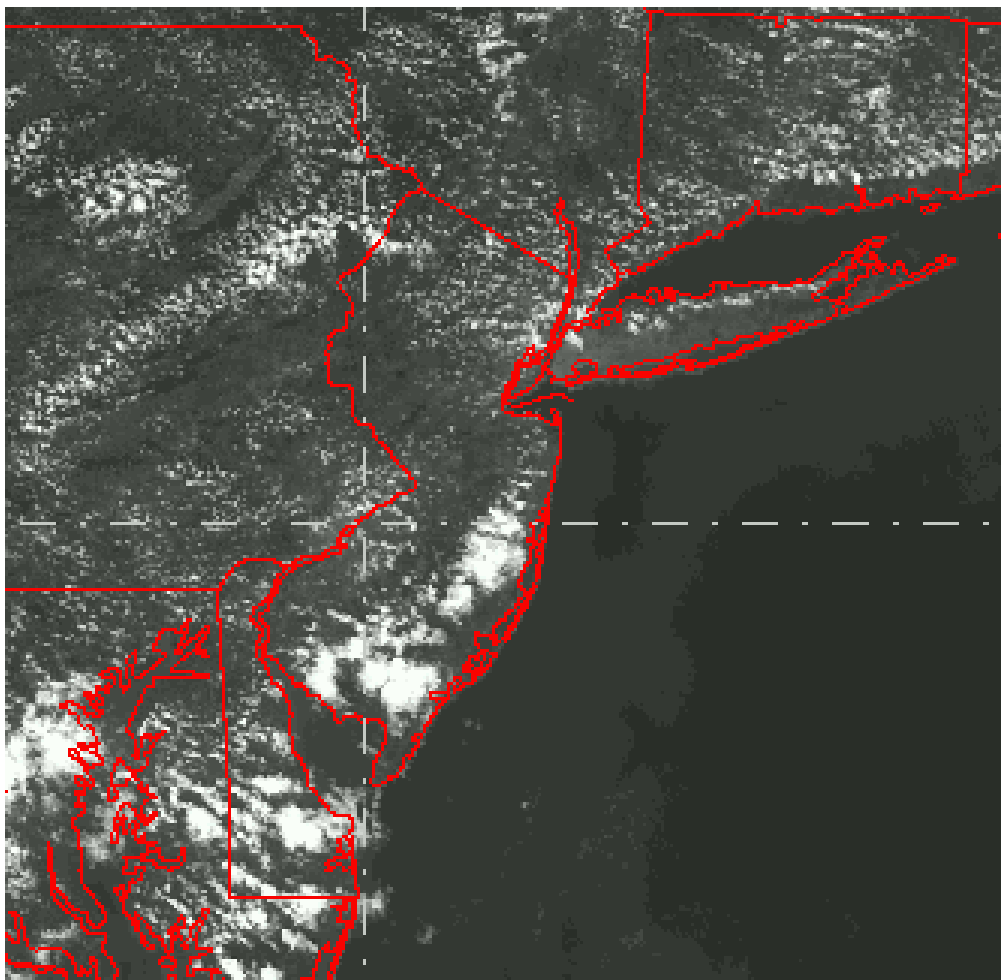


**Figure 10:** AVHRR Visible Satellite imagery from August 19, 2003 at 1841 GMT showing sea breeze front along the New Jersey coast.

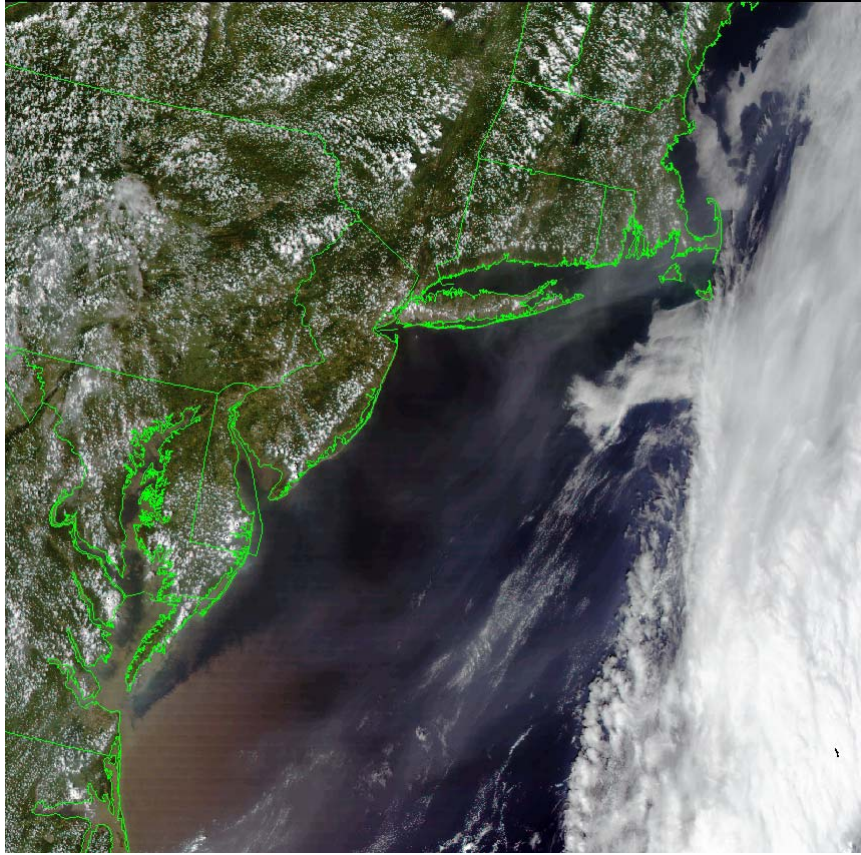


**Figure 11:** MODIS visible satellite image from July 21, 2004 showing sea breeze front along the coast (North to South). The Delaware Bay Breeze is shown along the New Jersey shore of Delaware Bay. The intersection of the sea breeze and bay breeze is noted along the Southern New Jersey coast by brighter cloud tops. Additional sea breezes can be seen along the coast from Maine to North Carolina.

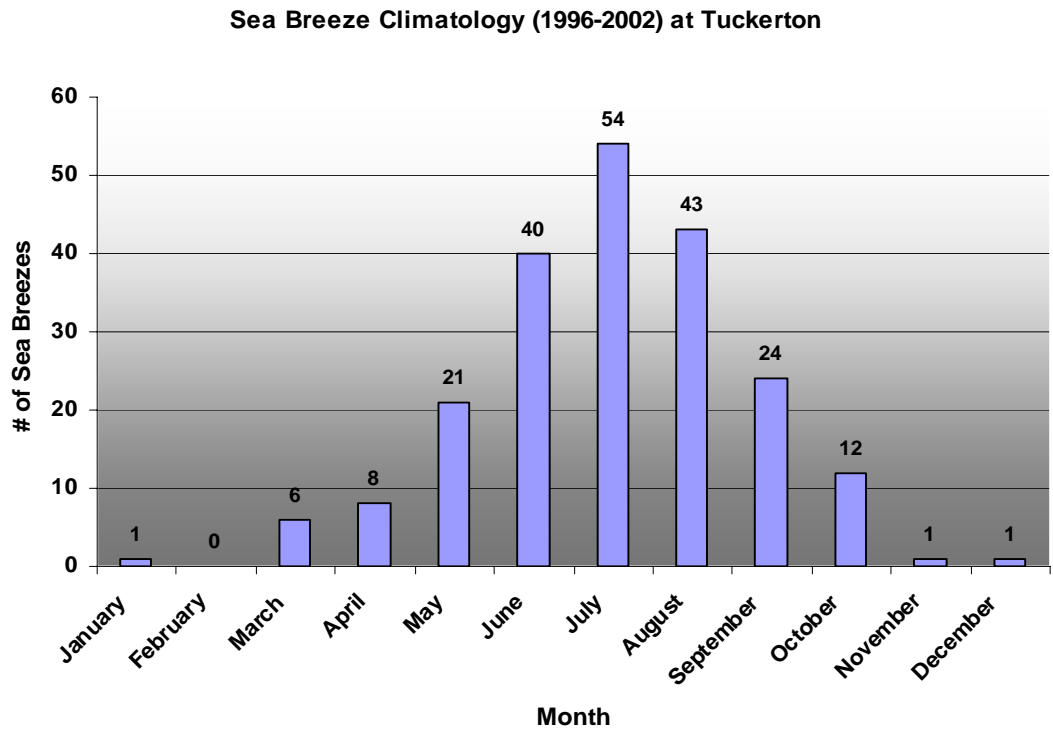


**Figure 12:** Sea breeze climatology at Tuckerton from 1996-2002. There were 211 sea breezes which passed the airport during the six year study. Sea breezes were noted in every month except February.

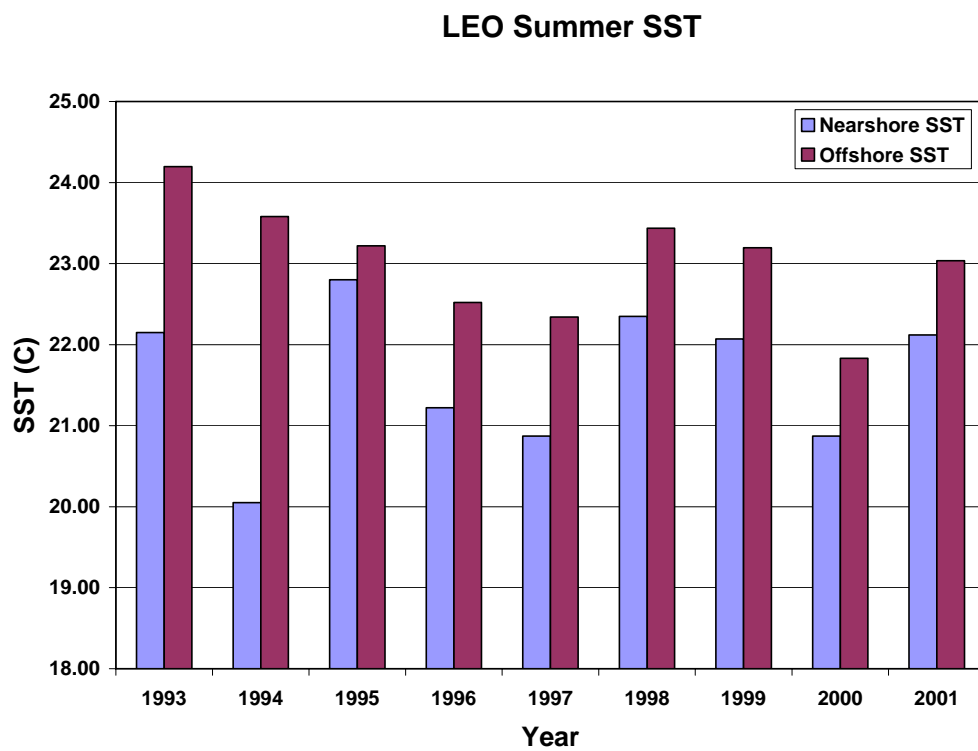


**Figure 13:** Sea surface temperature from AVHRR satellite at LEO-15 off of the coast from Tuckerton. Nearshore and offshore locations were used to combine annual statistics showing the summer season effect of coastal upwelling (Glenn et al., 2004).

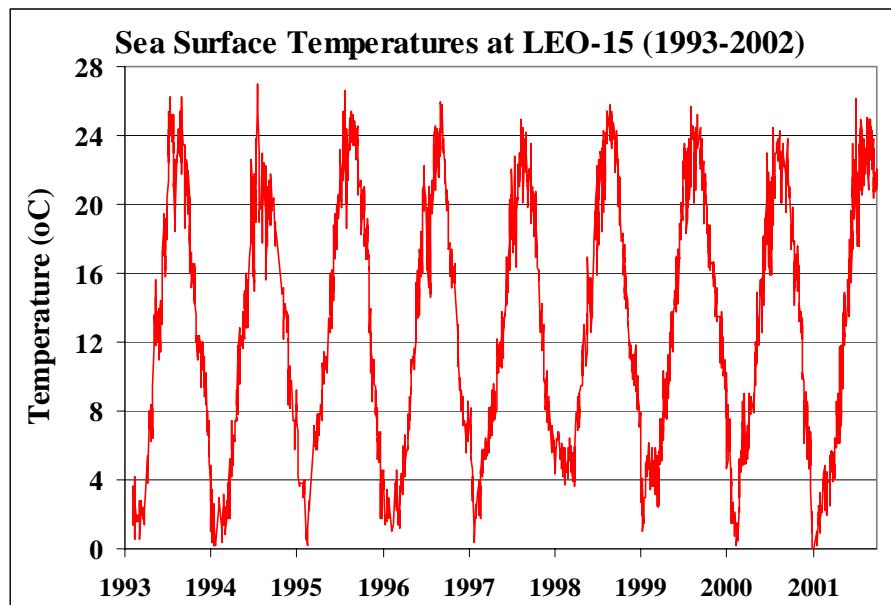


**Figure 14:** Annual sea surface temperature from 1993-2002 at LEO-15 derived from AVHRR satellite (Glenn et al., 2004) Note the maximum SST during this period is between 27° and 28°C.

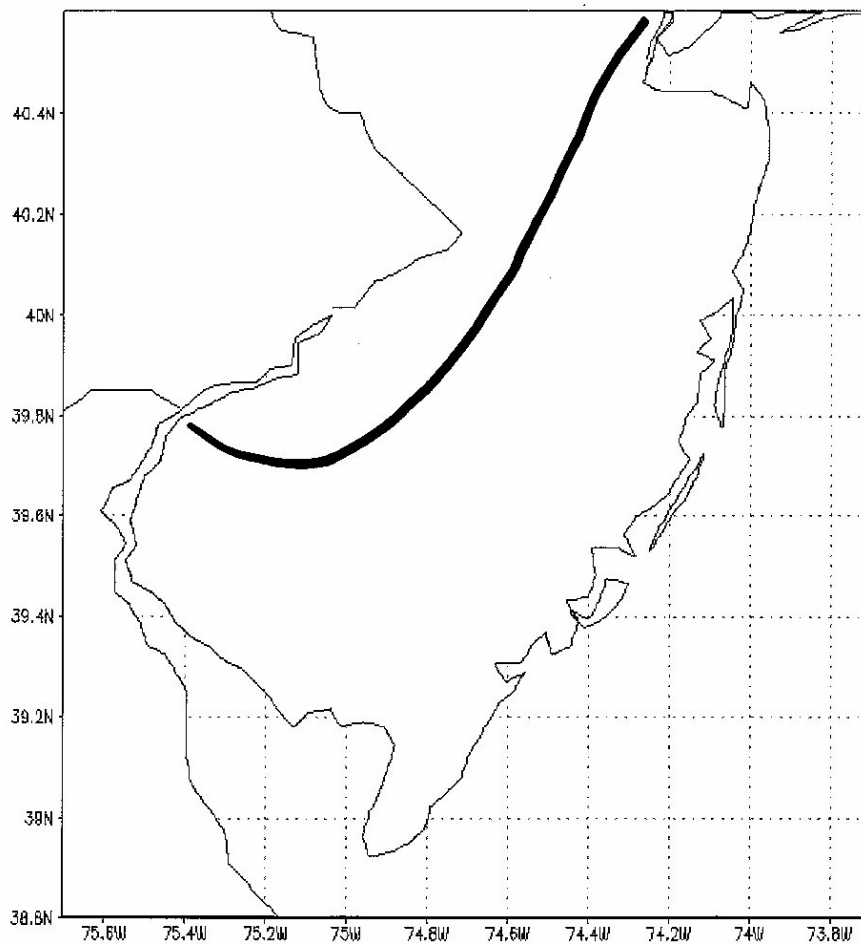


**Figure 15:** Radar reflectivity showing the maximum inland penetration of the sea breeze on June 29, 2003.

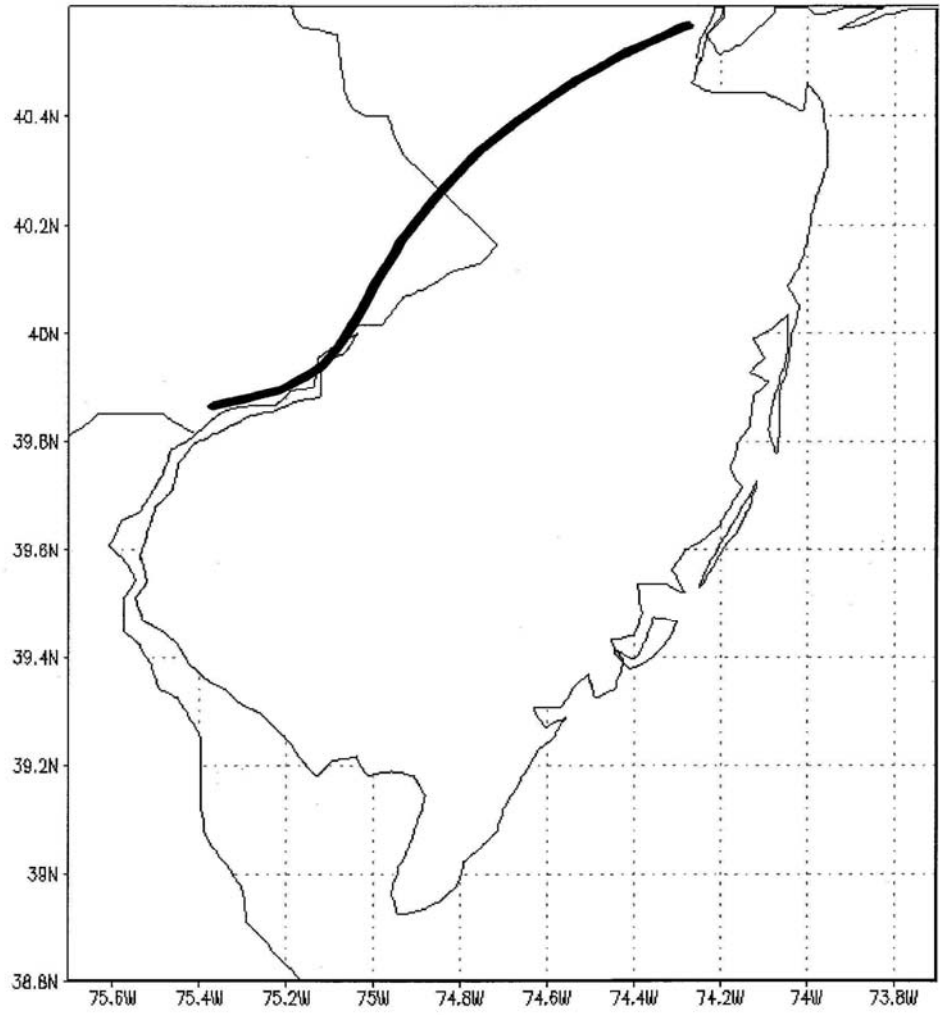


**Figure 16:** Radar reflectivity showing the maximum inland penetration of the sea breeze on June 30, 2003.

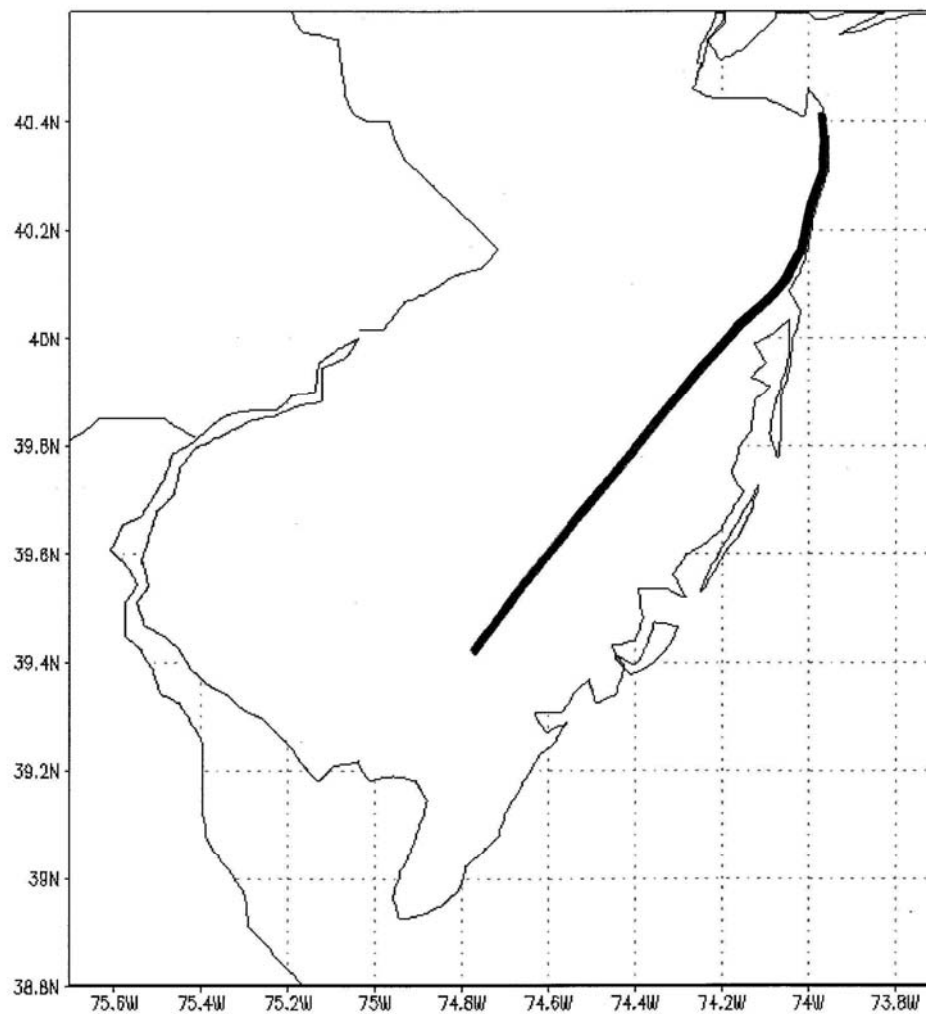


**Figure 17:** Radar reflectivity showing the maximum inland penetration of the sea breeze on July 1, 2003.

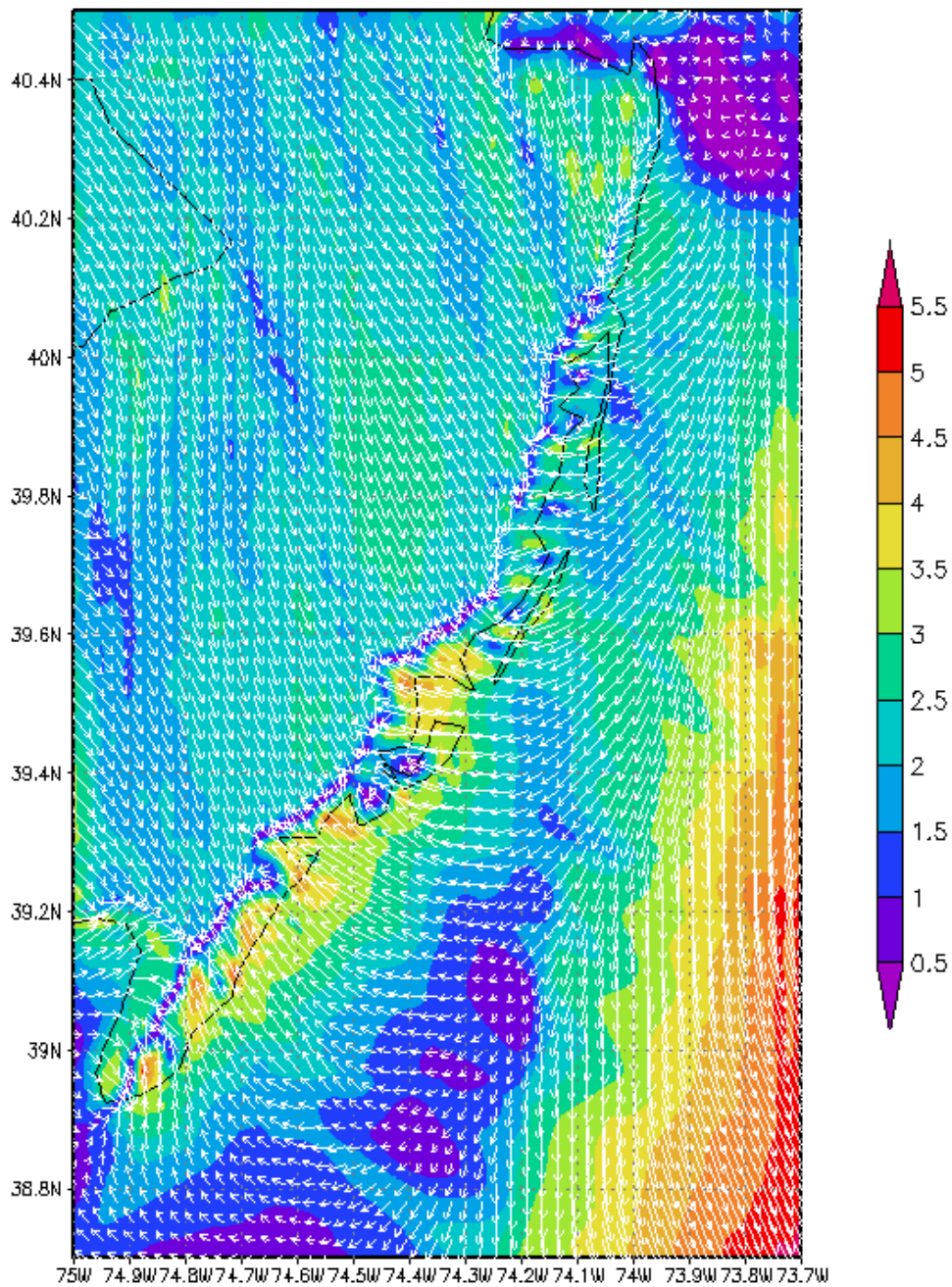


**Figure 18:** WRF model simulation for April 16, 2004 at 1800 GMT showing irregular inland penetration of sea breeze front near bays and estuaries. Wind speeds are in color and wind vectors are in white.

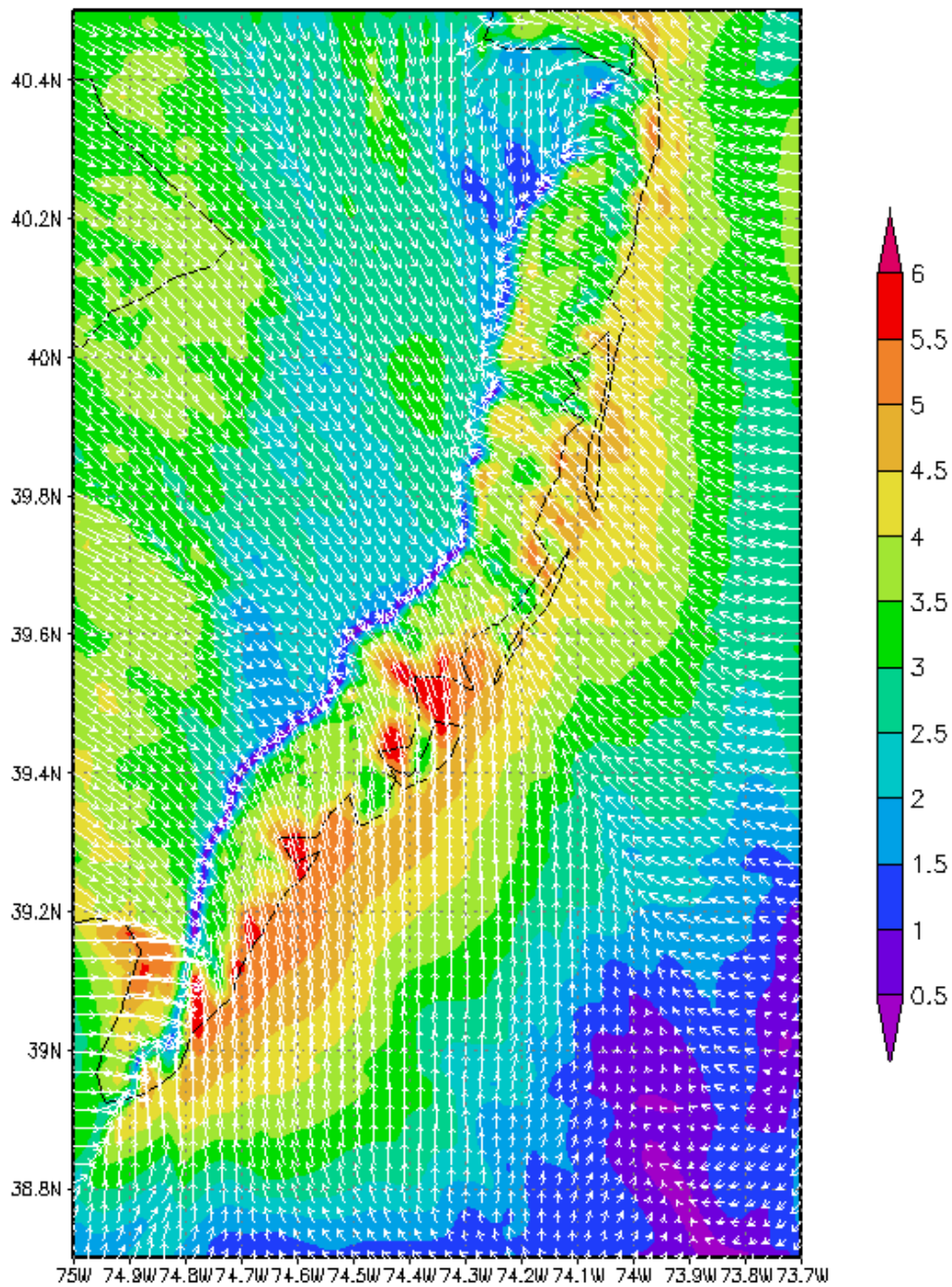


**Figure 19:** WRF model simulation for April 16, 2004 at 2000 GMT showing increasingly more homogeneous shape with increasing distance from shore.

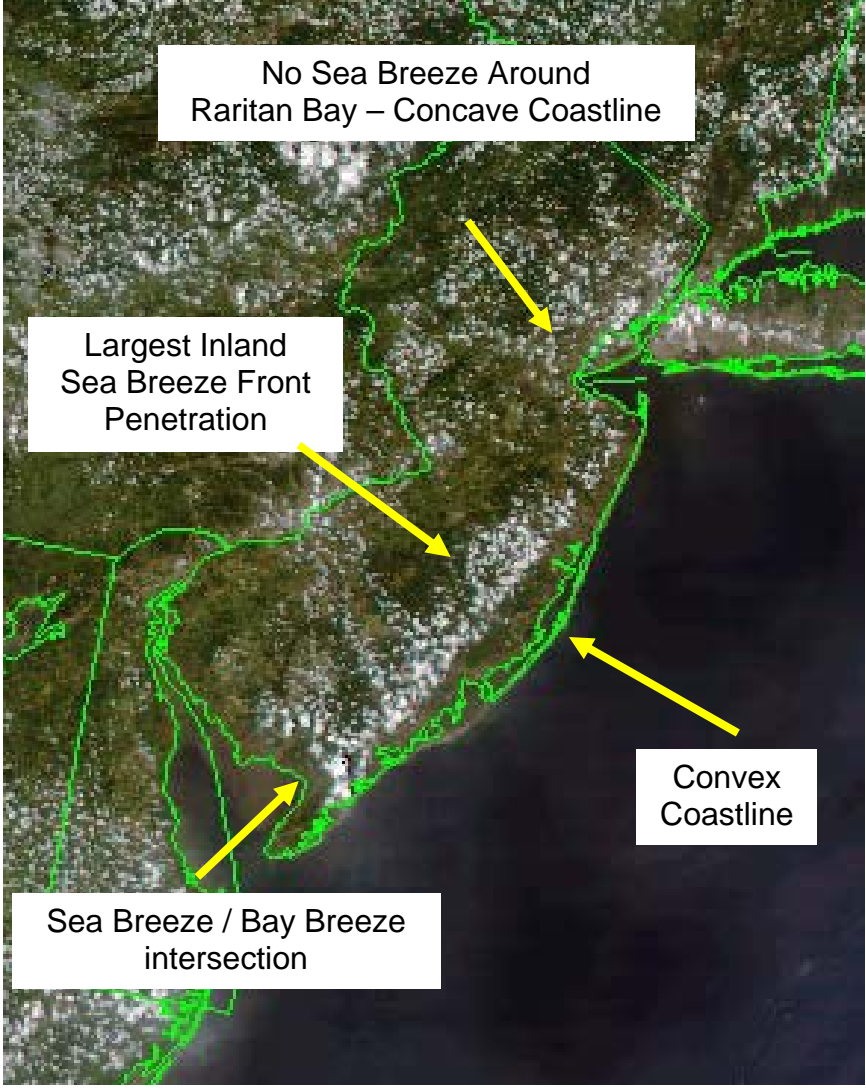


**Figure 20:** Zoomed in MODIS visible satellite image (Figure 7) showing the interaction of the sea breeze and the Delaware Bay breeze indicated by higher (brighter white) cloud tops. The location of the largest inland sea breeze penetration is referenced to the convex curvature (sea breeze favorable) of the New Jersey coastline. The lack of an identifiable Raritan Bay breeze just west of the bay is referenced to the concave coastline (sea breeze unfavorable) configuration of the bay.

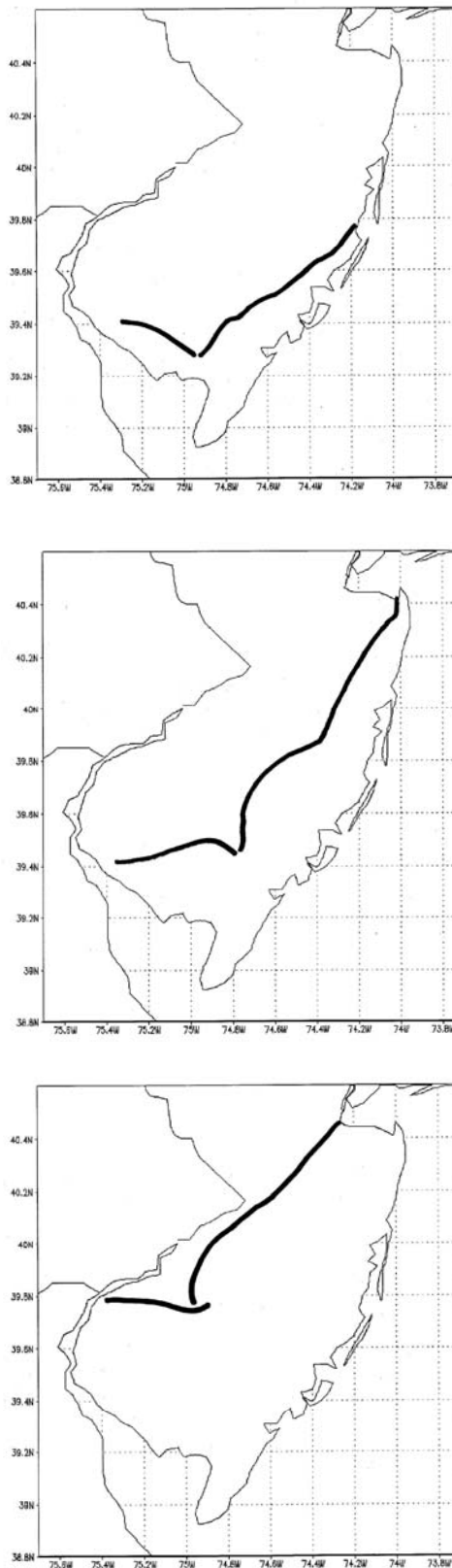


**Figure 21 a-c:** NWS Doppler radar indicated positions of the sea breeze and Delaware Bay breeze fronts at 1715 (a), 2111 (b), and 2359 (c) on July 1, 2003.

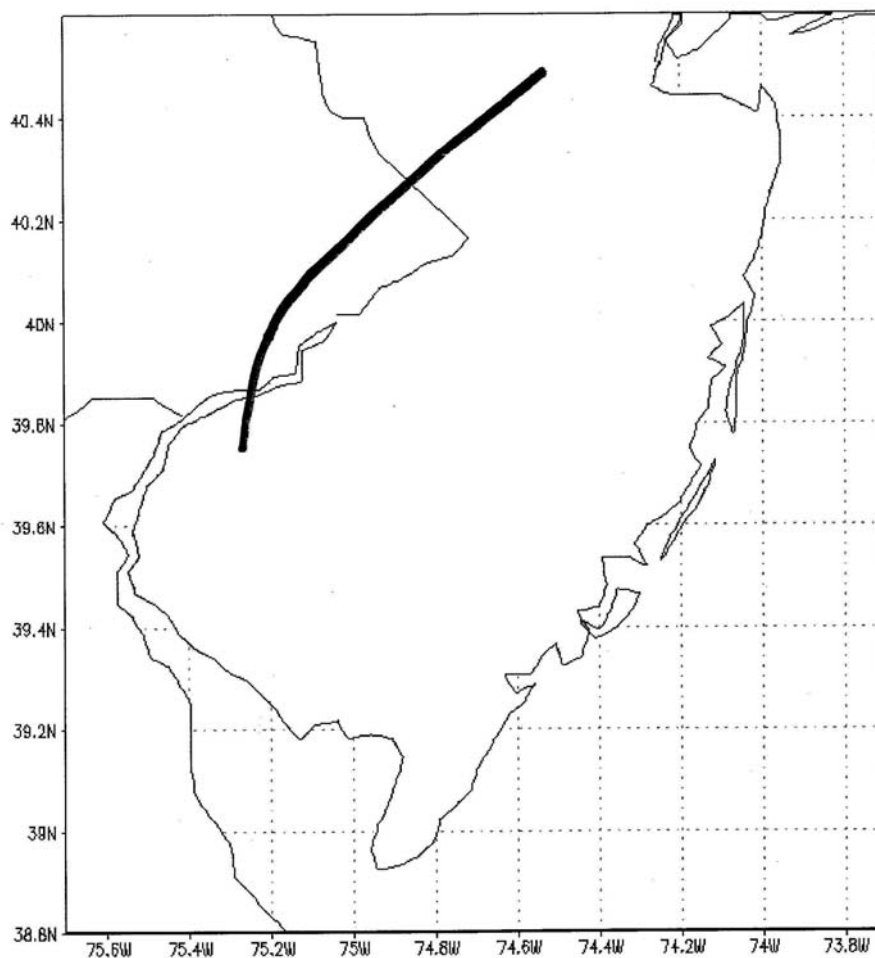


**Figure 22:** Maximum inland extent of the sea breeze on June 4, 1994.

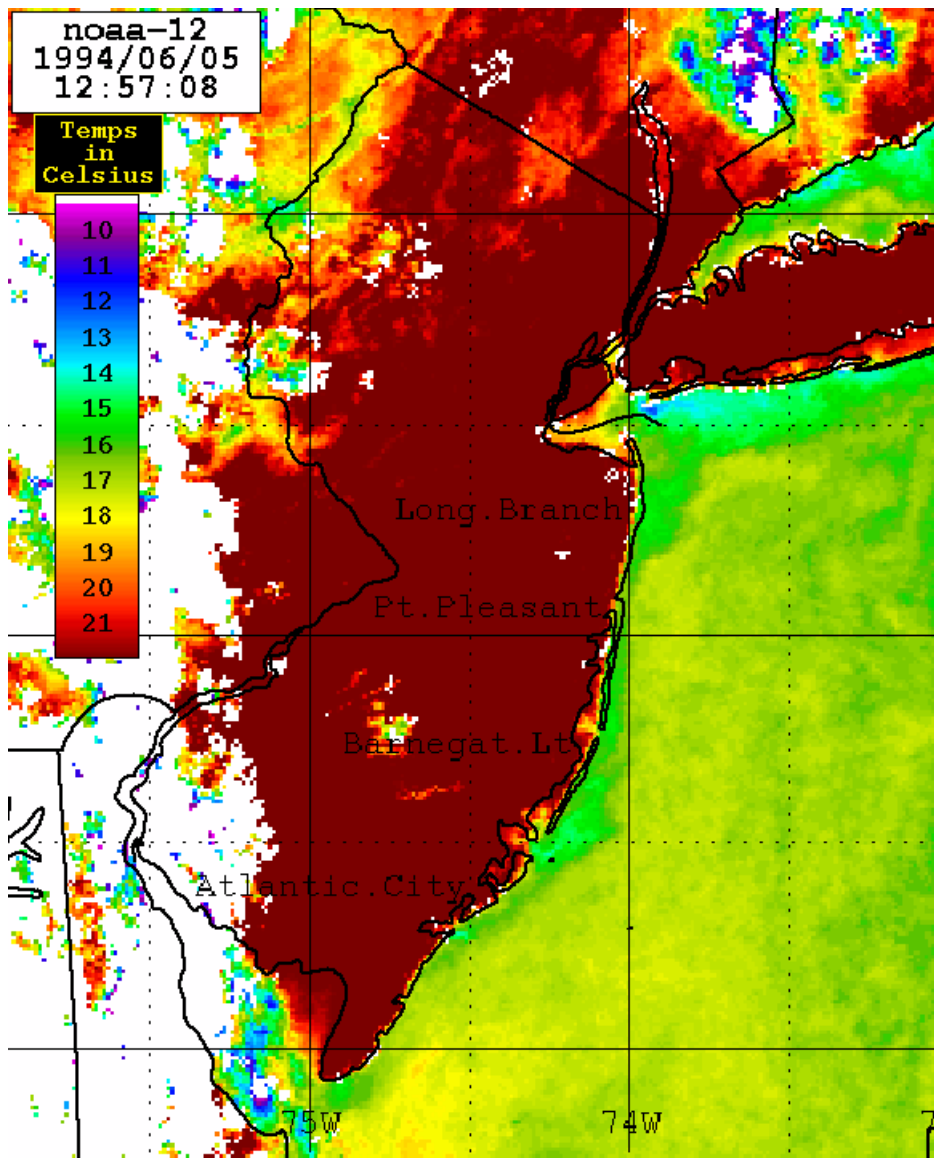


**Figure 23:** Sea surface temperature from AVHRR at 1257 GMT on June 5, 1994 showing slight coastal upwelling from Sandy Hook to Atlantic City.

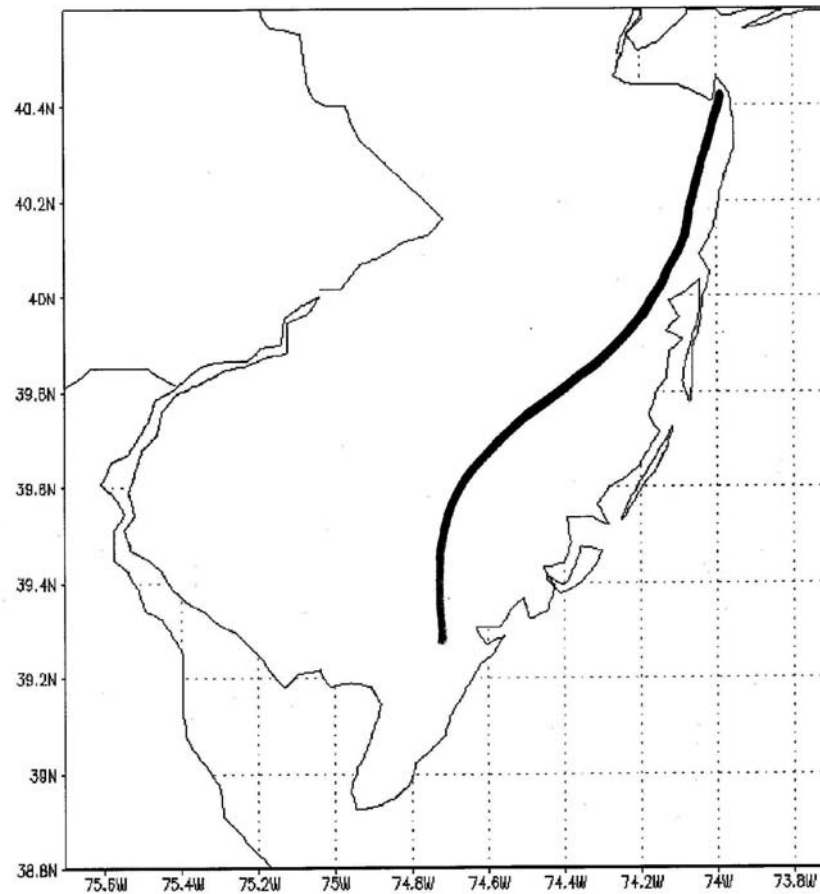


**Figure 24:** Maximum inland extent of the sea breeze front for June 26, 2001. Note the increased inland penetration of the sea breeze front inland from the upwelling center (Figure 25).

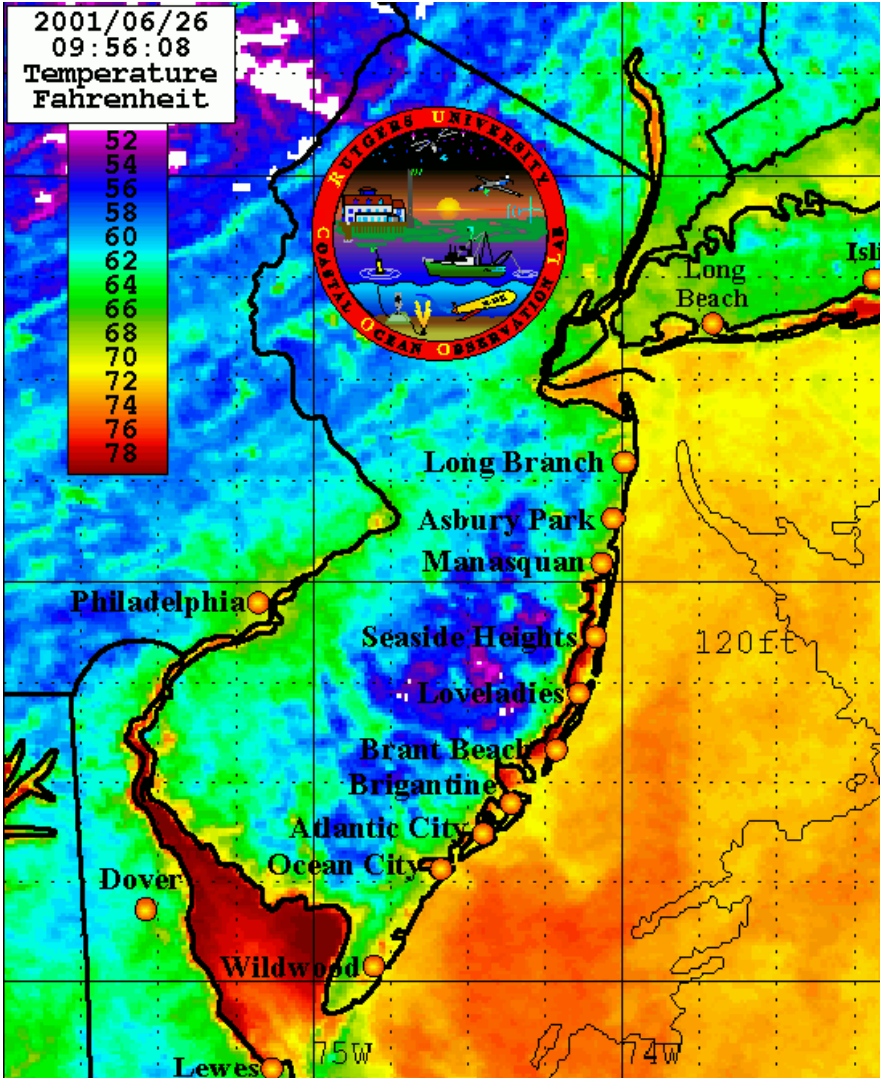


**Figure 25:** Sea surface temperature from AVHRR at 0956 GMT on June 26, 2001 showing slight coastal upwelling along Long Beach Island to Atlantic City.

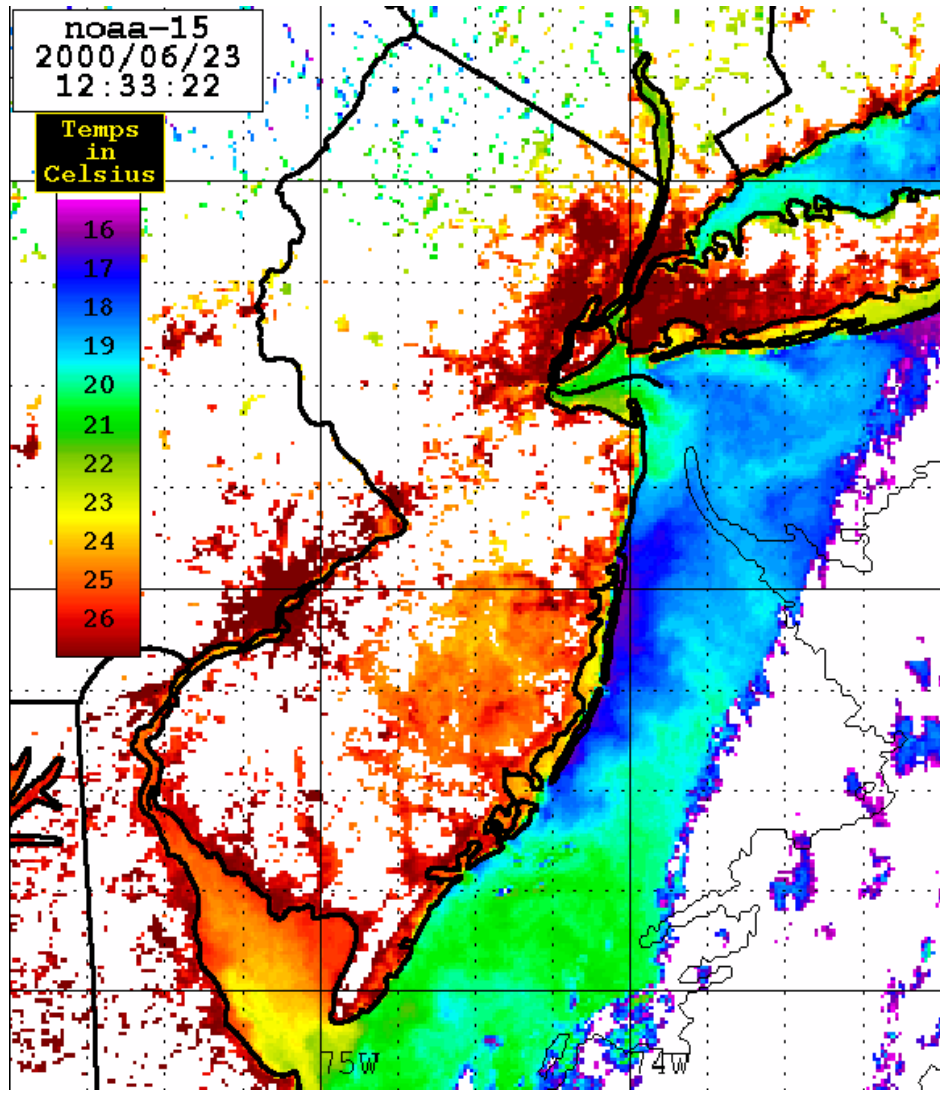


**Figure 26:** Sea surface temperature from AVHRR at 1233 GMT on June 23, 2000 showing strong coastal upwelling along Long Beach Island to Asbury Park.

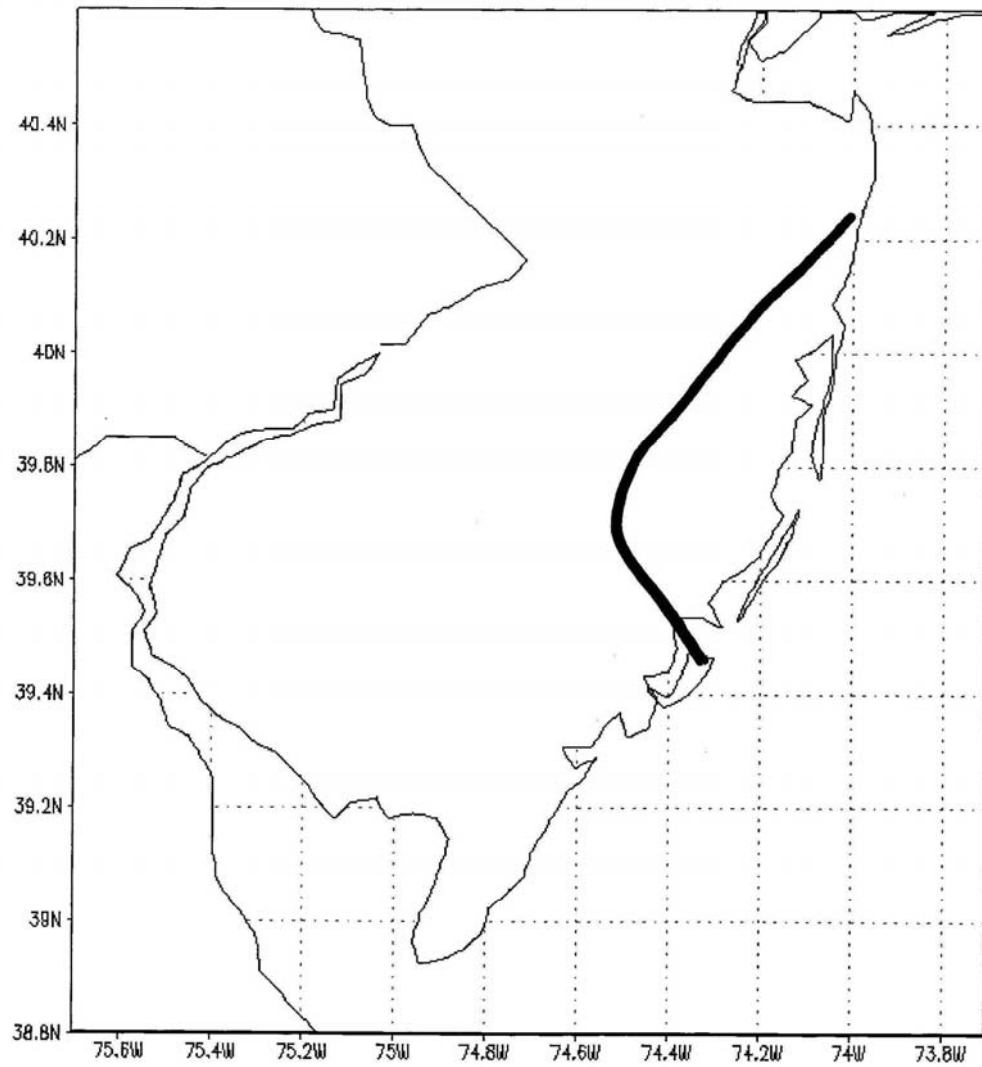


**Figure 27:** Maximum inland extent of sea breeze front on June 23, 2000. Note the increased inland penetration of the sea breeze front inland from the upwelling center (Figure 27).

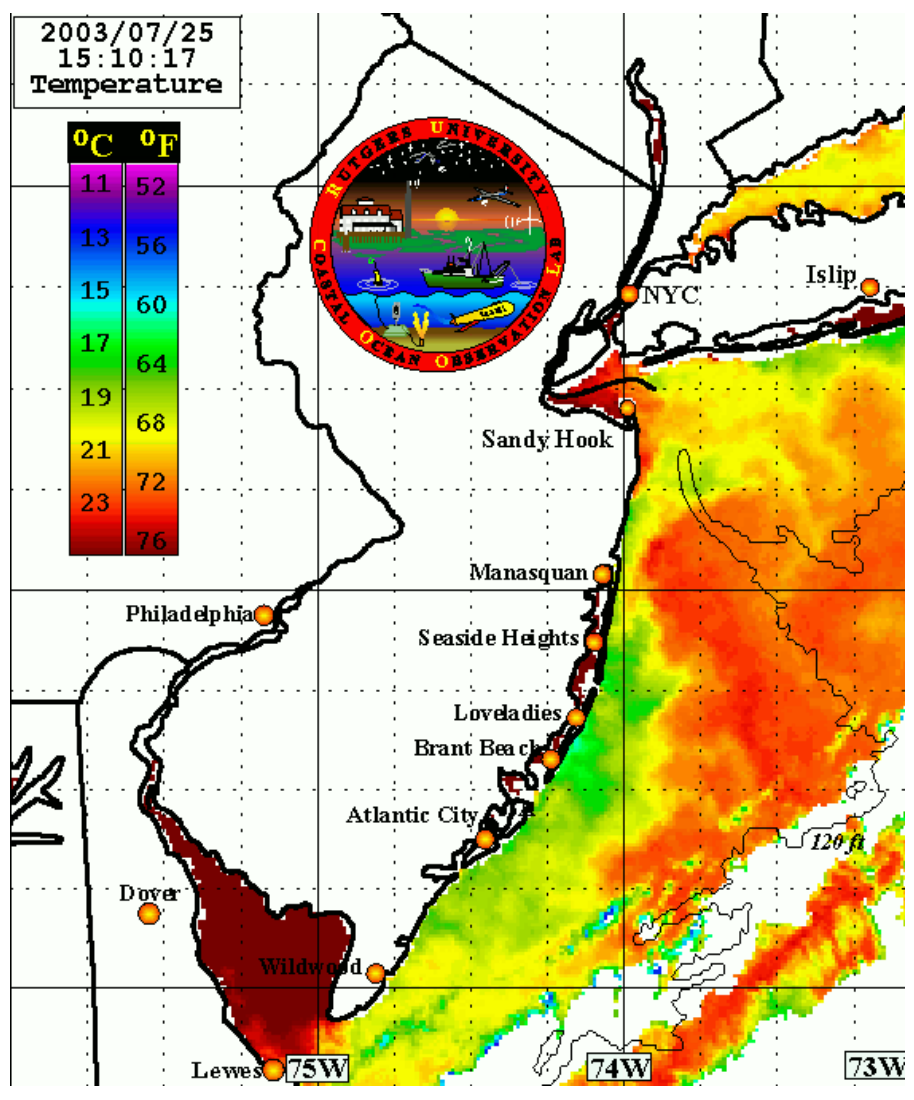


**Figure 28:** Sea surface temperature from AVHRR at 1510 GMT on July 25, 2003 showing coastal upwelling from Atlantic City to Asbury Park. Note the strong oceanic temperature front offshore which corresponds to the possible “offshore sea breeze front” in Figure 29.

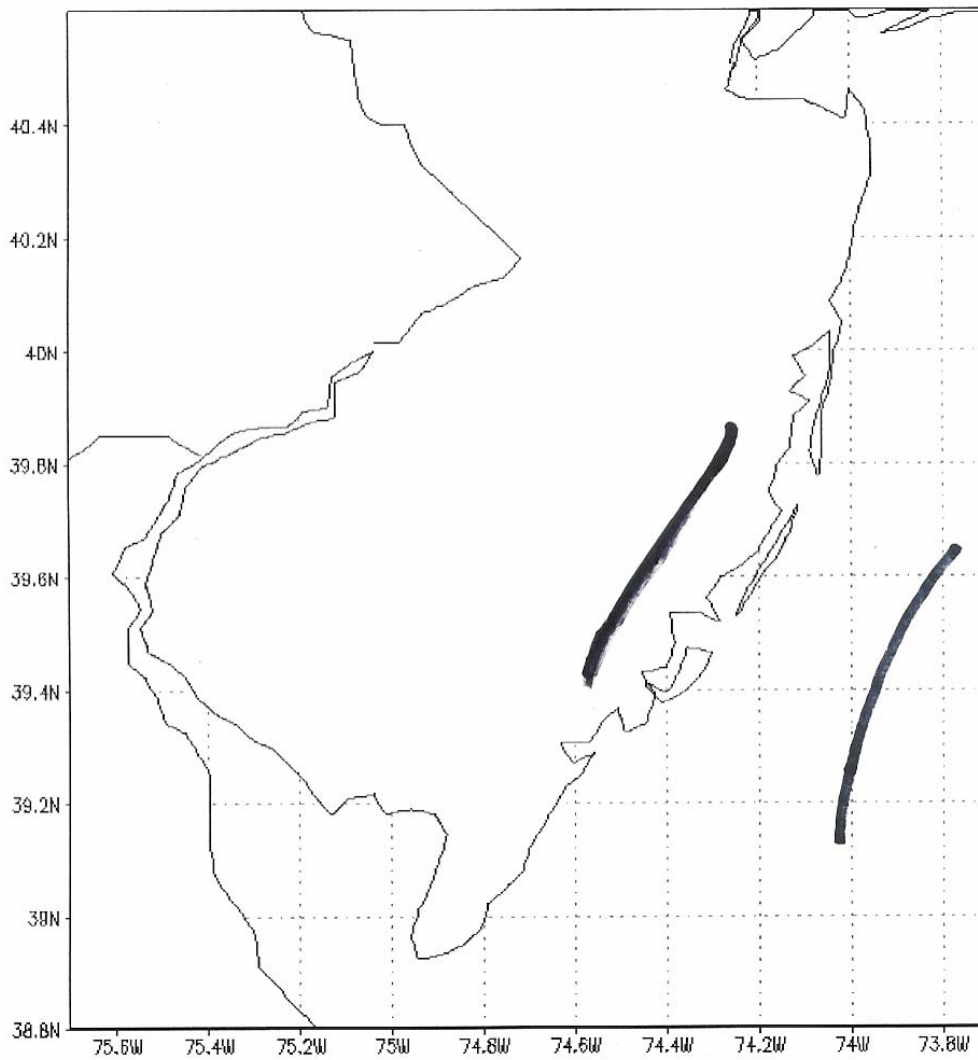


**Figure 29:** Radar reflectivity for July 26, 2003 at 1857 GMT showing sea breeze front inland and offshore extent (offshore sea breeze front?) of the sea breeze circulation offshore corresponding to the upwelling center in Figure 28.

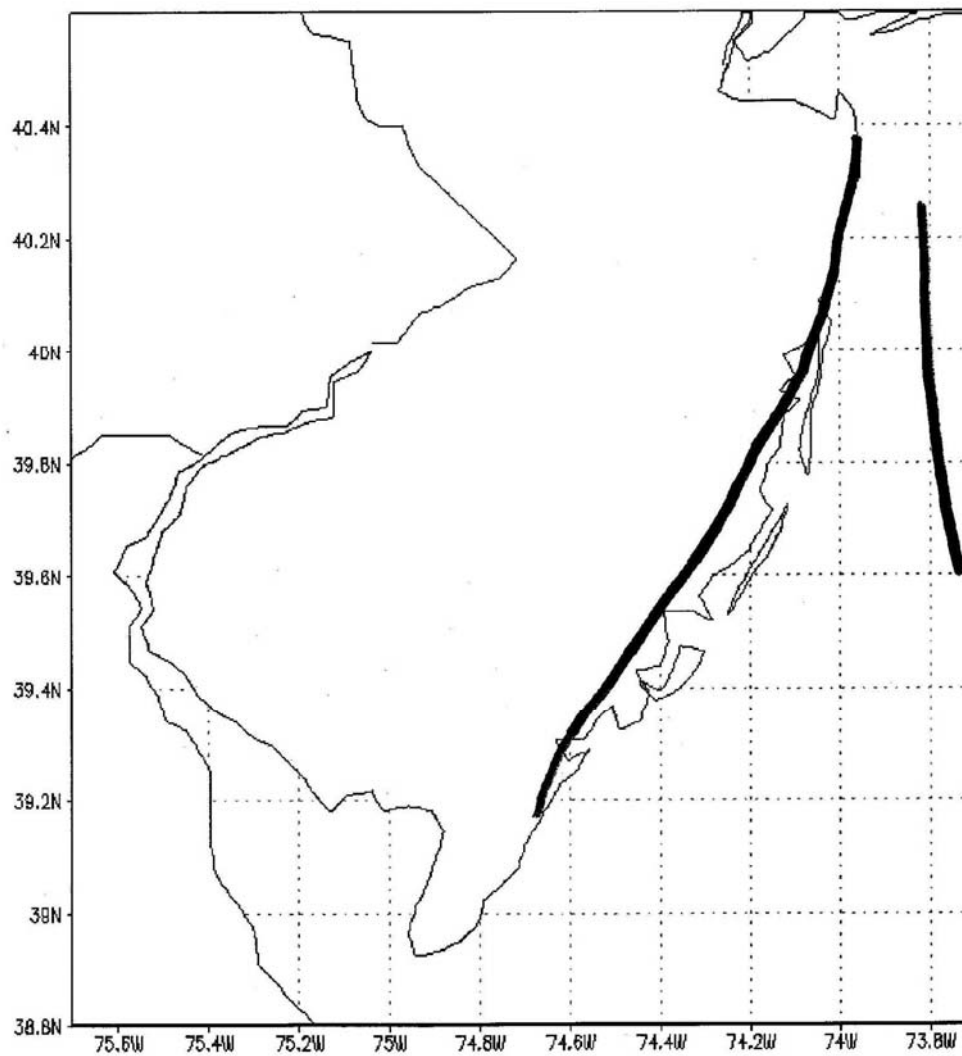


**Figure 30:** Radar indicated sea breeze frontal position and offshore extent of the sea breeze circulation offshore for August 2, 2001 at 2044 GMT.

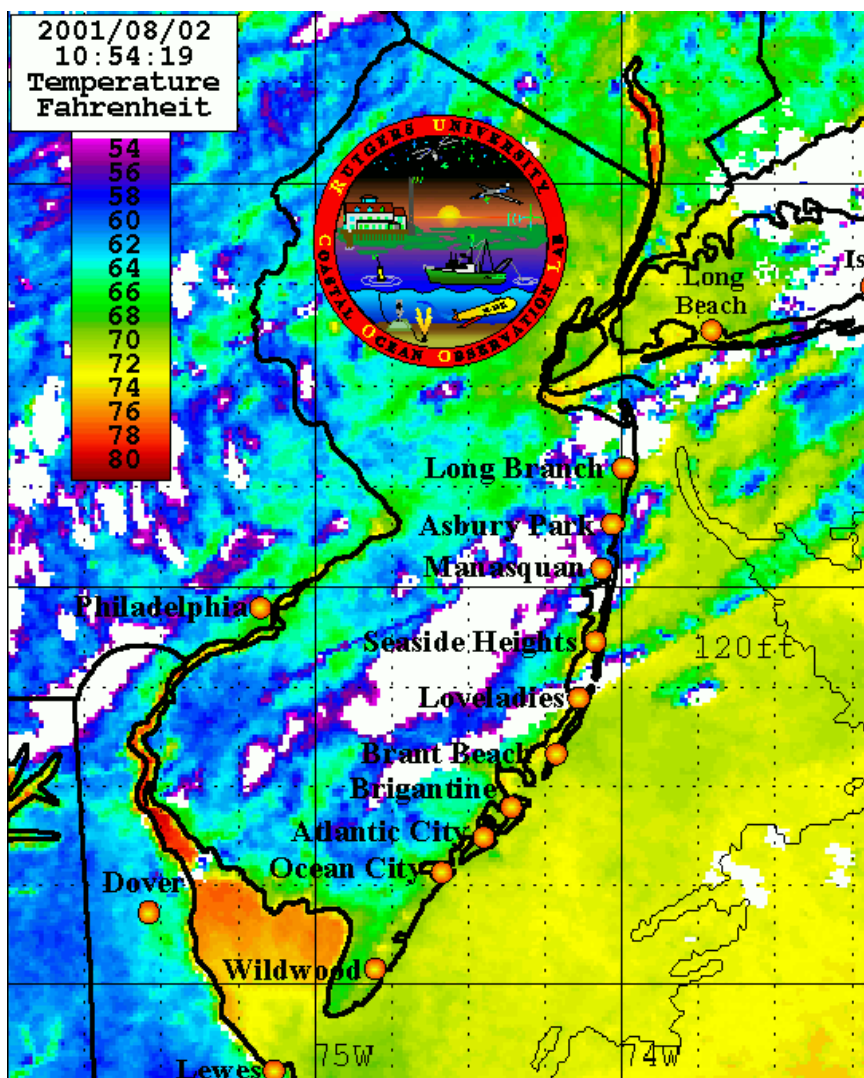


**Figure 31:** Sea surface temperature from AVHRR at 1054 GMT on August 2, 2001 showing no evidence of SST variation along the coast of New Jersey.

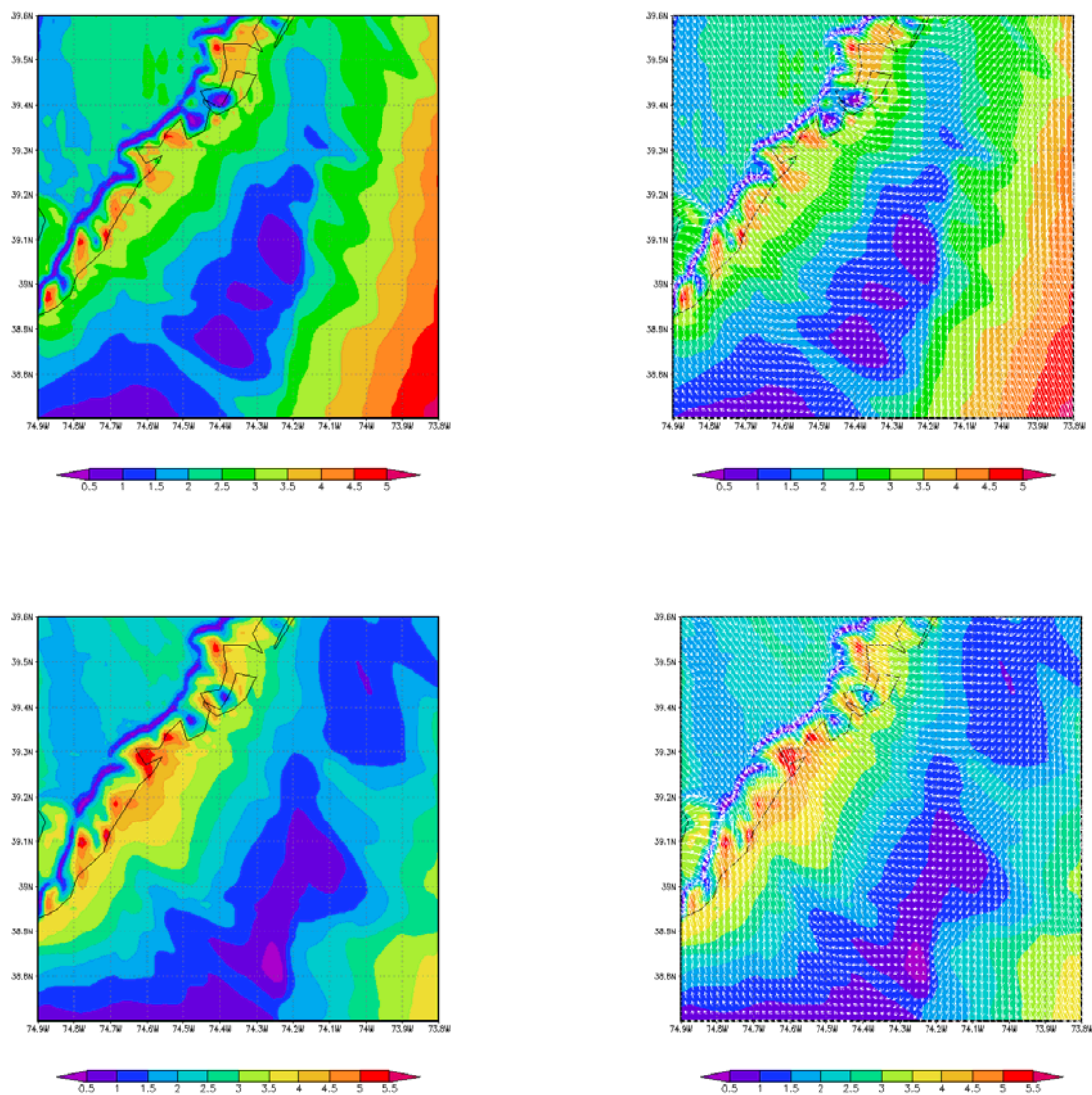


**Figure 32 a-d:** WRF model output for sea breeze simulation on April 16, 2004 zoomed into the offshore waters of southern New Jersey. Figure 24 a and b (upper-left and upper-right) show wind speed (m/s) (a) and wind speed and wind vectors (b) indicating zone of weak, divergent winds offshore at 1800 GMT. Figure 24 c and d (lower-left and lower-right) show the zone moving farther offshore as the inland penetration of the sea breeze front increases at 1900 GMT.

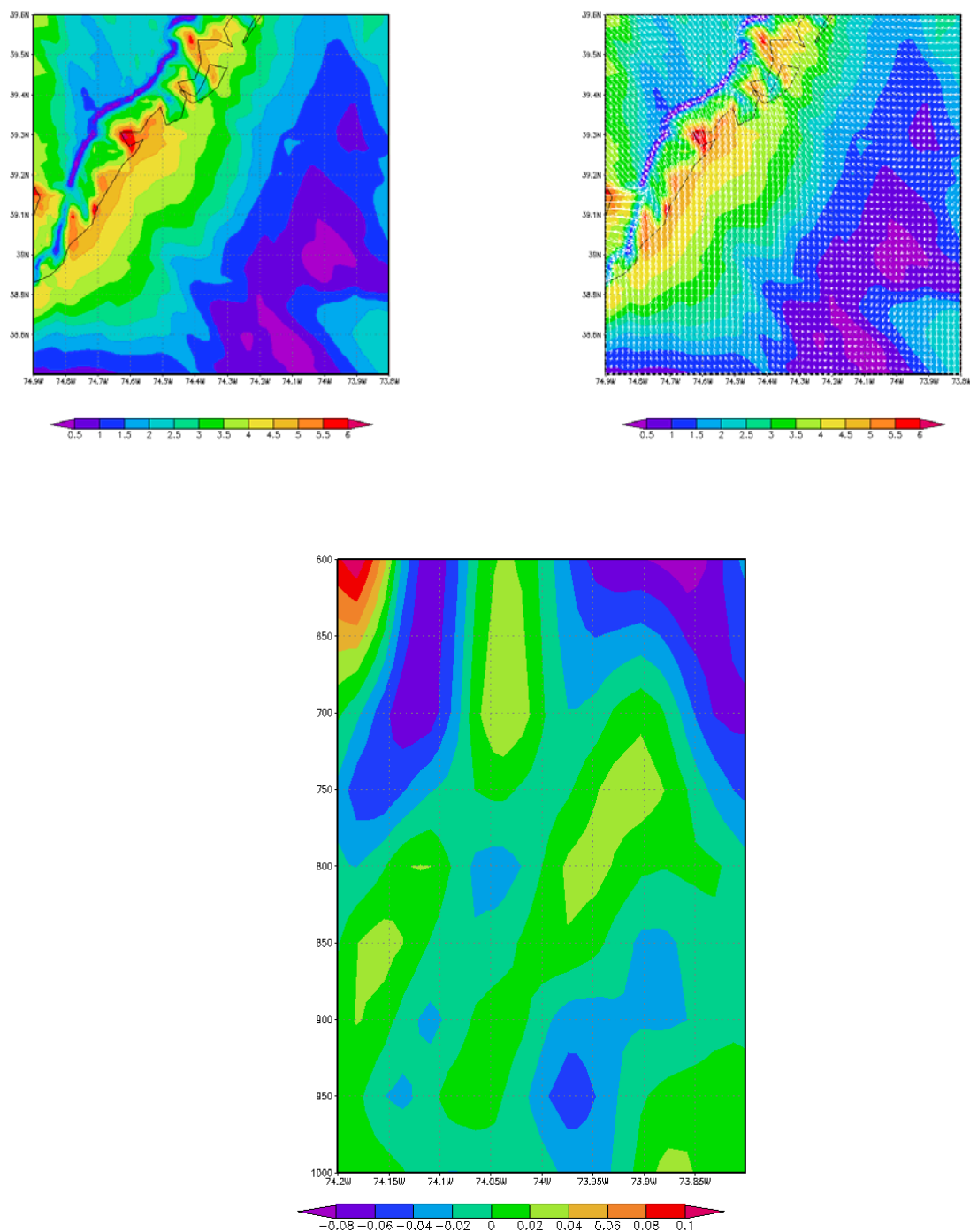


**Figure 32 e-g:** Figure 24 e and f (upper-left and upper-right) show wind speed and wind speed and wind vector for 2000 GMT indicating the zone of divergent winds moving increasingly farther offshore. Figure 24 g (bottom) shows a vertical cross-section through latitude  $39.0^{\circ}\text{N}$  from  $73.8^{\circ}\text{W}$  to  $74.2^{\circ}\text{W}$  of vertical velocity (m/s) at 2000 GMT. The largest sinking motion occurs in the center of the divergent wind zone.

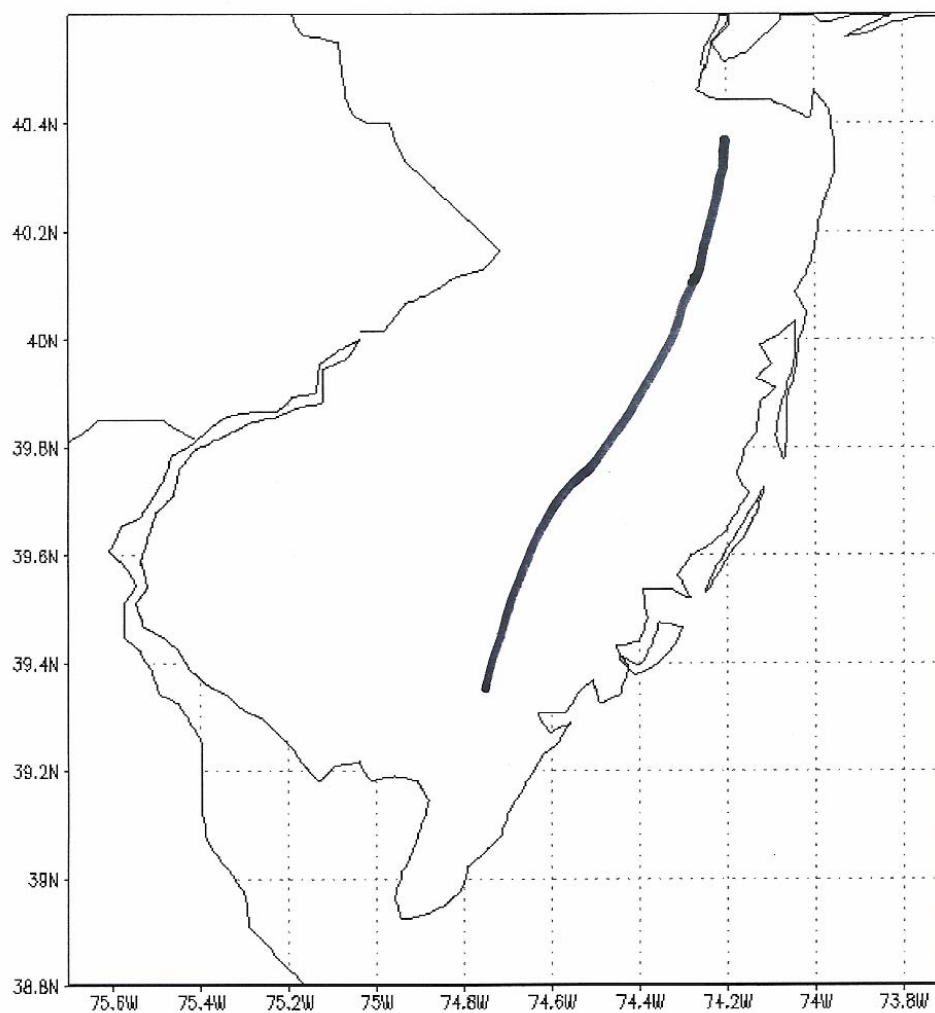


**Figure 33:** Radar reflectivity for July 5, 2004 at 2133 GMT showing the maximum inland extent of the sea breeze front.

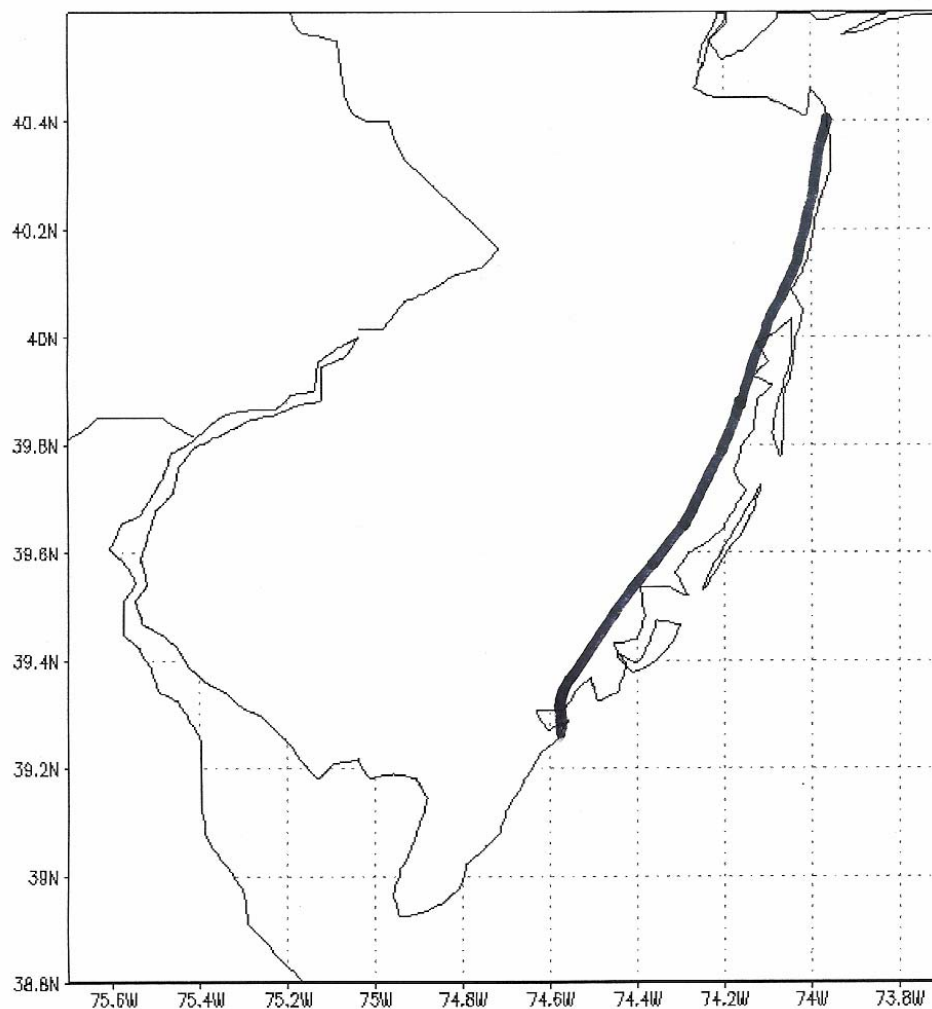


**Figure 34:** Radar reflectivity for July 6, 2004 at 2111 GMT showing the maximum inland extent of the sea breeze front.

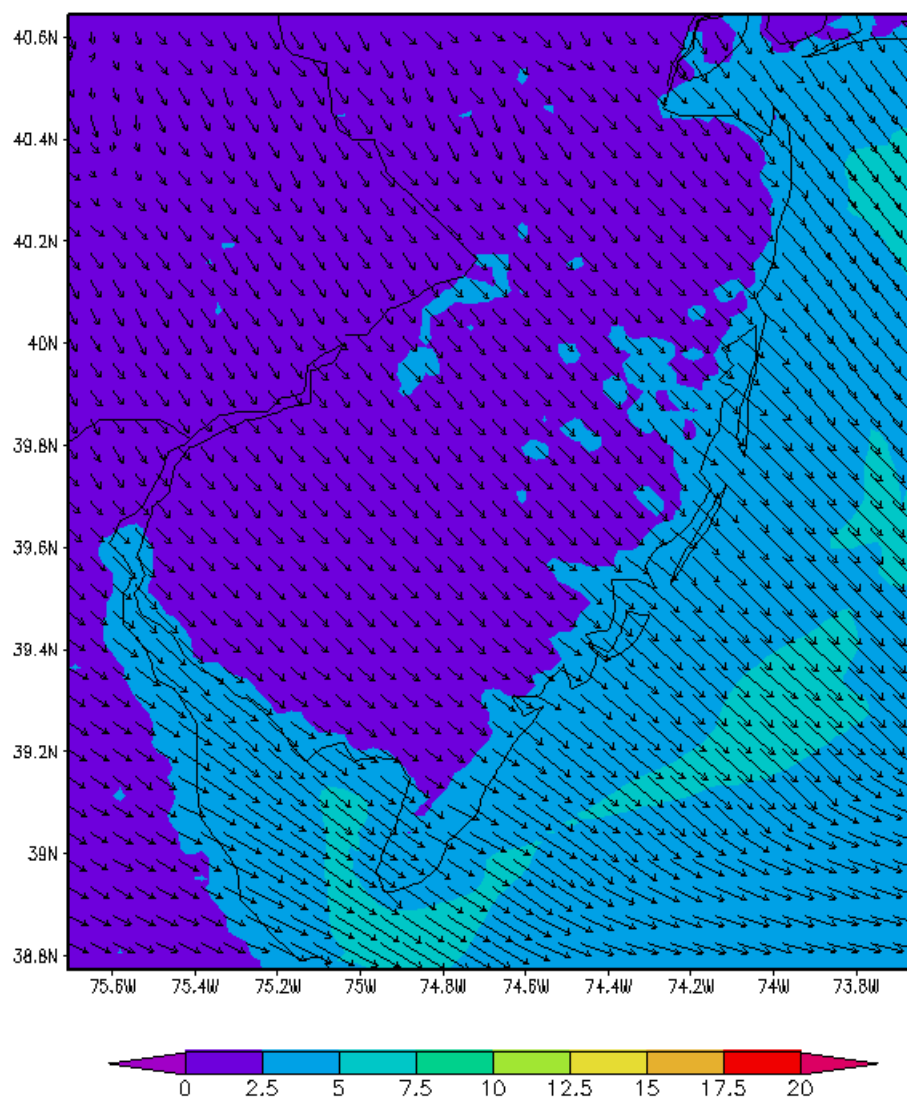


**Figure 35:** WRF model output showing 850 mb wind speed (m/s) and wind vector for July 5, 2004 at 1200 GMT.

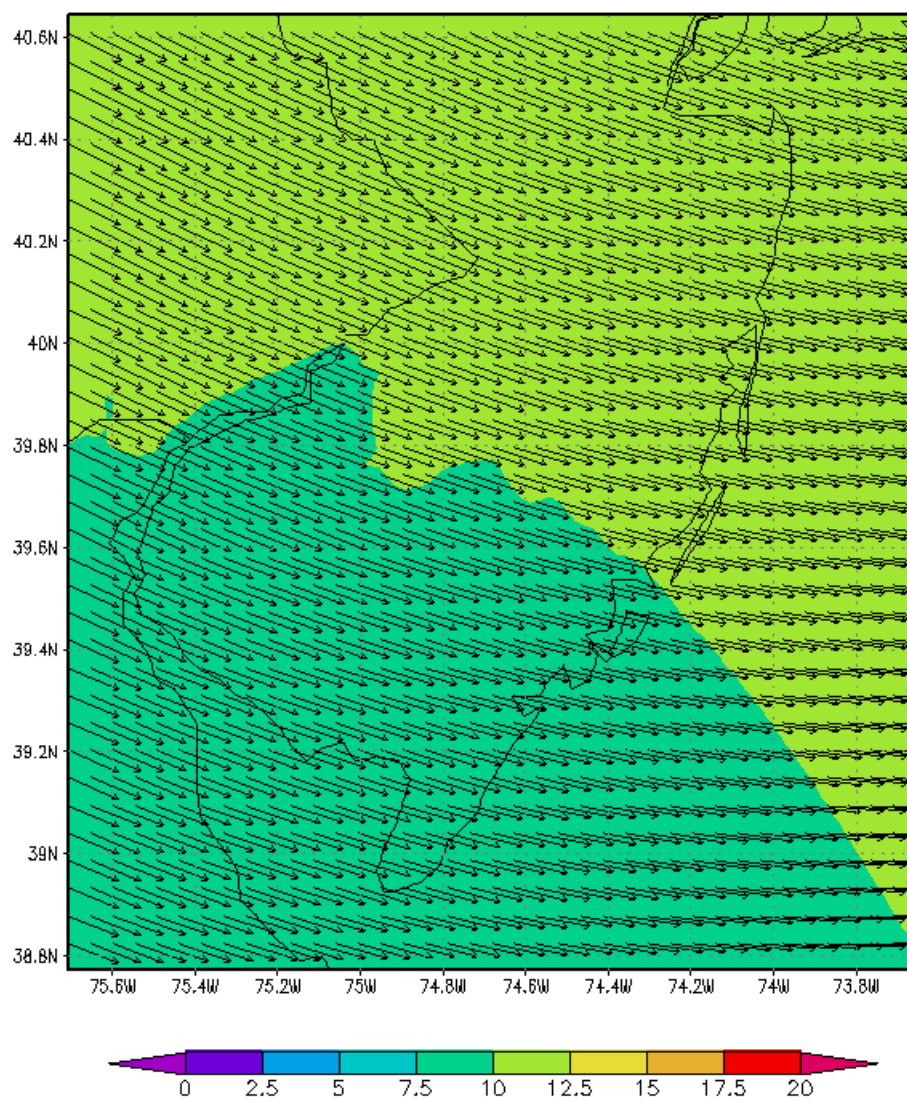


**Figure 36:** WRF model output showing 850 mb wind speed (m/s) and wind vector for July 6, 2004 at 1200 GMT.

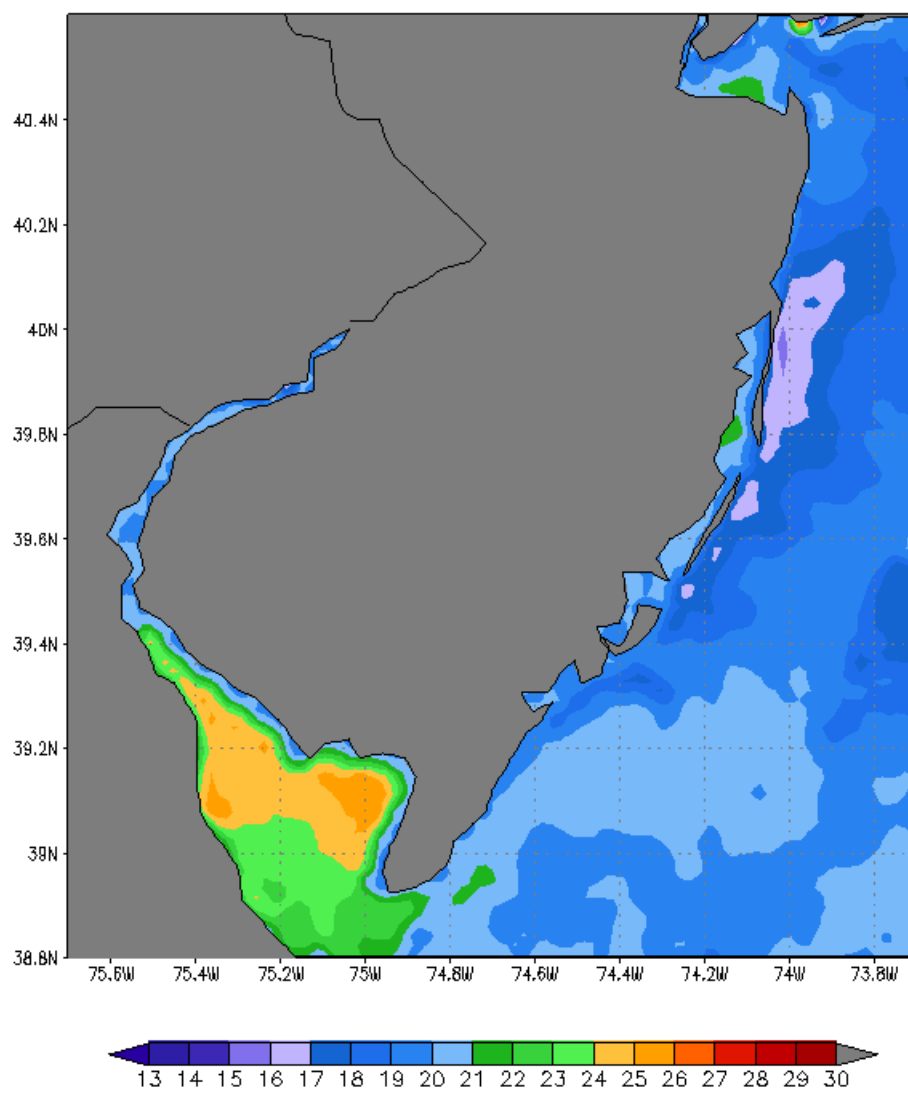


**Figure 37:** Sea surface temperature (°C) used for the actual SST case July 5, 2004.

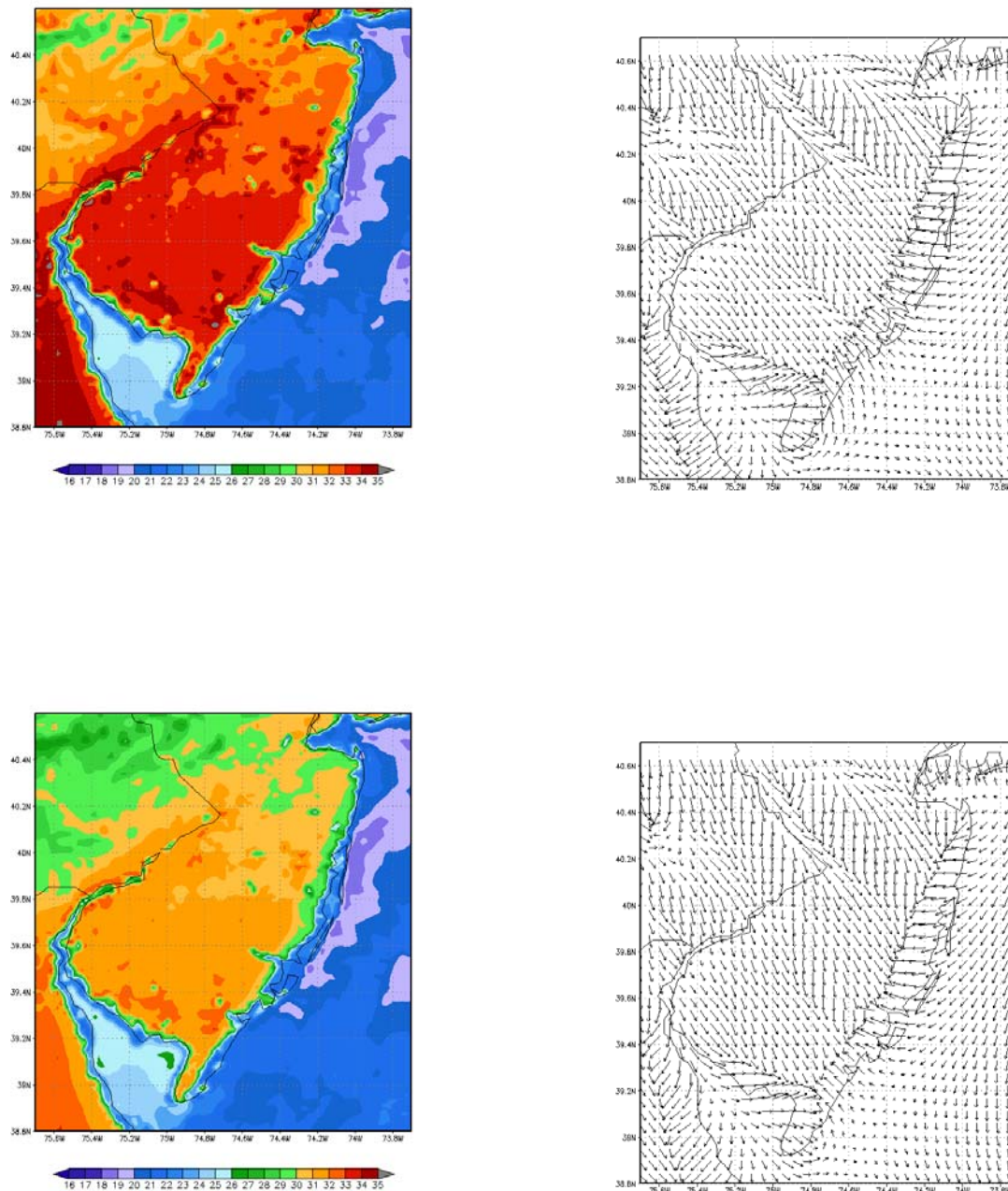


**Figure 38 a-d:** WRF model simulation output for the actual SST July 5, 2004 case study. Figure 29 (a, upper-left) and (b, upper-right) show 2 meter air temperature and wind vectors at 2000 GMT. Figure 29 (c, lower-left) and (d, lower-right) show the same, except for 2200 GMT.

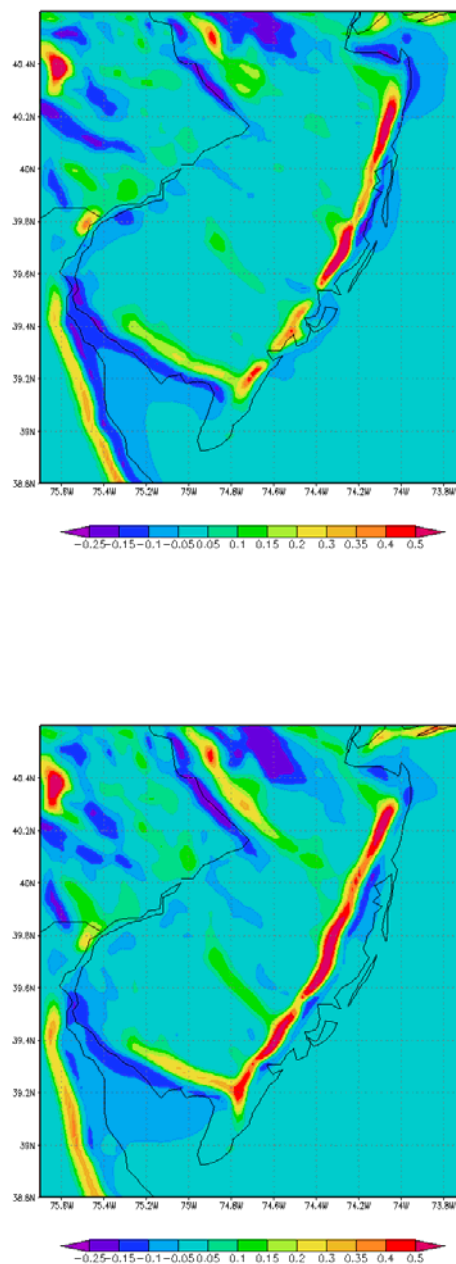


**Figure 39 a-b:** Vertical velocity at 500 m for 1700 GMT (a, top) and 2200 GMT (b, bottom). Areas of yellow and red (positive vertical velocity) along the coast correspond to the location of the sea breeze and Delaware Bay breeze fronts.

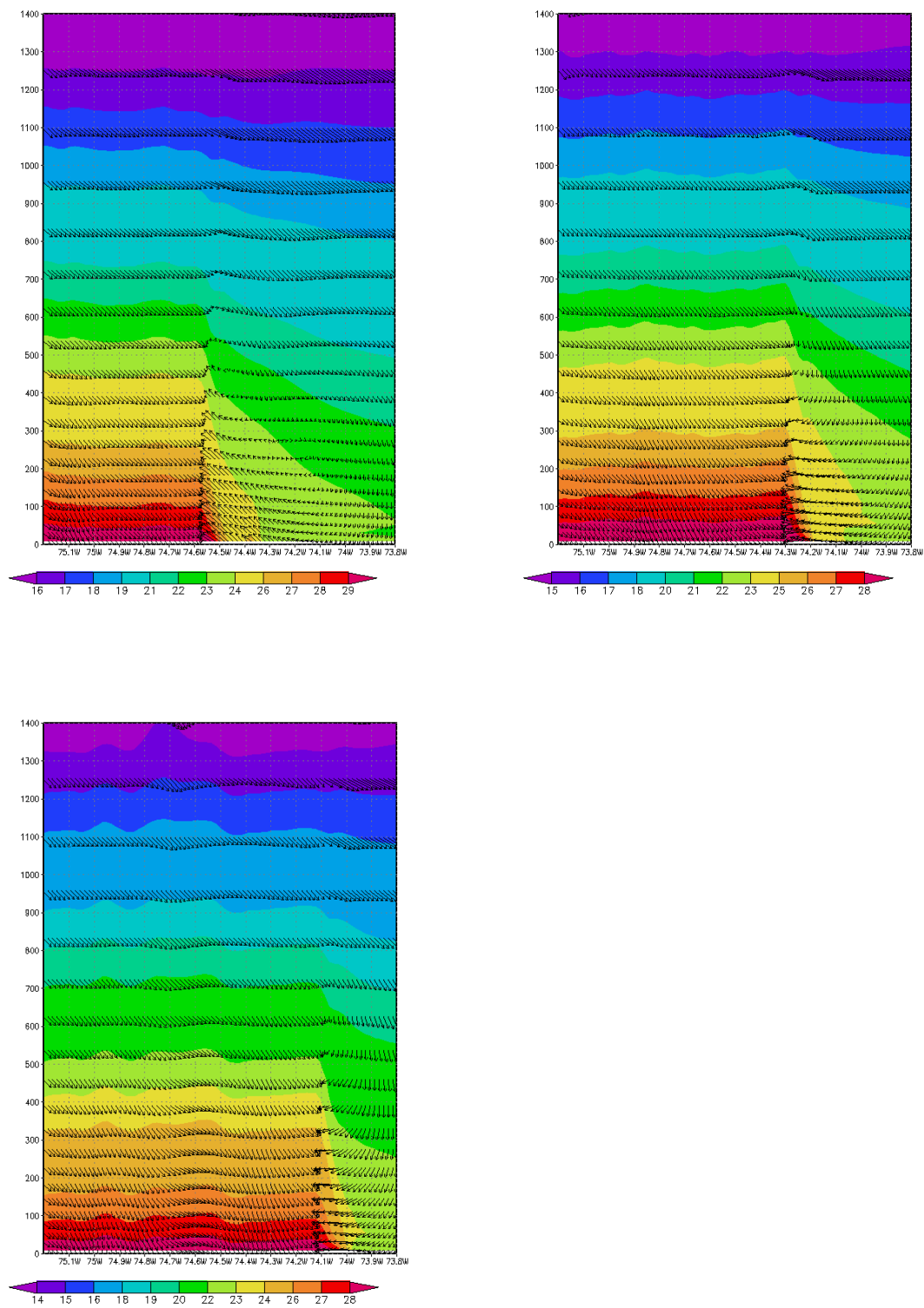


**Figure 40 a-c:** Vertical cross-section for 39.4°N (a, upper-left), 39.8°N (b, upper-right), and 40.2°N (c, lower-left) for 2000 GMT showing air temperature (°C) and wind vectors.

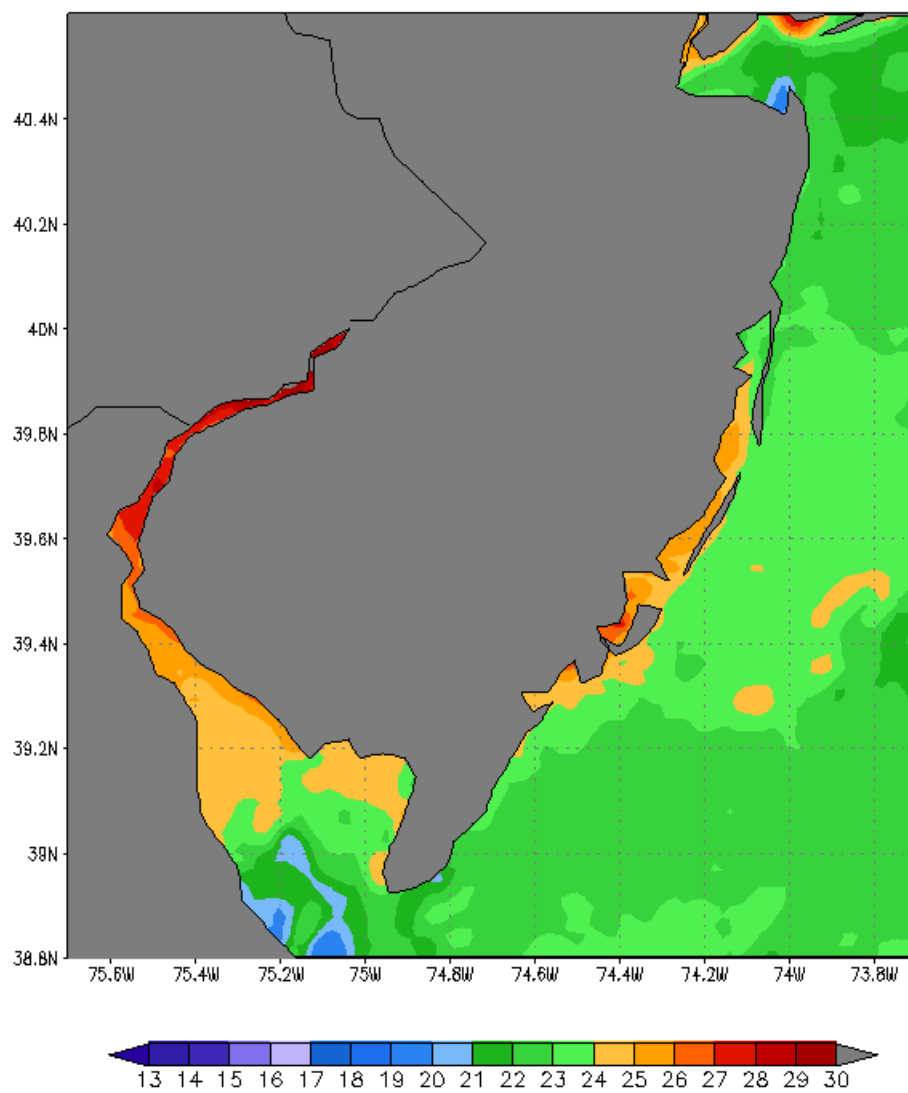


**Figure 41:** Sea surface temperature (°C) used for the July 16 SST case July 5, 2004.

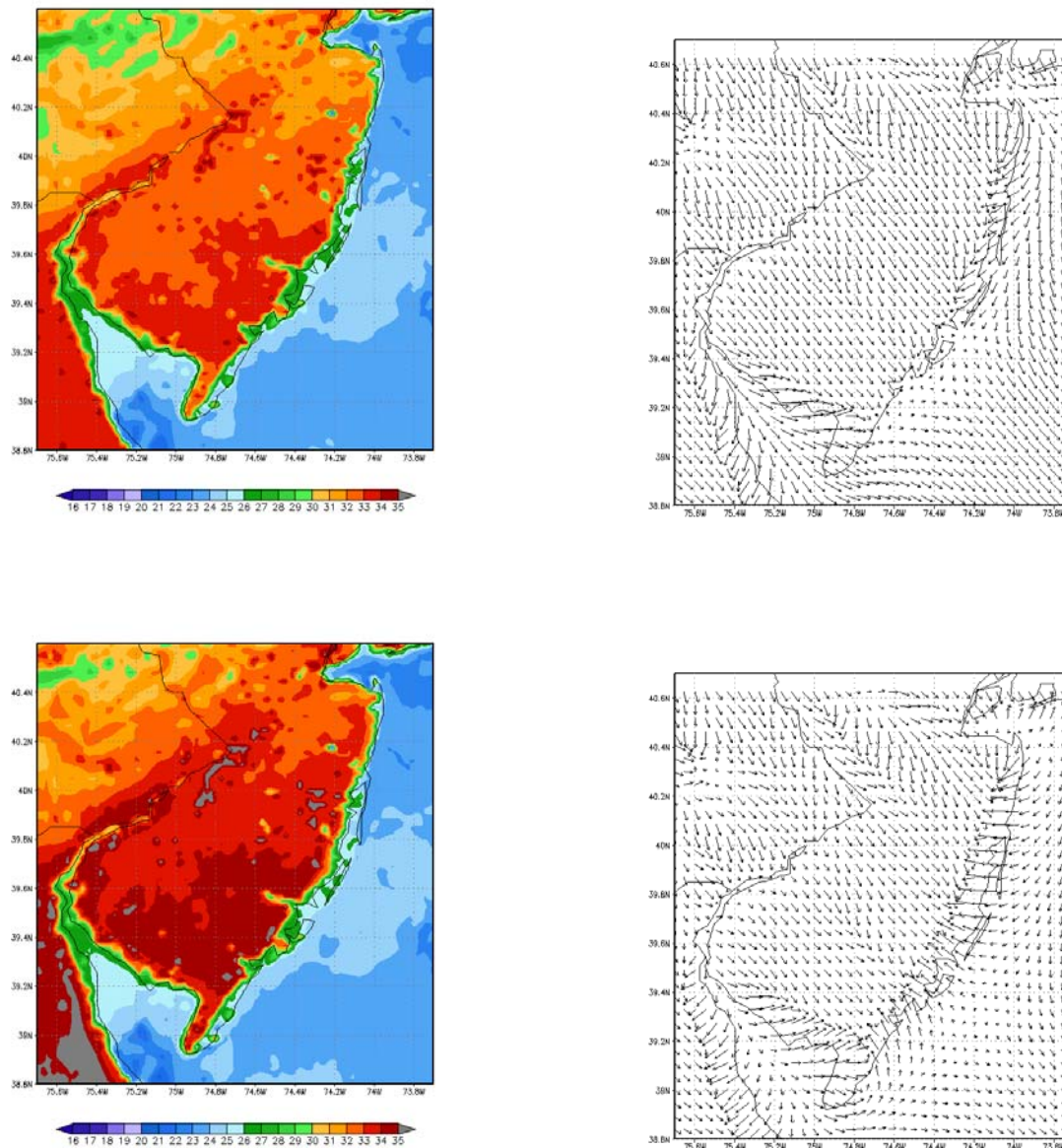


**Figure 42 a-d:** WRF model simulation output for the July 16 SST July 5, 2004 case study. Figure 33 (a, upper-left) and (b, upper-right) show 2 meter air temperature and wind vectors at 1600 GMT. Figure 33 (c, lower-left) and (d, lower-right) show the same, except for 1800 GMT.

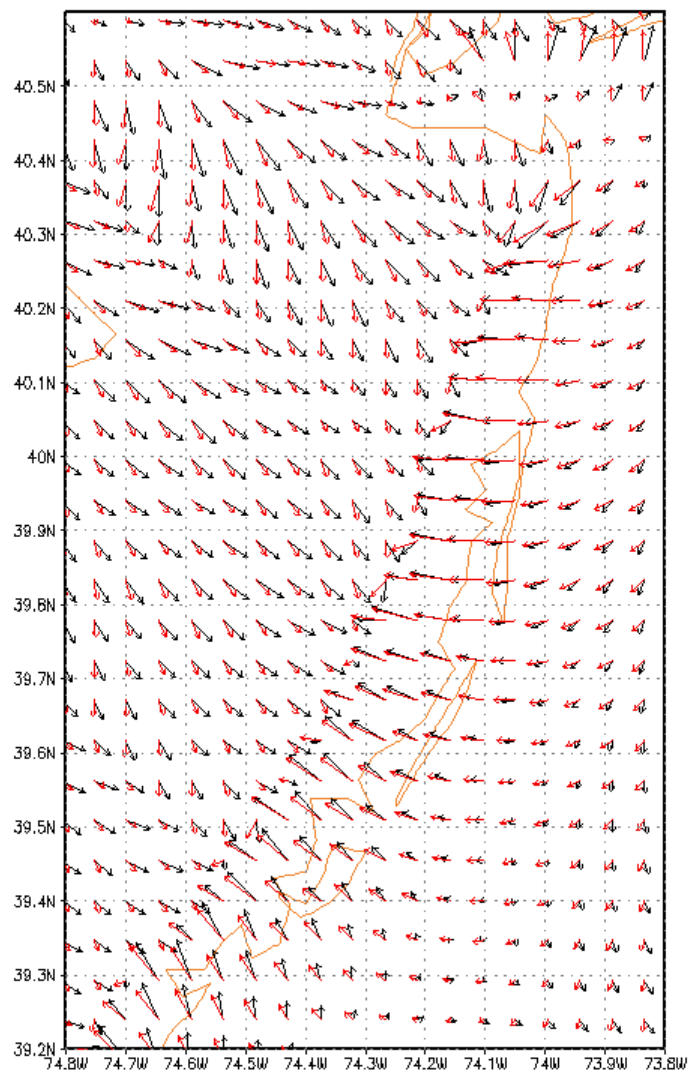


**Figure 43:** Wind vector difference at 2000 GMT. Wind vectors from the actual SST simulation are in red, and wind vectors from the July 16, 2004 SST, July 5 case study are in black. Very little difference is noted, except the wind vectors indicate slightly more inland penetration of the sea breeze front.

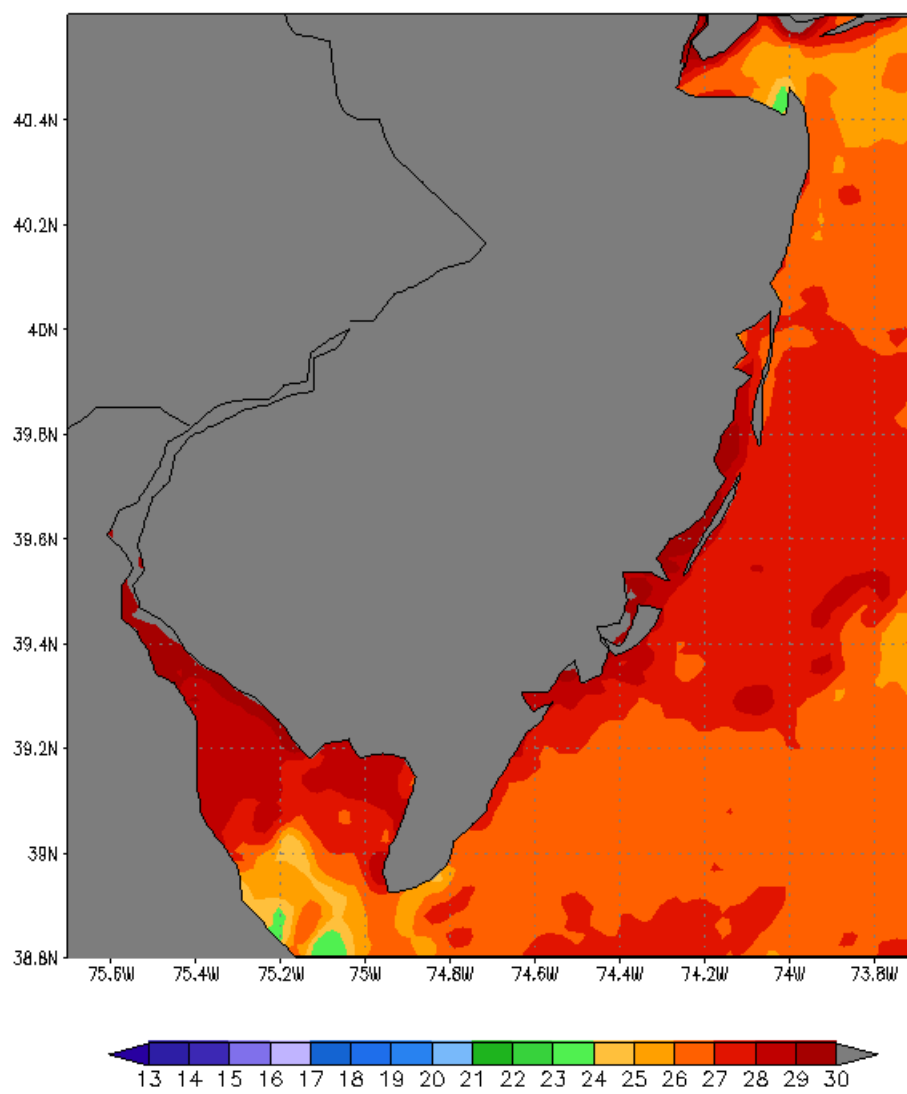


**Figure 44:** Sea surface temperature (°C) used for the Climatological Maximum SST case July 5, 2004.

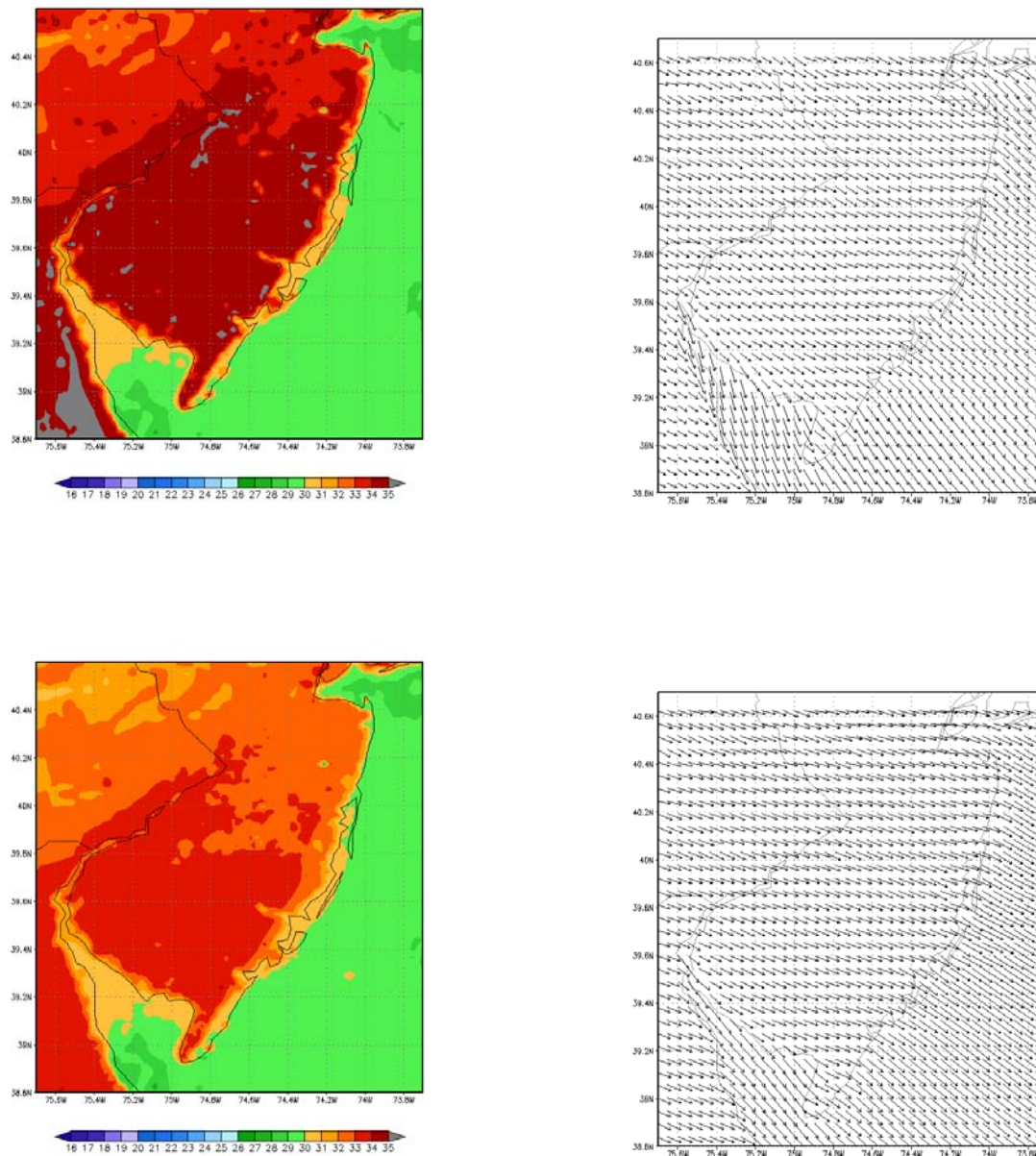


**Figure 45 a-d:** WRF model simulation output for the July 16 SST July 5, 2004 case study. Figure 36 (a, upper-left) and (b, upper-right) show 2 meter air temperature and wind vectors at 1800 GMT. Figure 36 (c, lower-left) and (d, lower-right) show the same, except for 2200 GMT.

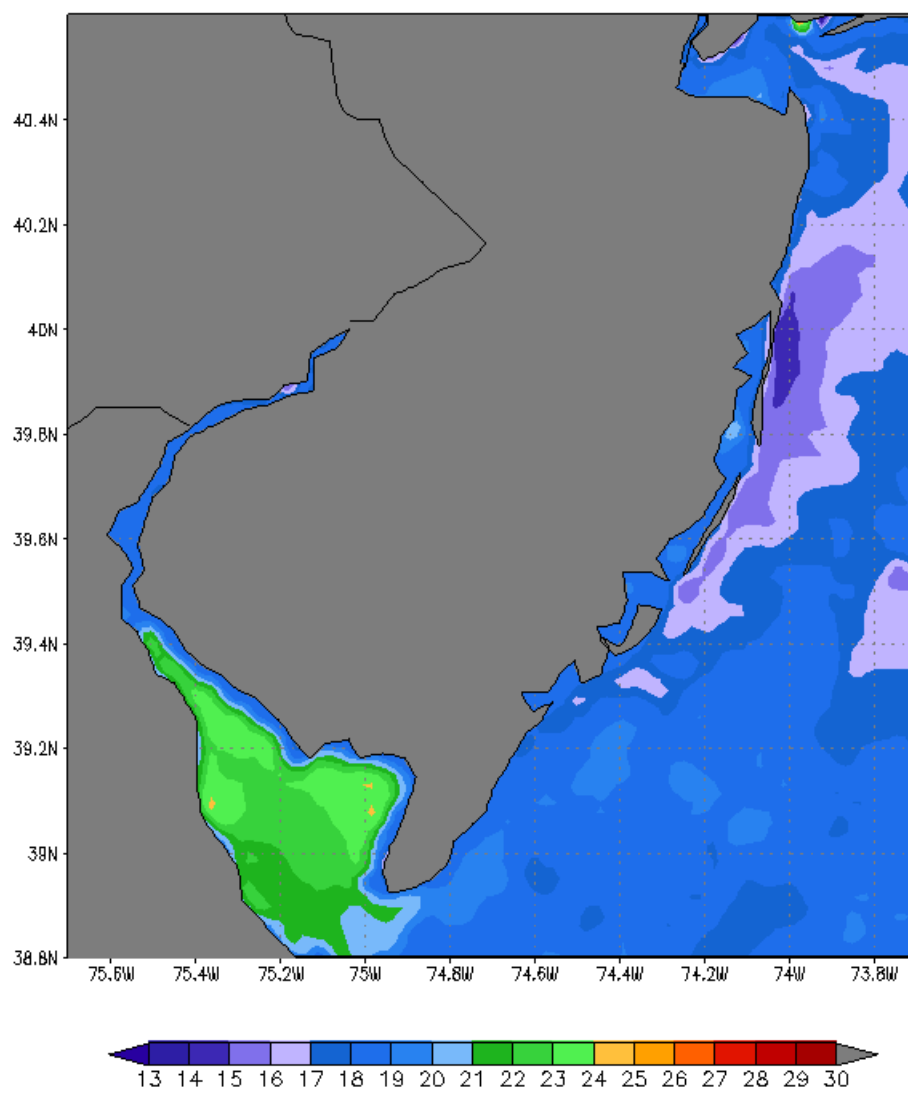


**Figure 46:** Sea surface temperature (°C) used for the actual SST case July 6, 2004.

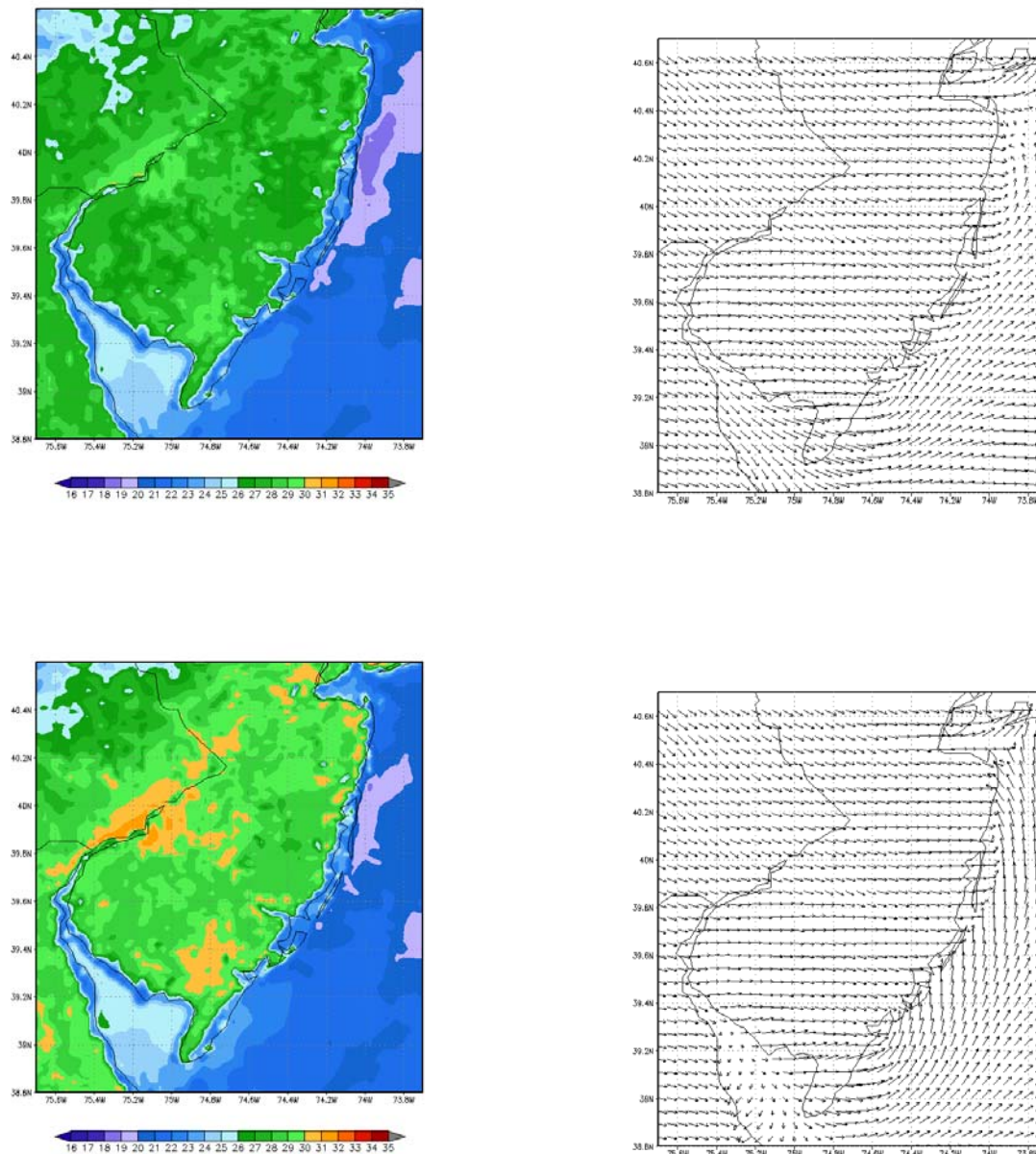


**Figure 47 a-d:** WRF model simulation output for the actual SST July 6, 2004 case study. Figure 39 (a, upper-left) and (b, upper-right) show 2 meter air temperature and wind vectors at 1600 GMT. Figure 39 (c, lower-left) and (d, lower-right) show the same, except for 1800 GMT.

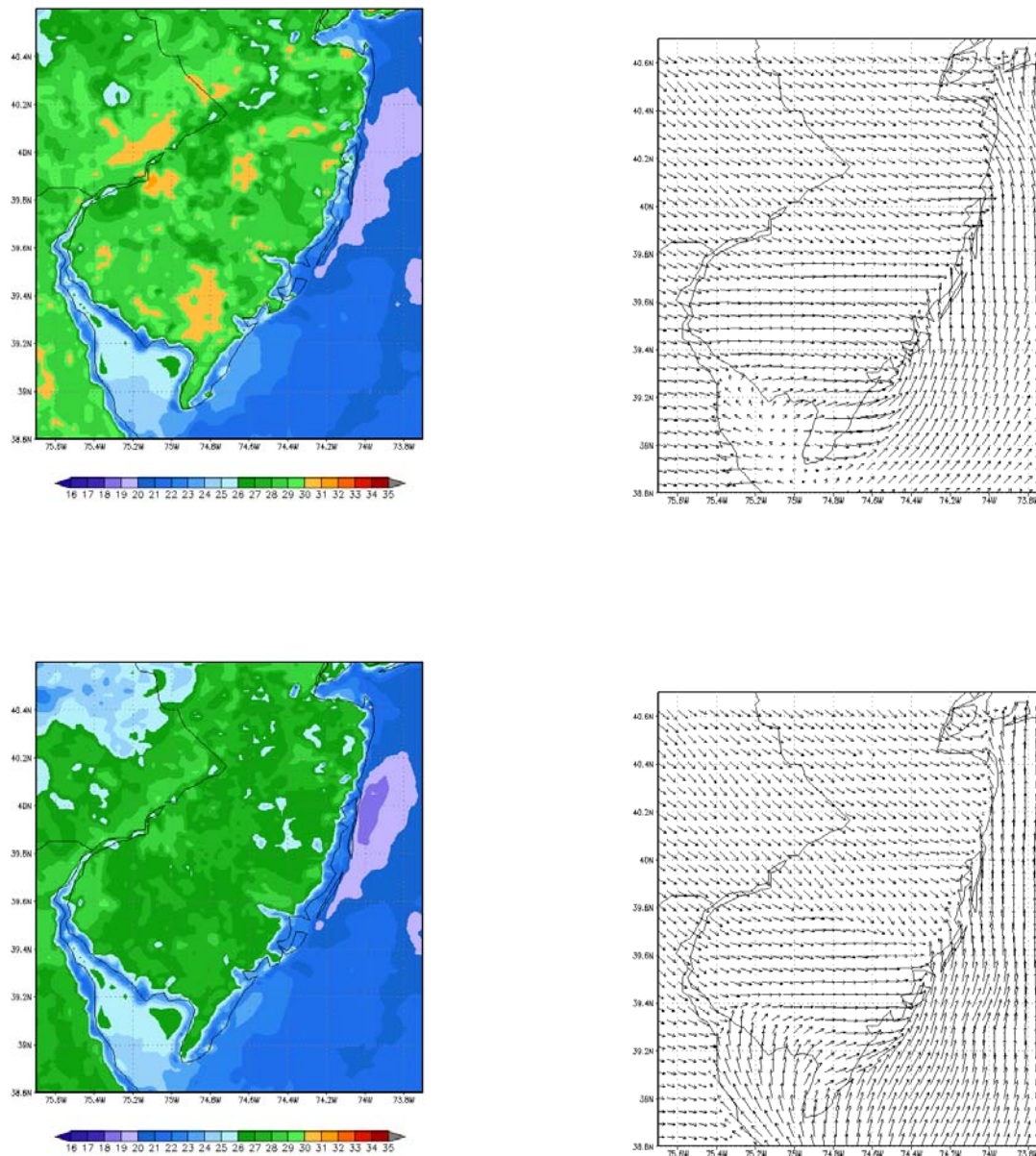


**Figure 47 e-h:** WRF model simulation output for the actual SST July 6, 2004 case study. Figure 39 (e, upper-left) and (f, upper-right) show 2 meter air temperature and wind vectors at 2000 GMT. Figure 39 (g, lower-left) and (h, lower-right) show the same, except for 2300 GMT.

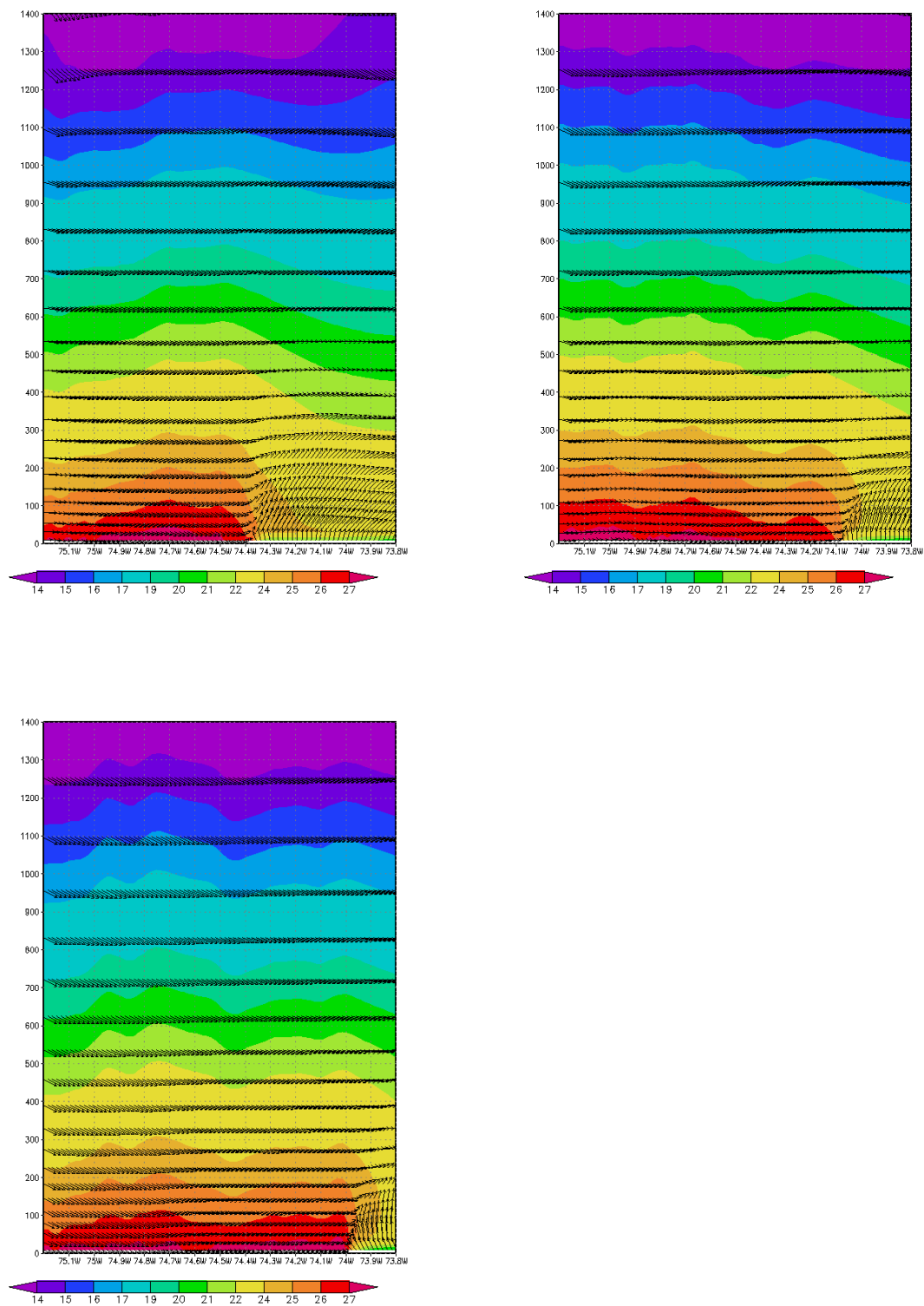


**Figure 48 a-c:** Vertical cross-section for 39.4°N (a, upper-left), 39.8°N (b, upper-right), and 40.2°N (c, lower-left) for 2000 GMT showing air temperature (°C) and wind vectors.

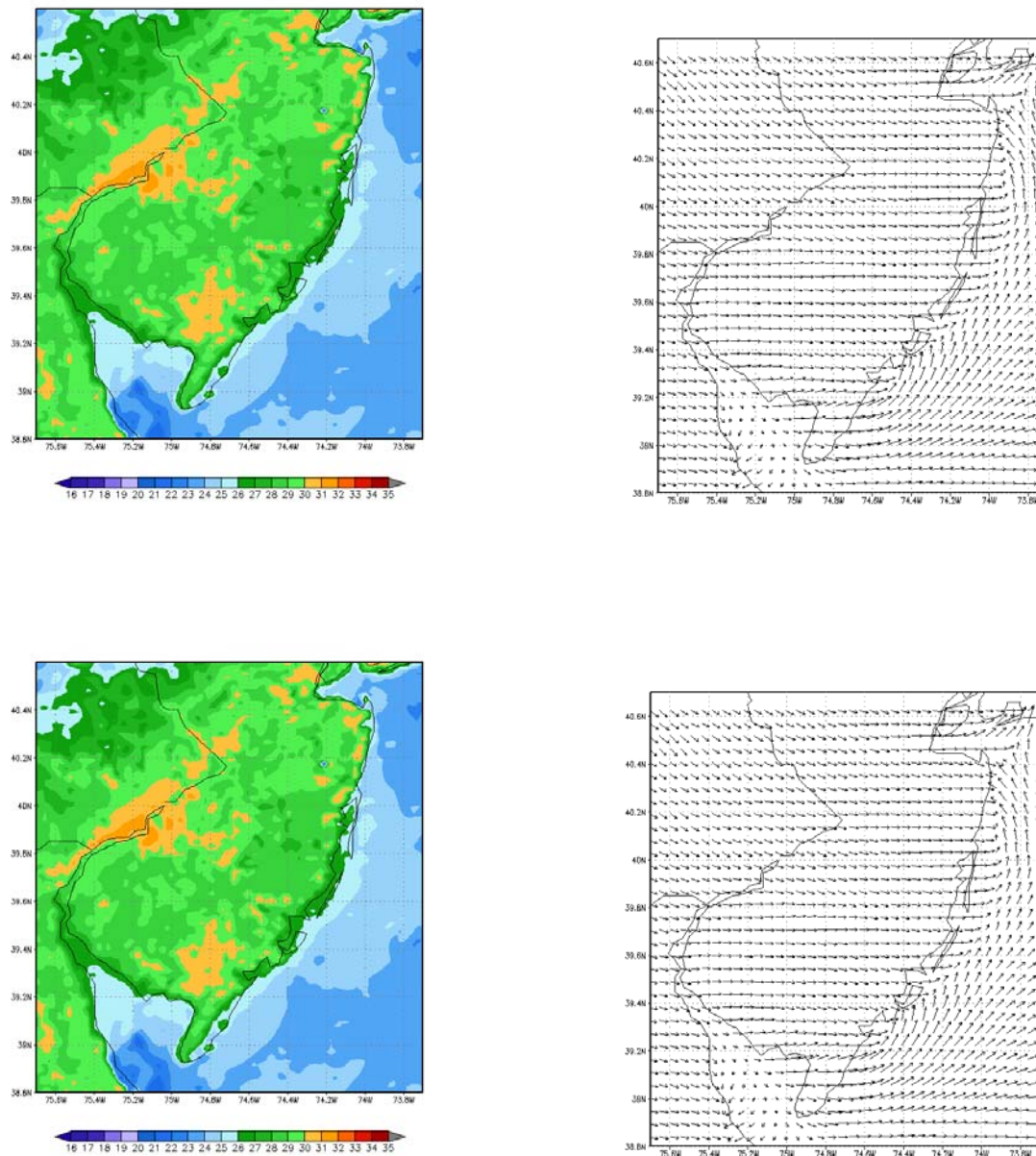


**Figure 49 a-d:** WRF model simulation output for the July 16, 2003 SST July 6, 2004 case study. Figure 41 (a, upper-left) and (b, upper-right) show 2 meter air temperature and wind vectors at 1600 GMT. Figure 39 (c, lower-left) and (d, lower-right) show the same, except for 1800 GMT.

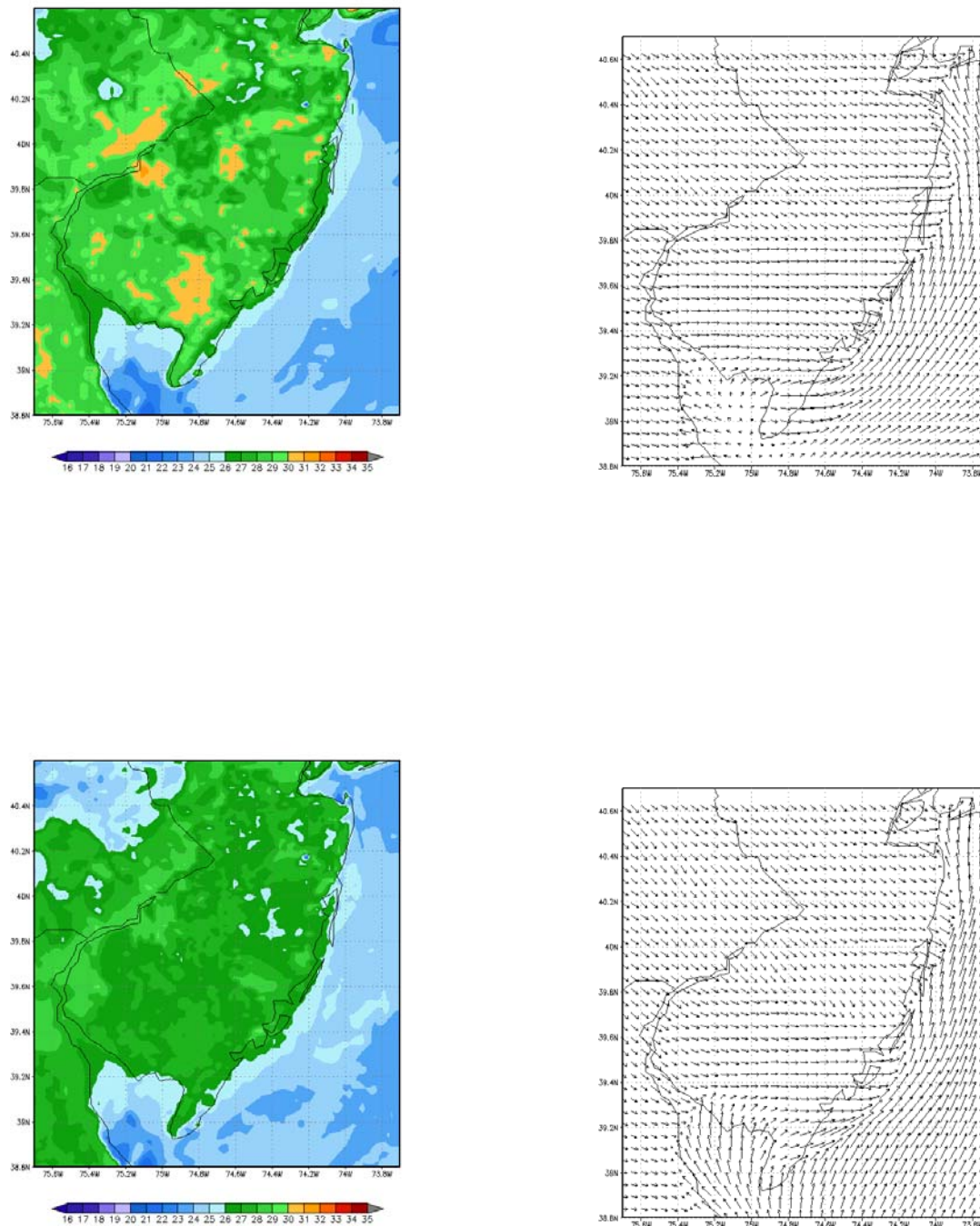


**Figure 49 e-h:** WRF model simulation output for the July 16, 2003 SST July 6, 2004 case study. Figure 41 (e, upper-left) and (f, upper-right) show 2 meter air temperature and wind vectors at 2000 GMT. Figure 41 (g, lower-left) and (h, lower-right) show the same, except for 2300 GMT.

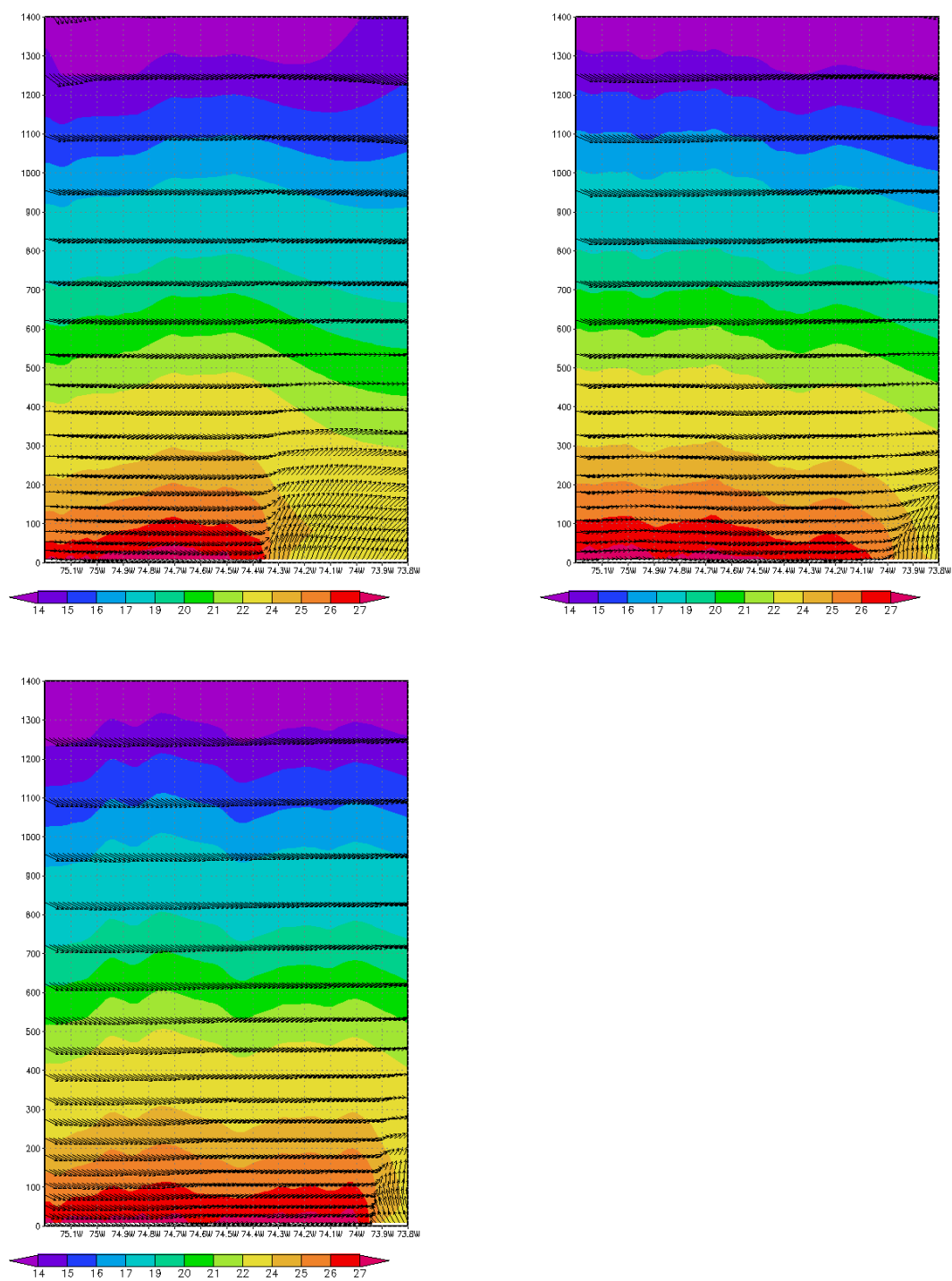


**Figure 50 a-c:** Vertical cross-section for 39.4°N (a, upper-left), 39.8°N (b, upper-right), and 40.2°N (c, lower-left) for 2000 GMT showing air temperature (°C) and wind vectors.

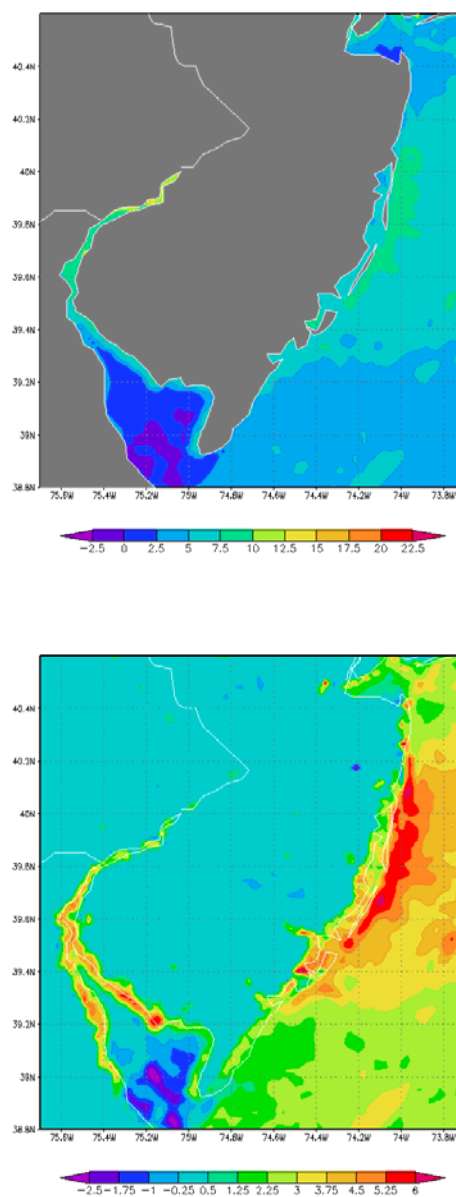


**Figure 51 a-b:** Figure 43 a (top) shows the difference in SST ( $^{\circ}\text{C}$ ) between the actual July 6, 2004 SST and the July 16, 2004 SST. A positive temperature difference indicates that the July 16, 2004 SST was warmer than the July 6, 2004 SST. Figure 43 b (bottom) shows the difference in 2 meter temperature between the two cases as 2000 GMT. A positive value indicates that the simulated 2 meter air temperature in the July 16, 2004 SST case is warmer than the air temperature from the July 6, 2004 SST case.

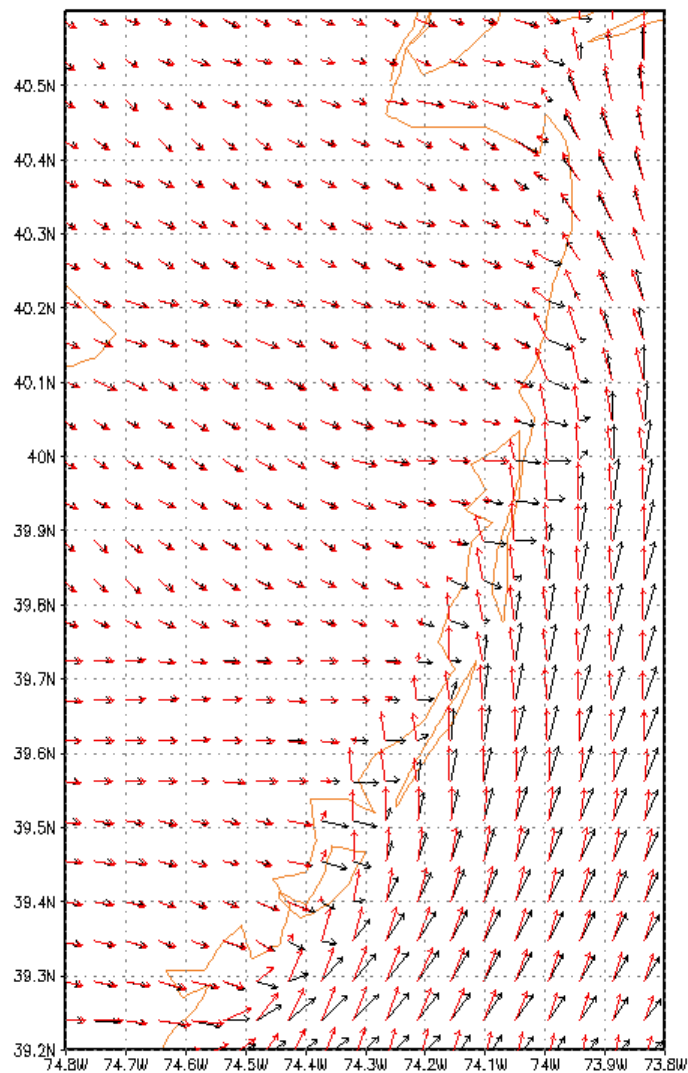


**Figure 51 c:** Wind vector difference at 2200 GMT. Wind vectors from the actual SST simulation are in red and wind vectors from the July 16, 2004 SST, July 6 case study are in black. A difference in the position of the sea breeze front of 6 km northern areas and 18 km in southern areas is noted. The largest change in wind direction is south of the upwelling region.

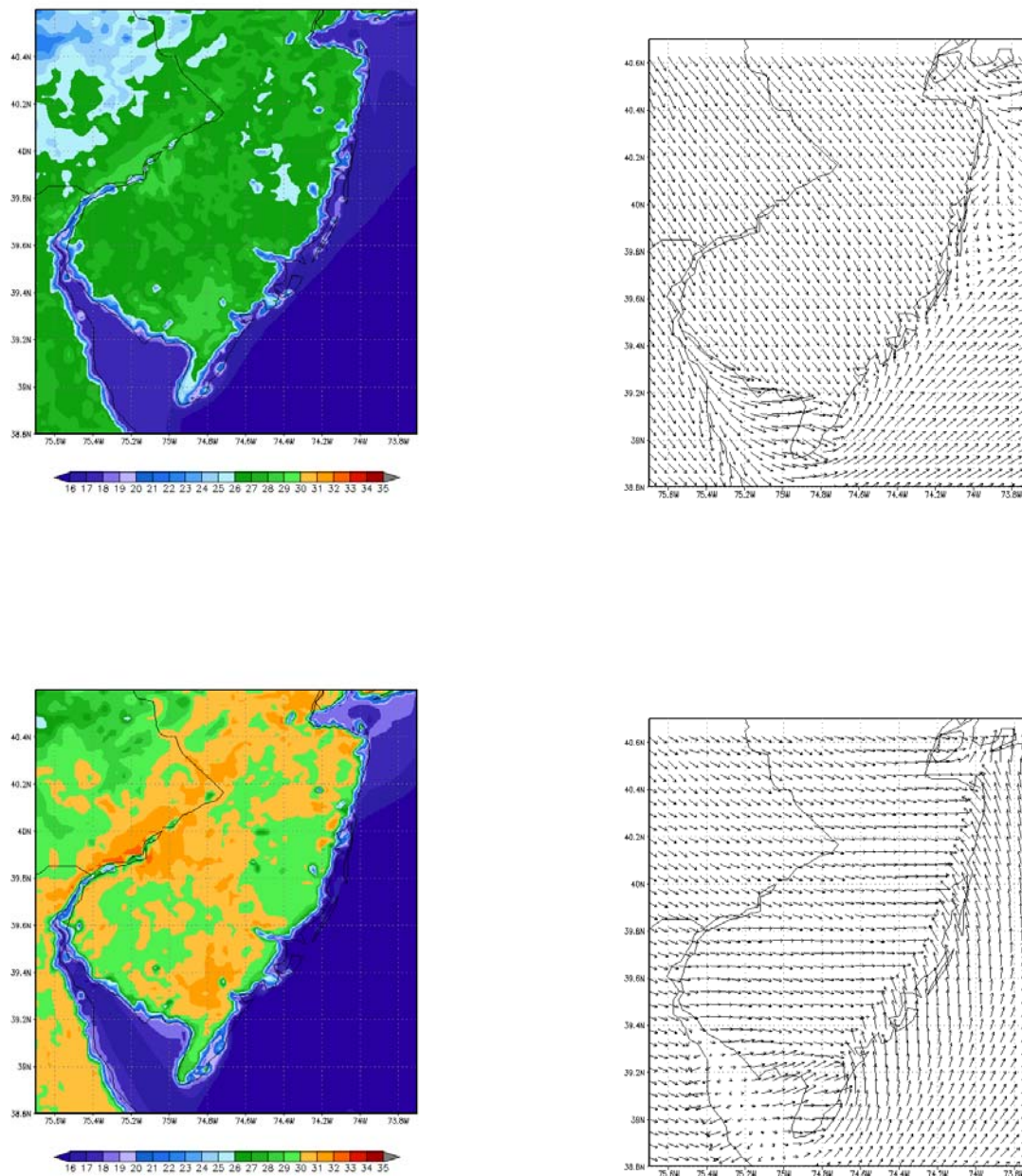


**Figure 52 a-d:** WRF model simulation output for the uniform 15°C July 6, 2004 sensitivity case study. Figure 45 (a, left) and (b, right) show 2 meter air temperature and wind vectors at 1500 GMT. Figure 45 (c, lower-left) and (d, lower-right) show the same, except for 1800 GMT.

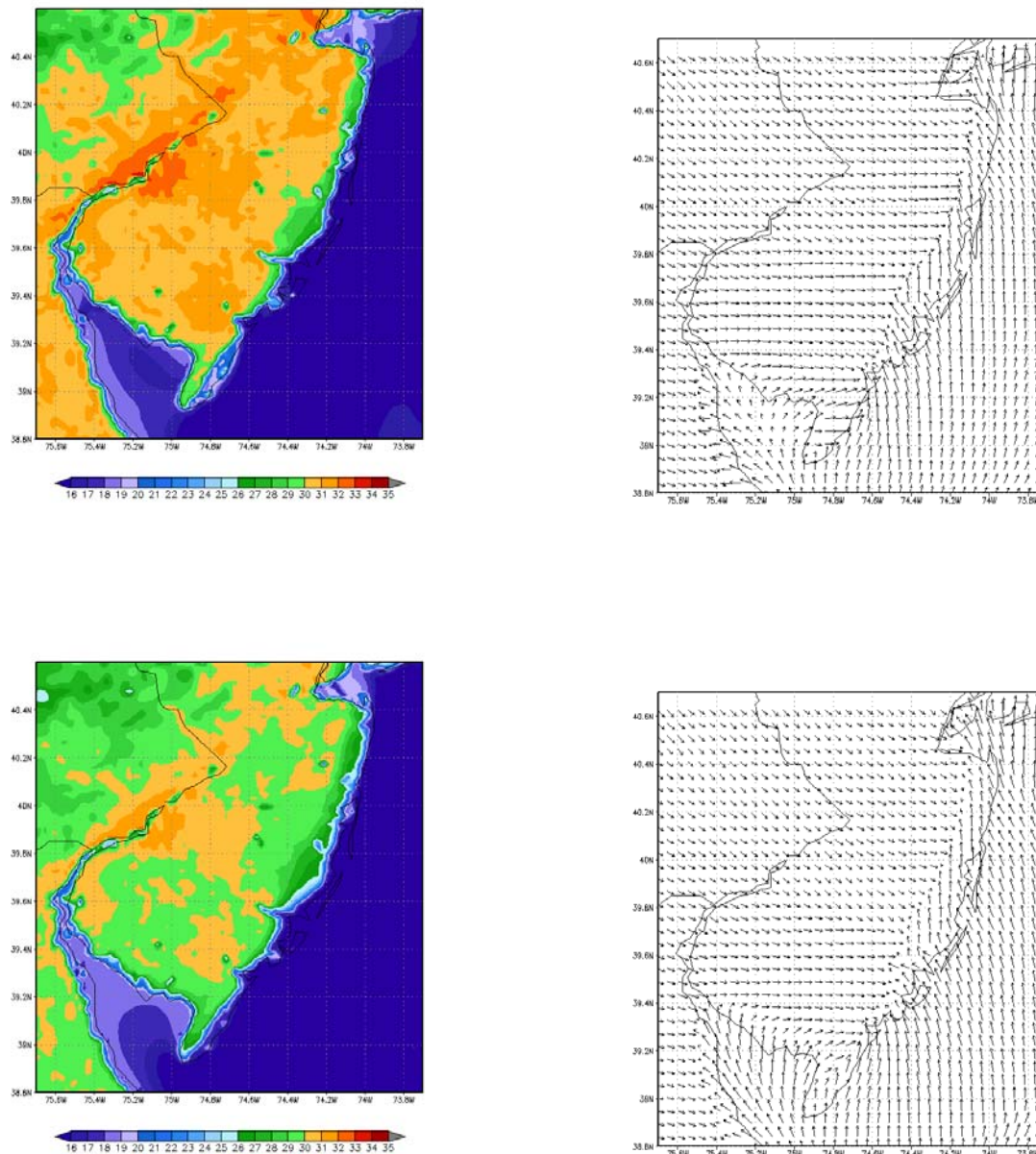


**Figure 52 e-h:** WRF model simulation output for the uniform 15°C July 6, 2004 sensitivity case study. Figure 45 (e, left) and (f, right) show 2 meter air temperature and wind vectors at 2000 GMT. Figure 45 (g, lower-left) and (h, lower-right) show the same, except for 2200 GMT.

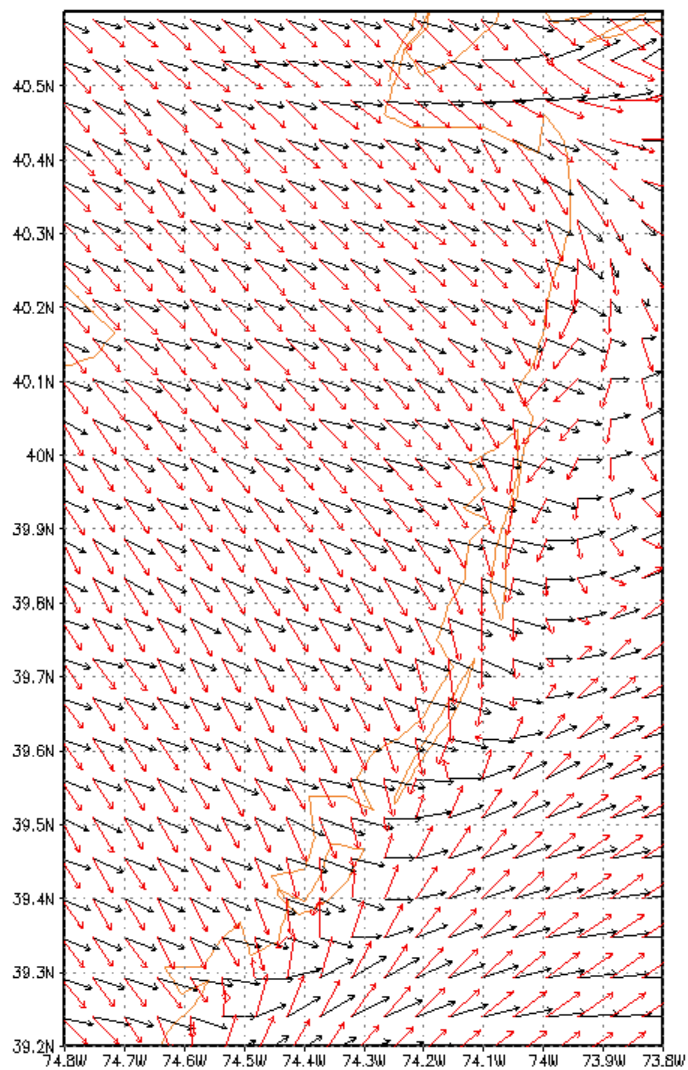


**Figure 53 a:** Wind vector difference at 1600 GMT. Wind vectors from the uniform 15°C SST simulation are in red and wind vectors from the uniform 17°C SST sensitivity case study are in black. Onshore wind vectors are noted near the shoreline in the 15°C SST case indicating the onset of the sea breeze.

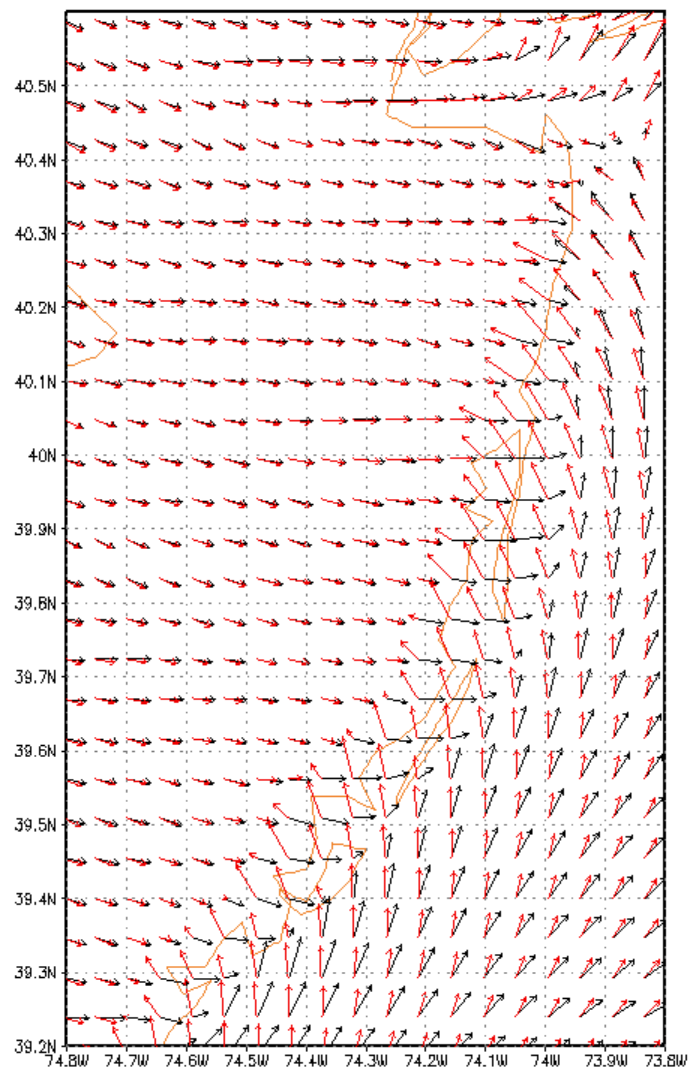


**Figure 53 b:** Wind vector difference at 1800 GMT. Wind vectors from the uniform 15°C SST simulation are in red and wind vectors from the uniform 17°C SST sensitivity case study are in black. An onshore component in the 15°C SST case is noted between 12 and 18 km farther inland than the 17°C SST wind vectors south of Asbury Park.

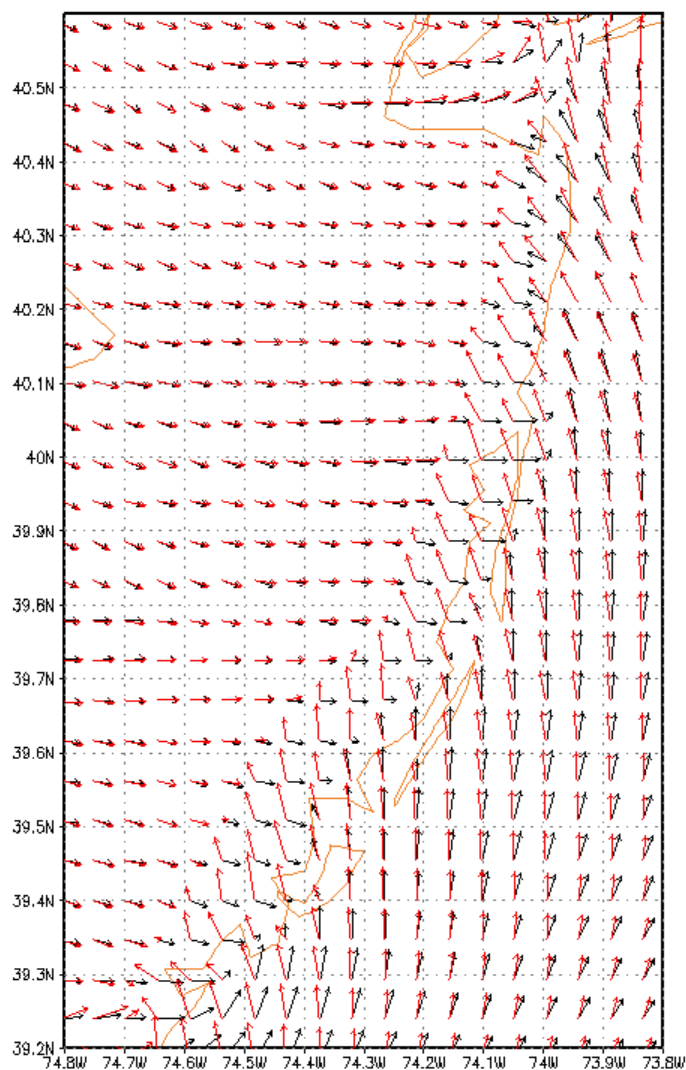


**Figure 53 c:** Wind vector difference at 2000 GMT. Wind vectors from the uniform 15°C SST simulation are in red and wind vectors from the uniform 17°C SST sensitivity case study are in black. An onshore component in the 15°C SST case is noted about 6 km along northern portions of the coastline and between 12 and 18 km farther inland than the 17°C SST wind vectors.

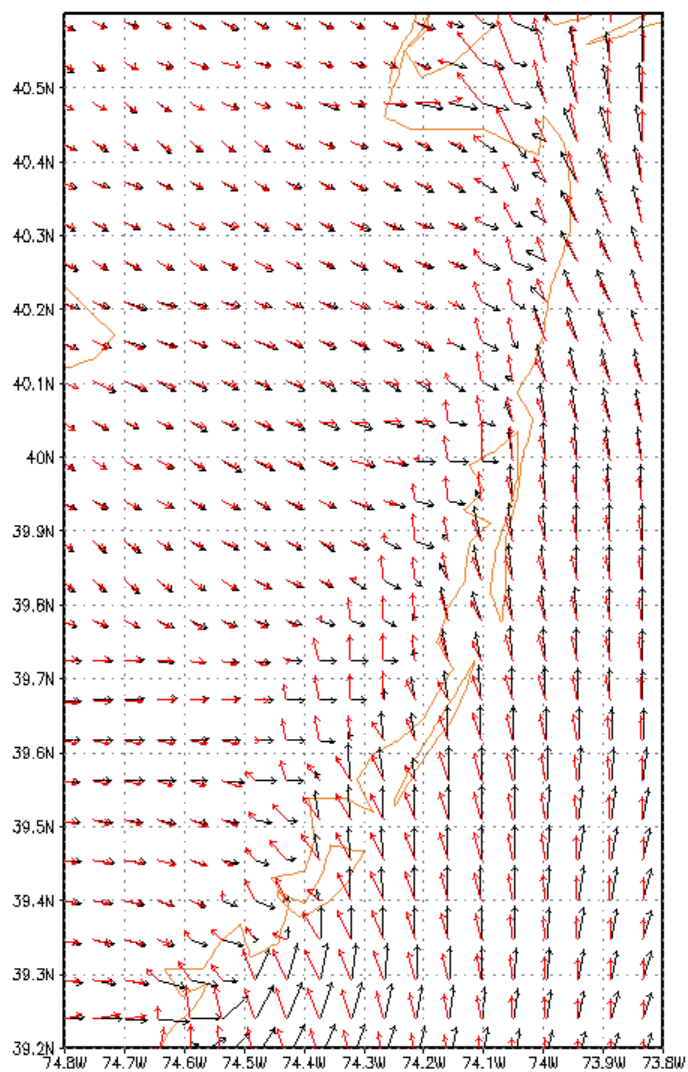


**Figure 53 d:** Wind vector difference at 2200 GMT. Wind vectors from the uniform 15°C SST simulation are in red and wind vectors from the uniform 17°C SST sensitivity case study are in black. An onshore component in the 15°C SST case is noted between 12 and 18 km farther inland than the 17°C SST wind vectors.

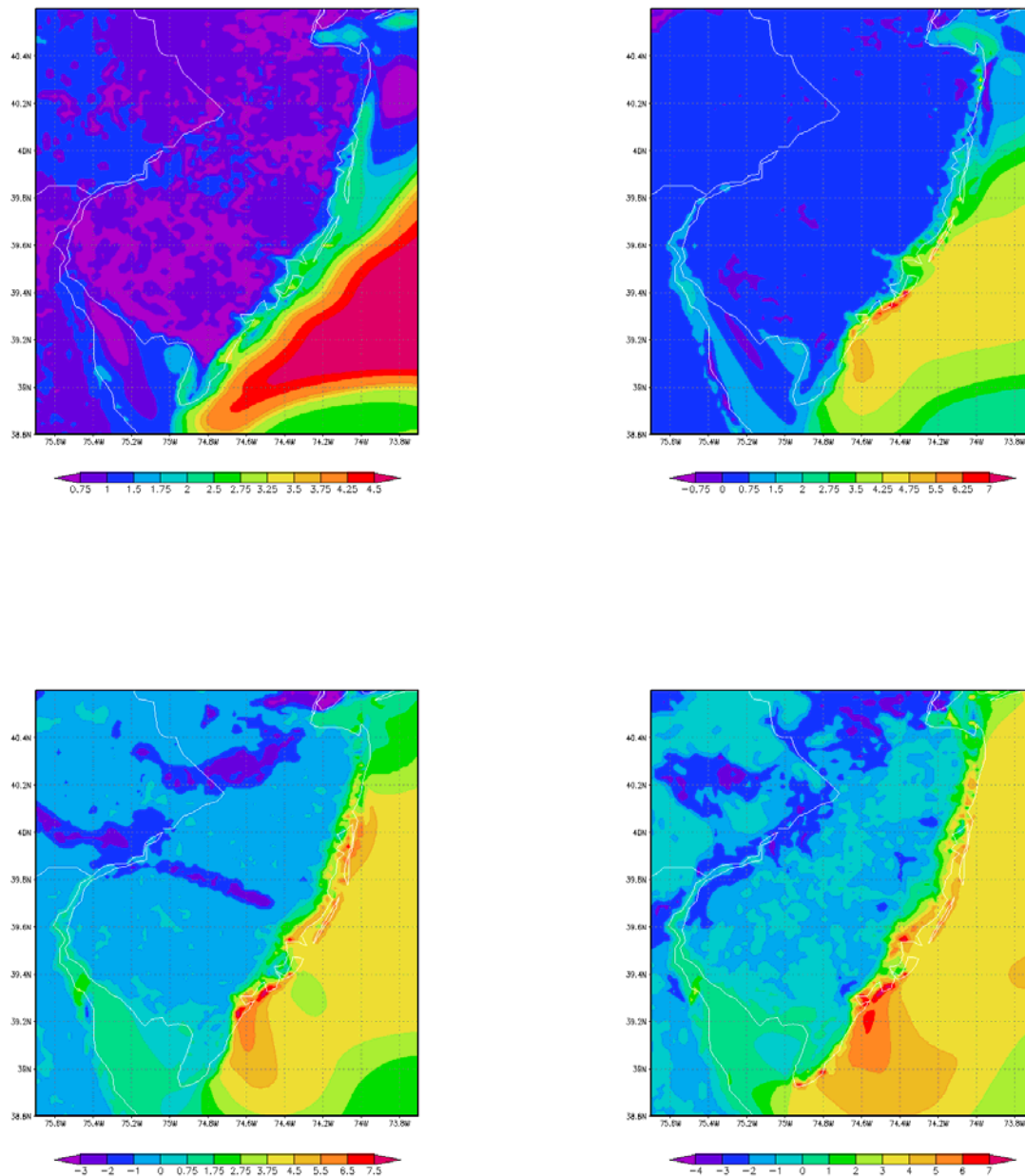


**Figure 54 a-d:** Air temperature at 2 meters difference ( $^{\circ}\text{C}$ ) between uniform  $15^{\circ}\text{C}$  July 6, 2004 and uniform  $17^{\circ}\text{C}$  July 6, 2004 sensitivity case studies. Figure 45 (a, upper-left) at 1600 GMT, (b, upper-right) at 1800 GMT, (c, lower-left) at 2000 GMT, and (d, lower-right) at 2200 GMT. Positive values indicate warmer 2 m air temperatures for the uniform  $17^{\circ}\text{C}$  sensitivity case.

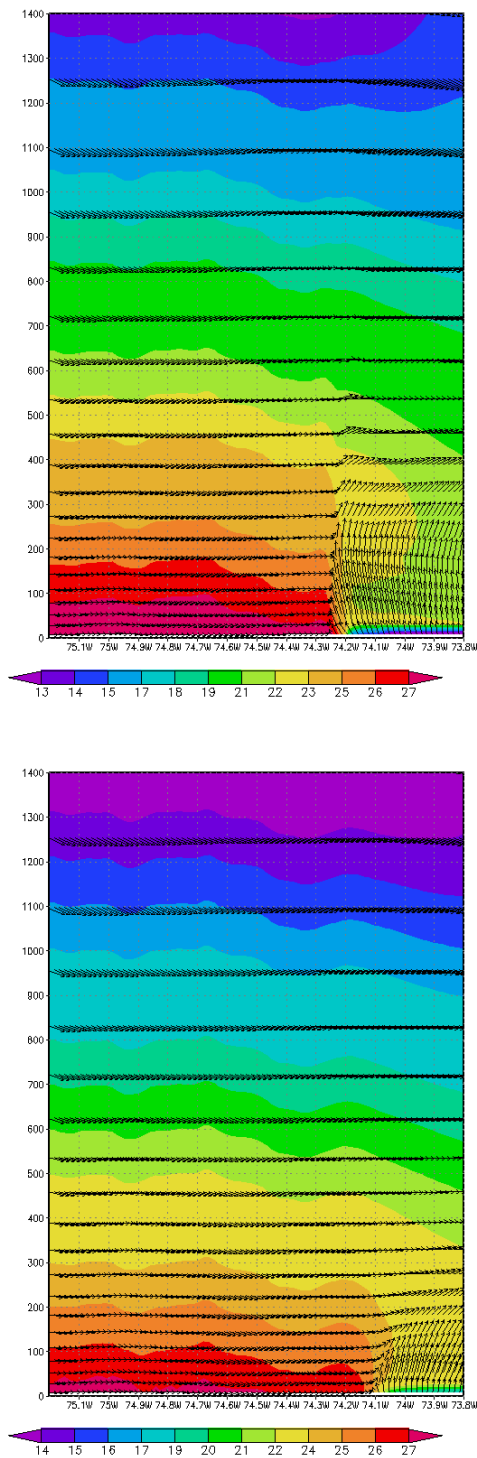


**Figure 55 a-b:** Vertical cross-sections for 39.8°N at 2000 GMT for the uniform 15°C July 6, 2004 sensitivity case study (a, top) and the uniform 17°C July 6, 2004 sensitivity case study (b, bottom) showing air temperature (°C) and wind vectors. The vertical extent of the sea breeze circulation is significantly deeper in the 15°C SST case study, and penetrates farther inland at low-levels.

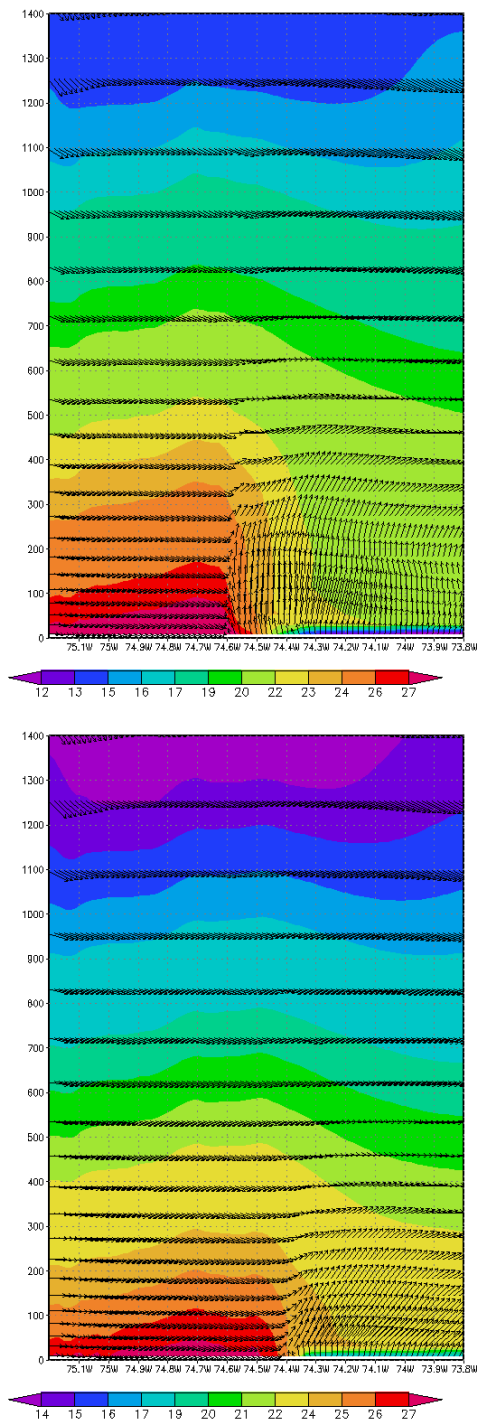


**Figure 56 a-b:** Vertical cross-sections for 39.4°N at 2000 GMT for the uniform 15°C July 6, 2004 sensitivity case study (a, top) and the uniform 17°C July 6, 2004 sensitivity case study (b, bottom) showing air temperature (°C) and wind vectors. The vertical extent of the sea breeze circulation is significantly deeper in the 15°C SST case study, and penetrates farther inland at low-levels.

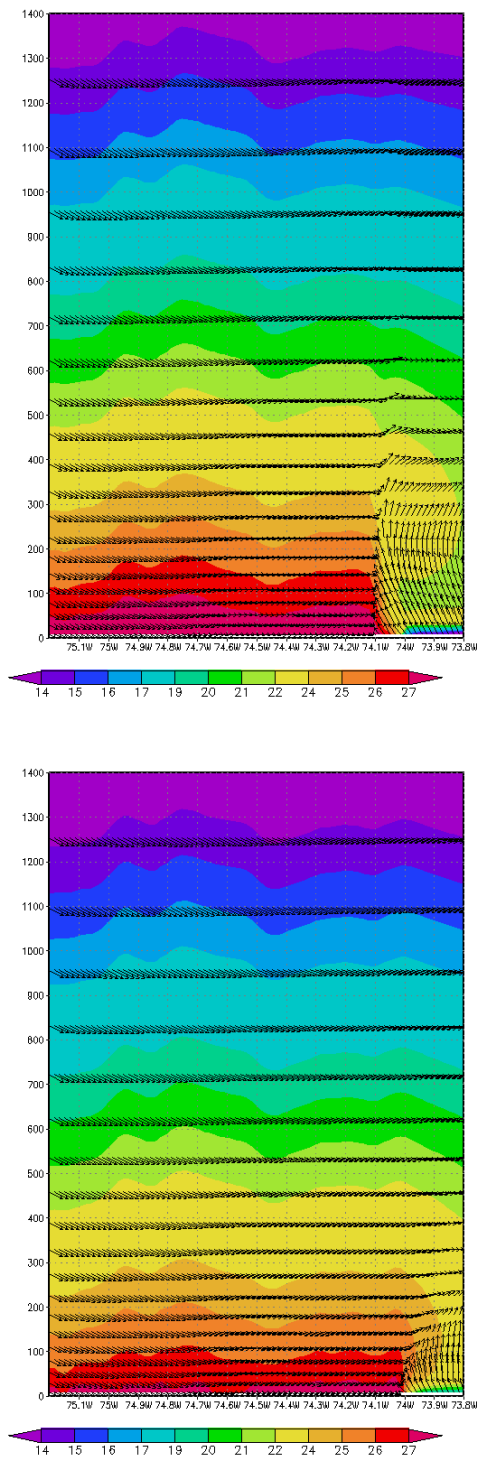


**Figure 57 a-b:** Vertical cross-sections for 40.2°N at 2000 GMT for the uniform 15°C July 6, 2004 sensitivity case study (a, top) and the uniform 17°C July 6, 2004 sensitivity case study (b, bottom) showing air temperature (°C) and wind vectors. The vertical extent of the sea breeze circulation is significantly deeper in the 15°C SST case study, and penetrates farther inland at low-levels.

## References

- Achtemeier, G. L., 1991: The Use of Insects as Tracers for “Clear-Air” Boundary-Layer Studies by Doppler Radar. *Journal of Atmospheric and Oceanic Technology*, **8**, 746-765.
- Alpert, P., D. S. Tannhauser, Y. Leshem, A. Kravitz, and M. Rabinovitch-Hadar, 2000: Migrating Soaring Birds Align along Sea Breeze Fronts; First Evidence from Israel. *Bulletin of the American Meteorological Society*, **81**, 1599-1601.
- Angell, J. K., and D. H. Pack, 1965: A Study of the Sea Breeze at Atlantic City, New Jersey Using Tetroons as Lagrangian Tracers. *Monthly Weather Review*, **93**, 475-493.
- Arritt, R. W., 1993: Effects of the Large-Scale Flow on Characteristic Features of the Sea Breeze. *Journal of Applied Meteorology*, **32**, 116-125.
- Atkins, N. T., and R. M. Wakimoto, 1997: Influence of the Synoptic-Scale Flow on Sea Breezes Observed During CaPE. *Monthly Weather Review*, **125**, 2112-2130.
- Atlas, D., 1960: Radar Detection of the Sea Breeze. *J. Meteorology*, **17**, 244-258.
- Banta, R. M., L. D. Oliver, and D. H. Levinson, 1993: Evolution of the Monterrey Bay Sea-Breeze Layer As Observed by Pulsed Doppler Lidar. *Journal of the Atmospheric Sciences*, **50**, 3959-3982.
- Bechtold, P. J., J. Pinty, and P. Mascart, 1991: A numerical investigation of the influence of large-scale winds on the sea-breeze and inland-breeze type circulations. *Journal of Applied Meteorology*, **30**, 1268-1279.
- Bourne, K., D. Chen, and M. Nunez, 1998: A Method for Finding Sea Breeze Days Under Stable Synoptic Conditions and its Application to the Swedish West Coast. *International Journal of Climatology*, **18**, 901-914.
- Chant, R. J., 2001: Evolution of Near-Inertial Waves During an Upwelling Event on the New Jersey Inner Shelf. *Journal of Physical Oceanography*, **31**, 746-764.
- Chiba, O., F. Kobayashi, G. Naito, and K. Sassa, 1999: Helicopter Observations of the Sea Breeze over a Coastal Area. *Journal of Applied Meteorology*, **38**, 481-492.
- Clancy, R. M., J. D. Thompson, H. E. Hurlburt, and J. D. Lee, 1979: A Model of Mesoscale Air-Sea Interaction in a Sea Breeze-Coastal Upwelling Regime. *Monthly Weather Review*, **107**, 1476-1505.

- Colby, F. P. Jr., 2004: Simulation of the New England Sea Breeze: The Effect of Grid Spacing. *Weather and Forecasting*, **19**, 277-285.
- Crum, T. D., R. L. Alberty, 1993: The WSR-88D and the WSR-88D Operational Support Facility. *Bulletin of the American Meteorological Society*, **74**, 1669-1687.
- Eastwood, Dr. E., and G. C. Rider, 1961: A radar observation of a sea breeze front. *Nature*, **189**, 978-980.
- Estoque, M.A., 1962: The sea breeze as a function of the prevailing synoptic situation. *Journal of Atmospheric Science*, **19**, 244-250.
- Fett, R., and P. Tag, 1984: The Sea-Breeze-Induced Coastal Calm Zone as Revealed by Satellite Data and Simulated by a Numerical Model. *Mon. Wea. Rev.*, **112**, 1226-1233.
- Finkele, K.J., M. Hacker, H. Kraus, and R.A.D. Byron-Scott, 1995: A complete sea-breeze circulation cell derived from aircraft observations. *Boundary Layer Meteorology*, **73**, 299-317.
- Frizzola, J. A., and E. L. Fisher, 1963: A Series of Sea Breeze Observations in the New York City Area. *Journal of Applied Meteorology*, **2**, 722-739.
- Glenn, S. M., Crowley, M., Haidvogel, D., and Song, Y. T., 1996: Underwater observatory captures coastal upwelling events off New Jersey. *EOS Trans AGU*, **77**, 233-236.
- Glenn, S. M., Grassle, J. F., and von Alt, C. J., 2000. A Well-Sampled Ocean; The Leo Approach. *Oceanus*, **42**, 28-30.
- Glenn, S. M., Arnone, R., Bergmann, T., Bissett, W. P., Crowley, M., Cullen, J., Gryzmski, J., Haidvogel, D., Kohut, J., Moline, M. A., Oliver, M., Orrico, C., Sherrell, R., Song, T., Weidemann, A., Chant, R., and Schofield, O., 2004. The Biogeochemical impact of summertime coastal upwelling in the Mid-Atlantic Bight. *Journal Geophysical Research*.
- Hicks, D. C., and J. R. Miller, 1980: Meteorological forcing and bottom water movement off the northern New Jersey coast. *Estuarine Coastal Marine Science*, **11**, 563-571.
- Huschke, R. E., editor, 1959: Glossary of Meteorology, American Meteorological Society, Boston. 638 pp.
- Ingham, M. C., and J. Eberwine, 1984: Evidence of Nearshore Summer Upwelling off Atlantic City, New Jersey. NOAA Technical Memorandum NMFS-F/NEC-31. 10pp.

- Kwiatkowski, J. J., 1999: Observations and Analysis of the New Jersey Sea Breeze. M.S. Thesis. The Graduate School. Rutgers University. 79 pp..
- Mahrer, Y., and M. Segal, 1985: On the Effects of Islands' Geometry and Size on Inducing Sea Breeze Circulation. *Monthly Weather Review*, **113**, 170-175.
- McPherson, R.D., 1970: A Numerical Study of the Effect of a Coastal Irregularity on the Sea Breeze. *Journal of Applied Meteorology*, **9**, 767-777.
- Pearson, R. A., G. Carboni, and G. Brusasca, 1983: The sea breeze with mean flow. *Quarterly Journal of the Royal Meteorological Society*, **109**, 809-830.
- Pedgeley, D. E., 1990: Concentration of flying insects by the wind. *Philosophical Transactions of the Royal Society of London*, **328**, 631-653.
- Pielke, R.A., 1984: *Mesoscale meteorological modeling*. Academic Press, Orlando, 612 pp.
- Russell, R. W., and J. W. Wilson, 2001: Spatial dispersion of aerial plankton over east-central Florida: aeolian transport and coastline concentrations. *International Journal of Remote Sensing*, **22**, 2071-2082.
- Sabins, F. F., 1987: *Remote Sensing Principles and Interpretation*, New York: W. H. Freeman and Company, 449 pp.
- Schofield, O., T. Bergmann, W.P. Bissett, F. Grassle, D. Haidvogel, J. Kohut, M. Moline and S. Glenn, 2002. The Long-term Ecosystem Observatory: An integrated coastal observatory, *Journal of Oceanic Engineering*, **27**, 146-154.
- Simpson, J. E., 1964: Aerial and radar observations of some sea-breeze fronts. *Weather*, **22**, 306-316.
- Simpson, J.E., and R.E. Britter, 1980: A laboratory model of an atmospheric mesofront. *Quarterly Journal of the Royal Meteorological Society*, **106**, 485-500.
- Simpson, J.E., 1994: *Sea Breeze and local winds*. Cambridge University Press, Cambridge, 234 pp.
- Simpson, J. E., 1996: Diurnal Changes in Sea-Breeze Direction. *Journal of Applied Meteorology*, **35**, 1166-1169.
- Simpson, J. E., 1997: *Gravity Currents in the Environment and the Laboratory*. Cambridge University Press, Cambridge, 244 pp.

Song, Y. T., D. B. Haidvogel, and S. M. Glenn, 2001: Effects of topographic variability on the formation of upwelling centers off New Jersey: A theoretical model. *Journal of Geophysical Research*, **106**, 9223-9240.

Stephan, K., H. Kraus, C. M. Ewenz, and J. M. Hacker, 1999: Sea-breeze Front Variations in Space and Time. *Meteorology and Atmospheric Physics*, **70**, 81-95.

Tjim, A.B.C., and A.J. Van Delden, 1999: The role of sound waves in sea-breeze initiation. *Q. J. R. Meteorol. Soc.*, **125**, 1997-2018.

Tijm, A. B. C., A. A. M. Holtstag, and A. J. van Delden, 1999: Observations and Modeling of the Sea Breeze with the Return Current. *Monthly Weather Review*, **127**, 625-640.

Yoshikado, H., 1990: Vertical Structure of the Sea Breeze Penetrating through a Large Urban Complex. *Journal of Applied Meteorology*, **29**, 878-891.

Zhong, S. and E. S. Takle, 1993: The Effects of Large-Scale Winds on the Sea-Land Breeze Circulations in an Area of Complex Coastal Heating. *Journal of Applied Meteorology*, **32**, 1181-1195.